

Aus dem Institut für Humangenetik
Theoretische Medizin und Biowissenschaften
der Medizinischen Fakultät
der Universität des Saarlandes, Homburg/Saar

Functional screening for anti-apoptotic genes using RNAi technology

*Dissertation zur Erlangung des Grades eines Doktors der Naturwissenschaften
der Medizinischen Fakultät*

der UNIVERSITÄT DES SAARLANDES

2009

vorgelegt von Maria Shahmoradgoli Najafabadi
geb. am 19.08.1978 in Esfahan

Content

| | |
|---|-----|
| Content | II |
| Summary | VI |
| Zusammenfassung | VII |
| Abbreviation | IX |
| I Introduction | 1 |
| I-1 Apoptosis | 1 |
| I.1.2 Morphological features and detection of apoptosis | 1 |
| I.1.3 Apoptotic pathways..... | 2 |
| I.1.3.1 The death receptor-mediated apoptotic pathway (extrinsic pathway) | 3 |
| I.1.3.2 The mitochondria-mediated apoptotic pathway (intrinsic pathway) | 3 |
| I.1.4 Regulation and molecular mechanism of apoptosis..... | 5 |
| I.1.4.1 Caspases | 5 |
| I.1.4.2 Caspase regulators..... | 5 |
| I.1.4.3 Bcl-2 family proteins | 6 |
| I.1.4.4 TNF family and receptors | 6 |
| I.2 Cancer | 7 |
| I.2.1 Apoptosis and Cancer | 8 |
| I.2.2 Breast cancer | 9 |
| I.2.2.1 Breast cancer and apoptosis | 10 |
| I.3 RNA interference | 10 |
| I.3.1 RNA interference mechanism | 11 |
| I.3.2 Applications of RNA interference | 12 |
| I.4 Reverse transfection cell array | 15 |
| I.5 Aim of this project | 17 |
| II Materials and methods | 18 |
| II.1 Materials | 18 |
| II.1.1 Instruments | 18 |
| II.1.2 Chemical reagents and general materials | 19 |
| II.1.3 Cell Culture..... | 20 |
| II.1.4 Kits..... | 20 |
| II.1.5 Antibodies..... | 21 |
| II.1.6 sh-RNAs and plasmid DNA | 21 |

| | |
|---|----|
| II.1.7 Oligonucleotides Primers..... | 22 |
| II.1.8 siRNAs..... | 22 |
| II.1.9 Cell lines | 23 |
| II.1.10 Media, Solutions and Buffers | 23 |
| II.1.11 Antibiotics..... | 25 |
| II.2 Methods | 26 |
| II.2.1 General molecular biology methods | 26 |
| II.2.1.1 Transformation in competent bacteria | 26 |
| II.2.1.2 Mini-preparation of plasmid DNA | 26 |
| II.2.1.3 RNA isolation and quality assessment | 27 |
| II.2.1.4 Protein isolation with RIPA buffer | 27 |
| II.2.1.5 Protein quantification (BCA Protein Quantification)..... | 28 |
| II.2.1.6 DNA sequencing..... | 28 |
| II.2.1.7 Quantitative real time -PCR primer design | 28 |
| II.2.1.8 cDNA synthesis | 29 |
| II.2.1.9 Real-Time PCR analysis..... | 29 |
| II.2.1.10 Western blot analysis..... | 30 |
| II.2.1.11 Immunostaining of fixed cells | 30 |
| II.2.2 Cell culture..... | 31 |
| II.2.2.1 Cell maintenance | 31 |
| II.2.2.2 Reverse transfection cell array..... | 31 |
| II.2.2.3 Standard transfection of HEK293T cells..... | 32 |
| II.2.2.4 Transfection of MCF7 and other breast cancer cells | 33 |
| II.2.3 Expression arrays..... | 33 |
| II.2.3.1 Illumina expression array | 33 |
| II.2.3.1.1 RNA preparation and quality analysis | 34 |
| II.2.3.1.2 cRNA synthesis, purification and labeling | 34 |
| II.2.3.1.3 Probe labeling and Illumina Sentrix BeadChip array hybridization | 34 |
| II.2.3.1.4 Scanning and data analysis | 35 |
| II.2.3.2 Pathway analysis..... | 35 |
| II.2.3.2.1 Comprehensive gene pathway analysis..... | 35 |
| II.2.3.2.2 Ingenuity pathway analysis | 36 |
| II.2.4 Functional analysis | 36 |
| II.2.4.1 Apoptosis assay | 36 |

| | |
|---|----|
| II.2.4.2 Cell viability assay..... | 36 |
| II.2.4.3 Cell cycle analysis | 37 |
| II.2.4.4 Proliferation assay | 37 |
| II.2.4.5 Caspase activity measurement using the Caspase-Glo [®] Assay | 37 |
| II.2.4.6 NF-κB luciferase reporter assay (dual-luciferase reporter assay)..... | 38 |
| II.2.4.7 Flow cytometric analysis of cell surface death receptor..... | 39 |
| II.2.5 Statistical analysis..... | 39 |
| III Results | 40 |
| III.1 Short hairpin RNAi screen in normal cells | 40 |
| III.1.1 Reverse transfection cell array technology | 40 |
| III.1.2 Direct transfection and FACS analysis | 43 |
| III.1.2.1 Optimization of the screening set-up..... | 43 |
| III.1.3 Short hairpin RNA (shRNA) screen to identify putative anti apoptotic genes | 44 |
| III.1.4 Validation studies confirm the specificity of CHMP5 anti-apoptotic function..... | 45 |
| III.1.4.1 siRNAs targeting different segment of <i>CHMP5</i> RNA | 45 |
| III.1.4.2 Over expression and rescue assays..... | 47 |
| III.1.5 Functional characterization of CHMP5..... | 48 |
| III.1.5.1 CHMP5-silencing induces caspase activation..... | 48 |
| III.1.6 Expression array analysis | 50 |
| III.1.7 Pathway analysis | 53 |
| III.1.7.1 Comprehensive gene pathway analysis after CHMP5 modulation identifies relevant signaling cascades | 53 |
| III.1.7.2 Ingenuity pathway analysis and relevant NF-κB factors..... | 53 |
| III.1.8 Death receptor expression is influenced by CHMP5 | 55 |
| III.2 SiRNA screen in breast cancer cells..... | 57 |
| III.2.1 Background of selected genes for RNAi screening..... | 57 |
| III.2.2 Optimization of the screening set-up..... | 57 |
| III.2.3 SiRNA screen to identify genes involved in survival of breast cancer cells..... | 58 |
| III.2.4 Accuracy of screening readout | 60 |
| III.2.5 Validation of the cell death inhibitory function for candidate gene <i>PPP1R15B</i> ... | 61 |
| III.2.5.1 Efficacy of the PPP1R15B silencing phenotype | 61 |
| III.2.5.2 The impact of PPP1R15B knock-down at the protein level..... | 62 |
| III.2.5.3 Apoptosis induction upon PPP1R15B knock-down cells | 63 |
| III.2.6 Effect of PPP1R15B deficiency on caspase activation | 65 |

| | |
|--|-----|
| III.2.7 Apparent involvement of PPP1R15B in cell cycle regulation | 65 |
| III.2.8 Inhibition of proliferation by PPP1R15B silencing | 67 |
| III.2.9 <i>PPP1R15B</i> expression in different breast cancer cell lines..... | 68 |
| III.2.10 Investigation of PPP1R15B deficiency effect on cell viability in other breast cancer cell lines | 68 |
| IV Discussion | 70 |
| IV.1 shRNA screening in non-tumor cells | 70 |
| IV.1.1 An optimized method for screening of apoptotic phenotype mediated by loss-of-function experiments | 70 |
| IV.1.2 Identification of candidate genes on the bases of shRNA screen | 71 |
| IV.1.2.1 Validation of CHMP5 | 72 |
| IV.1.3 Further functional assays..... | 73 |
| IV.1.3.1 Caspase activity and apoptotic pathway | 73 |
| IV.1.3.2 Expression array analysis: genes and pathways affected by CHMP5 modulation..... | 74 |
| IV.1.3.2.1 Apoptosis related genes and expression changes induced by CHMP5 silencing..... | 74 |
| IV.1.3.2.2 Pathways affected by CHMP5 modulation | 74 |
| IV.1.4 Charged multivesicular body protein 5 (<i>CHMP5</i>); One gene, multiple functions | 76 |
| IV.2 RNAi screen in the breast cancer cells..... | 77 |
| IV.2.1 Expression profiling revealed candidate genes for functional study | 77 |
| IV.2.2 siRNA screen and identification of genes involved in cell survival | 77 |
| IV.2.3 Validation of the candidate gene <i>PPP1R15B</i> | 78 |
| IV.2.4 PPP1R15B deficiency reduced cell proliferation and induced apoptosis in breast cancer cell line..... | 79 |
| IV.2.5 PPP1R15B, an interesting target for chemotherapeutic studies..... | 81 |
| V. Literature | 82 |
| VI. Supplementary data..... | 89 |
| Publications | 106 |
| Acknowledgments | 107 |
| Curriculum Vitae..... | 108 |

Summary

RNA interference (RNAi) is a natural mechanism by which small interfering RNA (siRNA) or short hairpin RNA (shRNA) can mediate inhibition of translation or degradation of a target RNA molecule in a sequence-specific manner. RNAi is widely used to uncover gene function or pathway context of novel genes. In this study, two loss-of-function screens are performed using RNAi for the identification of genes, which are involved in cell survival and/or apoptosis pathway. One screen was performed using short hairpin RNAs targeting 288 functionally uncharacterized or poorly characterized human genes to identify those with a capability to inhibit apoptosis in non-tumorigenic cells. In this study, we identified a new anti-apoptotic function for CHMP5 (Charged Multivesicular Body Protein 5), which was confirmed by caspase inhibition assays. Furthermore, upon over-expression of CHMP5 a regulatory role for CHMP5 on different signaling pathways, including NF- κ B, was revealed by expression profiling. The regulatory effect of CHMP5 on the NF- κ B-pathway was confirmed using luciferase reporter assays. Further investigation of upstream effectors, like membrane receptors, indicated that cellular surface appearance of death receptor TNFR1 is affected in CHMP5 modulated cells as well. Taken together, this study revealed an anti-apoptotic function of CHMP5, and provided evidence for TNFR1 surface expression as an upstream and NF- κ B signaling as a downstream factor with respect to CHMP5 function.

The second screen was performed in a breast cancer cell line. SiRNAs against 107 genes over-expressed in breast cancer patients resistant to the chemotherapy were applied to identify genes which have an impact on survival in breast cancer. It led to identification of *PPP1R15B* (Protein phosphatase 1 regulatory (inhibitor) subunit 15B) as a gene increasing survival of breast cancer cell line MCF7. Moreover, cell cycle analysis showed that *PPP1R15B* silencing inhibits cell cycle progression apparently through block of the G1/S checkpoint. Induction of apoptosis and inhibition of cell proliferation seem to be the mechanism through which deficiency of *PPP1R15B* affect survival of MCF7 breast cancer cells. These two studies provided evidence that loss-of-function screen using RNAi is a powerful approach to identify novel factors which are implicated in cell survival and apoptosis pathways in non-tumorigenic and in cancer cells. The profound influence of *PPP1R15B* silencing on viability of cancer cells, may open a possible avenue for treatment of patients resistant to chemotherapy in future.

Zusammenfassung

Interferenz (RNAi) ist ein natürlicher Vorgang im Zellgeschehen, bei dem *small interfering RNAs* (siRNA) oder *short hairpin RNAs* (shRNA) die Inhibition der Translation oder den Verdau von Ziel-RNAs bewirken, die sequenzhomolog erkannt werden. RNAi wird vielfältig eingesetzt, um die Funktion von Genen oder deren Einbindung in zelluläre Reaktionsketten zu untersuchen. In der vorliegende Arbeit werden zwei *loss-of-function screens* unter Verwendung von RNAi zur systematischen Suche nach Genen beschrieben, die für das Überleben von Zellen und/oder an der Apoptose beteiligt sind. Der erste Screen wurde mit shRNAs gegen 288 nicht oder kaum charakterisierten Zielgenen durchgeführt, um Kandidaten mit einem hemmenden Einfluss auf die Apoptose in nicht-Tumor Zellen zu bestimmen. Mit diesem Ansatz konnten wir eine neue anti-apoptotische Wirkung für CHMP5 (Charged Multivesicular Body Protein 5) nachweisen, was sich durch Caspase-Hemmung bestätigen ließ. Darüberhinaus zeigten Expressions-Profile nach Überexpressions von CHMP5 dessen regulierenden Einfluss auf unterschiedliche Signalwege, einschließlich NF- κ B. Der Einfluss von CHMP5 auf den NF- κ B-Signalweg wurde durch Luciferase-Reporter Analysen bestätigt. Weiterführende Untersuchungen an vorgeschalteten Effektoren, z.B. Membranrezeptoren, wiesen darauf hin, dass die Aktivierung des *death receptors* TNFR1 auf der Zelloberfläche ebenfalls von CHMP5 abhängig ist. Zusammenfassend zeigte die Studie eine anti-apoptotische Funktion von CHMP5 und ergab Hinweise darauf, dass die Oberflächen-Expression von TNFR1 ein CHMP5-vorgeschalteter, und NF- κ B signaling ein CHMP5-nachgeschalteter Faktor Vorgang sind.

Der zweite Screen wurde mit einer Brustkrebs-Zelllinie durchgeführt. SiRNAs gegen 107 Gene, die bekanntermaßen in chemotherapieresistenten Brustkrebspatientinnen überexprimiert sind, wurden eingesetzt, um Gene zu identifizieren, die für das Überleben von Brustkrebszellen wichtig sind. Dies führte zum Nachweis dafür, dass *PPP1R15B* (Protein phosphatase 1 regulatory (inhibitor) subunit 15B) das Überleben von MCF7 Zellen erhöht. Darüberhinaus zeigte eine Zellzyklus-Analyse, dass Unterdrückung von PPP1R15B den Ablauf des Zellzyklus' anscheinend durch Blockierung des G1/S checkpoint hemmt. Induktion von Apoptose und Hemmung der Zellvermehrung scheinen der Mechanismus zu sein, durch den ein Ausfall von PPP1R15B auf das Überleben von MCF7-Brustkrebs Zellen einwirkt.

Diese beiden Untersuchungen erbringen den Nachweis, dass *loss-of-function screens* mittels RNAi ein leistungsfähiger Ansatz sind, um neue Faktoren zu finden, die das Überleben von Zellen und deren Apoptose in nicht-neoplastischen, sowie in Tumorzellen beeinflussen. Der grundlegende Einfluss der Unterdrückung von PPP1R15B auf die Lebensfähigkeit von Krebszellen könnte einen Weg zur Behandlung von Chemotherapie-resistenten Patienten öffnen.

Abbreviation

| | |
|-----------------|--|
| ATP | Adenosine triphosphate |
| Birc | Baculovirus IAP repeat (BIR)-containing protein |
| BSA | Bovine serum albumin |
| bp | Base pair |
| cDNA | Complementary DNA |
| CGPA | Comprehensive Gene Pathway Analysis |
| <i>CHMP5</i> | Charged Multivesicularbody Protein 5 |
| dNTP | Desoxy-nucleotide triphosphate |
| ds | Double stranded |
| DNA | Desoxy-ribonucleic acid |
| DISC | Death-inducing signaling complex |
| DD | Death domain |
| ESCRT-III | Endosomal sorting complex required for transport III |
| eIF2 α | Eukaryotic translation initiation factor 2 α |
| <i>E. coli</i> | Escherichia coli |
| FACS | Fluorescence-activated cell sorting |
| GEO | Gene Expression Omnibus |
| GFP | Green fluorescent protein |
| IAP | Inhibitor of apoptosis proteins |
| IPA | Ingenuity Pathways analysis |
| RLU | Related light units |
| Luc | Luciferase |
| LB | Lysogeny Broth / Luria Broth |
| mRNAs | Messenger RNAs |
| NF- κ B | Nuclear Factor kappa B |
| PCD | Programmed cell death |
| <i>PPP1R15B</i> | Protein Phosphatase 1 Regulatory (inhibitor) Subunit 15B |

Abbreviation

| | |
|----------|---|
| PVDF | Polyvinylidene fluoride |
| PI | Propidium iodide |
| PBS | Phosphate buffered saline |
| qRT-PCR | Quantitative real-time polymerase chain reaction |
| RNAi | RNA interference |
| RISC | RNA-induced silencing complex |
| RT | Room temperature |
| RPM | Rotations per minute |
| RNA | Ribonucleic acid |
| SDS | Sodium dodecyl sulfate |
| SDS-PAGE | Sodium dodecyl sulfate polyacrylamide gel electrophoresis |
| Sh | Short hairpin |
| ShRNAs | Short hairpin RNAs |
| SiRNAs | Small interfering RNAs |
| TNFR1 | Tumour Necrosis Factor Receptor 1 |
| v/v | Volume per volume |
| Vol | Volume |
| W/v | Weight per volume |
| YFP | Yellow fluorescent protein |

I Introduction

I-1 Apoptosis

The physiological cell death that occurs in multicellular organisms is called 'programmed cell death' (PCD) or apoptosis. Apoptosis is derived from the Greek word for "falling off" of leaves from a tree. The term apoptosis (ap-op-toe-sis) was first used in a, now-classic, paper by Kerr, Wyllie, and Currie in 1972 to describe a morphologically distinct form of cell death, although certain components of the apoptosis concept had been explicitly described many years previously (Kerr et al., 1972; Kerr, 2002; Chowdhury et al., 2006). Apoptosis is a crucial biological process and plays an essential role in regulating development, homeostasis, and immune defence. It is a biologically conserved phenomenon throughout evolution, and is observed from nematodes to mammals. The process of apoptosis is the end of an energy-dependent cascade of events initiated by death-inducing stimuli (Vaux and Strasser, 1996; Vaux and Korsmeyer, 1999; Chowdhury et al., 2006). The process of apoptosis is divided into different phases containing overlapping components:

- i. In the early or initiation phase a stimulus provokes or initiates the apoptotic response. This may be an external signal delivered through surface receptors, or may originate inside the cell from the action of a drug, toxin, or radiation.
- ii. The signal transduction phase, in which the detection of a signal or metabolic state results in the transduction of that signal to the cell death effector machinery, resulting in the activation of proteases.
- iii. The termination phase, in which results the cell's chromatin and DNA are degraded.

I.1.2 Morphological features and detection of apoptosis

Morphological alterations that occur upon apoptotic cell death involve both the nucleus and the cytoplasm. Light and electron microscopy have identified various changes, including cell shrinkage, surface convolution, and the formation of apoptotic bodies (Hacker, 2000). Using hematoxylin and eosin staining, an apoptotic cell appears as a round or oval mass with an intensely eosinophilic cytoplasm, and is accompanied by vacuolization and the presence of dense nuclear chromatin fragments. Apoptotic chromatin condensation and nuclear fragmentation occurs in two stages. Condensation starts peripherally along the nuclear

membrane, forming a crescent or ring-like structure. Chromatin cleavage occurs rapidly thereafter by topoisomerase II and DNase I/DNase II mediated enzyme activity, resulting in the formation of oligonucleosome-sized fragments (Earnshaw, 1995; Chowdhury *et al.*, 2006). A number of techniques are available for the detection of apoptosis (Barrett *et al.*, 2001):

- i. Detection of a so-called ladder of degenerated DNA fragments, which can be identified by DNA agarose gel electrophoresis (Wyllie, 1980).
- ii. Flow cytometry assays for the detection of apoptosis. Flow cytometric analyses are based on the detection of signals changed due to DNA fragmentation, DNA loss, or membrane changes. The easiest and quickest method for measuring apoptosis is DNA staining with PI (Nicoletti *et al.*, 1991), which is particularly suitable for large scale in vitro studies of late apoptosis. In addition, due to the plasma membrane changes during apoptosis, Hoechst and annexin V-FITC dyes can be used for early detection of apoptosis. (Hardin *et al.*, 1992) (Koopman *et al.*, 1994).
- iii. Terminal deoxynucleotidyl transferase-mediated dUTP-digoxigenin nick-end labeling (TUNEL). DNA strand breaks occurring in apoptotic cells as a result of endonuclease(s) activation can be labeled in situ in individual fixed, permeabilized cells or in tissue sections by the terminal deoxynucleotidyl transferase mediated dUTP nick end labeling (TUNEL) technique (Sgonc *et al.*, 1996), which transfers biotin labeled-dUTP to these strand breaks of cleaved DNA by terminal transferase.
- iv. Detection of activated caspases. Active caspases (see section I.1.4.1) can be detected using different methods such as flow cytometry, immunostaining and luminescent assays.

I.1.3 Apoptotic pathways

Apoptotic pathways can potentially be modulated to maintain cell viability. In mammals, apoptosis is initiated by two major pathways:

- i. The extrinsic pathway, which can be triggered by activation of transmembrane death receptors and subsequent caspase-8 activation;
- ii. The intrinsic or mitochondrial pathway, which is initiated by cellular stress followed by activation of caspase-9.

Each of these pathways converges to a common execution phase of apoptosis that requires proteolytic activation of caspases-3 and/or -7 from their inactive zymogens (Thornberry and Lazebnik, 1998). Biochemically, the main features of apoptosis include caspase cascade activation and DNA fragmentation (Adams, 2003).

I.1.3.1 The death receptor-mediated apoptotic pathway (extrinsic pathway)

The receptors triggering this pathway are located in the cell membrane and are activated by extra cellular ligands. Typical death receptors are Fas (also called Apo-1 or CD95) and tumor necrosis factor receptor (TNF-R) 1; they belong to the TNF-R family and contain a cytosolic death domain. Activation of death receptors causes formation of death-inducing signaling complexes (DISC) in which the adaptor proteins such as FADD bind with their death domain (DD) to a DD in the cytoplasmic region of the receptors (Ashkenazi and Dixit, 1998; Schulze-Osthoff *et al.*, 1998; Peter and Krammer, 2003). The receptor-induced pathway leads to the recruitment of caspase-8 or -10 (initiator caspases) to the DISC (Bodmer *et al.*, 2000). The activated caspase then proteolytically activates downstream effector caspases that degrade cellular targets and mediates cell death. There is a cross-link between the two-apoptotic pathways, in which caspase-8 can also cleave the protein Bid. The resulting truncated Bid (tBid) then moves to the mitochondria and induces cytochrome c release, leading to activation of caspase-9 and caspase-3. DISC signalling can be inhibited by expression of c-FLIP, an inactive homolog of caspase-8 (Li and Yuan, 2008) (Figure 1).

I.1.3.2 The mitochondria-mediated apoptotic pathway (intrinsic pathway)

The intrinsic or mitochondrial pathway is activated by a variety of extra- and intracellular stresses, including oxidative stress, irradiation, and treatment with cytotoxic drugs, oncogene activation or DNA damage (Figure 1). Mitochondria play a key role in mediating apoptosis induced by diverse stimuli (Wang, 2001). They release pro-apoptotic proteins (cytochrome c, Smac, Omi, Aif, and EndoG) whose release from the intermembrane space of mitochondria into the cytosol is regulated by proteins belonging to the Bcl2 family (see section I.1.4.3). Perhaps the most intriguing one of these proteins is cytochrome c, which binds to, and activates, the protein APAF1 in the cytoplasm. The binding of cytochrome c to APAF1 induces a conformational change that allows APAF1 to bind to ATP/dATP in order to form the apoptosome, which mediates the activation of caspase-9 (Li *et al.*, 1997; Rodriguez and Lazebnik, 1999; Jiang and Wang, 2000; Riedl and Shi, 2004), thereby triggering a cascade of caspase activation.

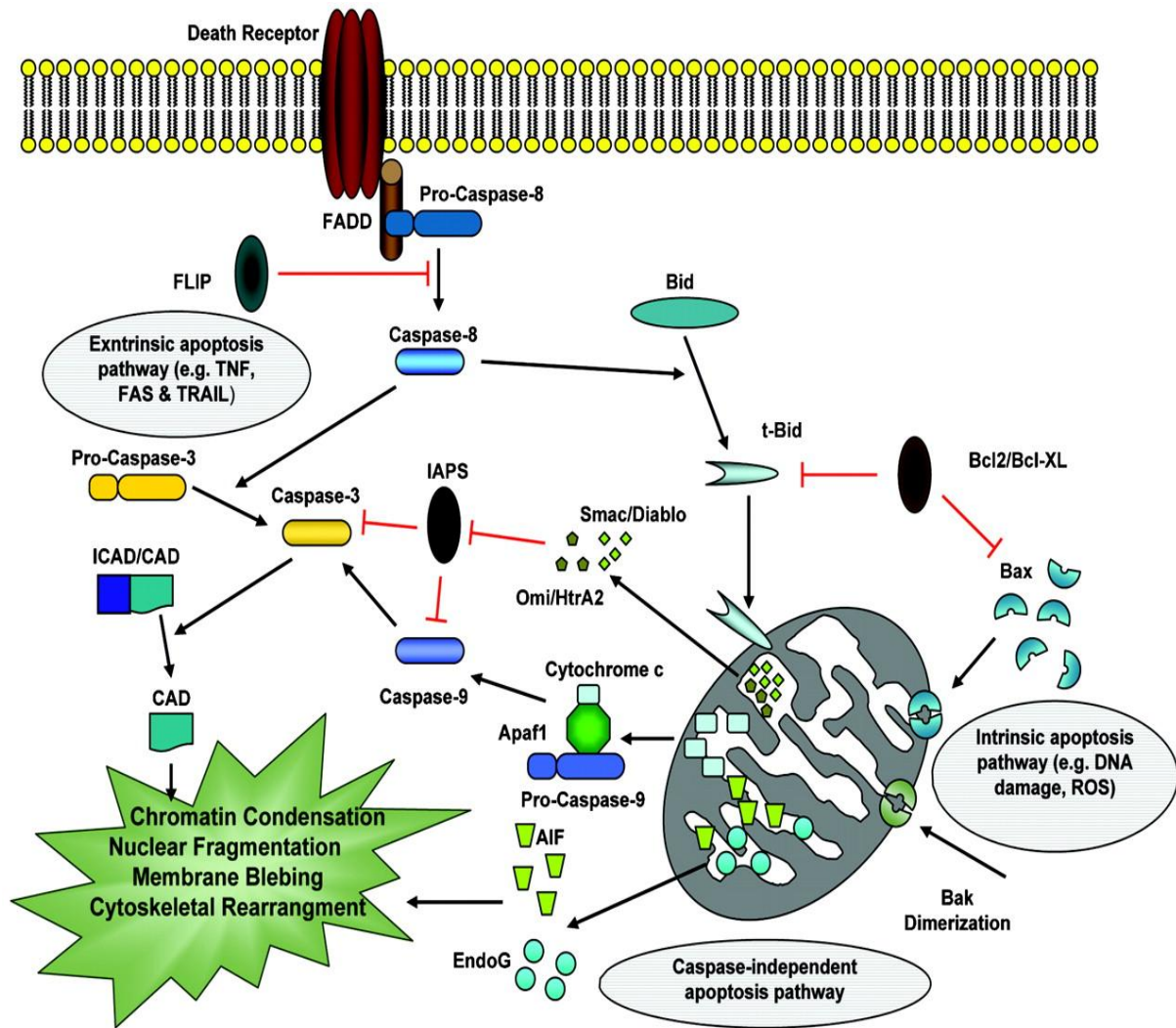


Figure 1- **The molecular mechanisms of apoptosis.** Apoptosis pathways can be initiated via different stimuli, i.e. at the plasma membrane by death receptor ligation (extrinsic pathway) or at the mitochondria (intrinsic pathway). Stimulation of death receptors results in receptor aggregation and recruitment of the adaptor molecule Fas-associated death domain (FADD) and caspase-8. Upon recruitment, caspase-8 becomes activated and initiates apoptosis by direct cleavage of downstream effector caspases. Mitochondria are engaged via the intrinsic pathway, which can be initiated by a variety of stress stimuli, including ultraviolet (UV) radiation, γ -irradiation, heat, DNA damage, the actions of some oncoproteins and tumor suppressor genes (i.e., *p53*), viral virulence factors and most chemotherapeutic agents (Ghavami *et al.*, 2009a).

I.1.4 Regulation and molecular mechanism of apoptosis

Each step of apoptosis requires many proteins (Barrett *et al.*, 2001) and among the most crucial are the caspases. Caspase activities are tightly regulated by the inhibitor of apoptosis proteins (IAP). Other families of cellular proteins are also involved in the regulation of apoptosis at different stages. These proteins are categorized as the Bcl-2/ Bax family and TNF family (Chowdhury *et al.*, 2006; Ghavami *et al.*, 2009b) .

I.1.4.1 Caspases

Caspases, a family of cysteine proteases, play a central role in apoptosis. They are a conserved family of enzymes that initiates a process resulting in cell death. At least 14 distinct mammalian caspases have been identified, of which 11 are present in human beings (Salvesen and Dixit, 1997; Shi, 2002; Riedl and Shi, 2004; Lavrik *et al.*, 2005). Among them, caspases 1, 4, and 5 play roles in inflammatory responses and caspase 2, 8, 9, and 10 are responsible for the initiation of apoptosis. All caspases are produced in cells as catalytically inactive zymogens (inactive enzyme precursors) and must undergo proteolytic processing and activation during apoptosis (Yan and Shi, 2005; Chowdhury *et al.*, 2006). Caspases become active in response to specific signals generated by selective proteolytic processing at specific aspartic acid residues, which produce subunits that form an active protease, which initiates apoptosis (Lavrik *et al.*, 2005). Activation of a caspase can be initiated by different mechanisms. Initiator caspases can be activated at the plasma membrane upon activation of death receptors, or by releasing of factors such as cytochrome c from mitochondria (see section I.1.3.1 and I.1.3.2).

I.1.4.2 Caspase regulators

In normal living cells, caspase activation and activity are carefully regulated at several levels by a family of cellular proteins called the inhibitor of apoptosis proteins (IAP). IAPs, also known as baculovirus IAP repeat (Bir)-containing proteins (Bircs), are evolutionarily conserved and structurally similar proteins. They share one to three copies of a conserved domain of about 70 amino-acids, named Bir. They have been identified in a large range of organisms including yeast, nematode, drosophila, fish and mammals. Eight members of this family have been described in humans (Birc1/Naip, Birc2/cIAP1, Birc3/cIAP2, Birc4/XIAP, Birc5/Survivin, Birc6/Apollon, Birc7/MI-IAP and Birc8/ILP2) (LaCasse *et al.*, 1998;

Salvesen and Duckett, 2002).

Most of IAPs are able to bind to several apoptotic caspases. The capacity of Birc4/XIAP to inhibit the catalytic activity of caspases-3, -7 and -9 is well known (Shiozaki et al., 2003). A group of IAPs like XIAP, cIAP1 and cIAP2 can prevent the proteolytic processing of pro-caspases -3, -6 and -7 by blocking the cytochrome c-induced activation of pro-caspase-9. In contrast, these IAP family proteins do not prevent caspase-8-induced proteolytic activation of pro-caspase-3. However, they subsequently can inhibit active caspase-3 directly, thus blocking downstream apoptotic events, such as further activation of other caspases (Deveraux et al., 1998).

I.1.4.3 Bcl-2 family proteins

The Bcl-2 (B-cell CLL/Lymphoma 2) family proteins are known to play a crucial role in the regulation of apoptosis. This family consists of both pro- and anti-apoptotic members, which elicit opposing effects on mitochondria. Pro-apoptotic members such as Bax can induce mitochondrial membrane permeability, which results in the release of factors including cytochrome c, AIF, Endo G, Smac/Diablo and Htra2/Omi. Anti-apoptotic members, such as Bcl-2, Mcl-1 and Bcl-XL, preserve mitochondrial integrity and, therefore, potentially block the release of soluble membrane proteins (Figure 1).

The members of this family possess conserved Bcl-2 homology domains (BH), and can be divided into three categories (Borner, 2003; Chowdhury *et al.*, 2006):

- i. The multi-domain pro-apoptotic members such as Bax, Boc and Bak possess BH1, BH2 and BH3 domains.
- ii. The 'BH3-only' pro-apoptotic members such as Bid, Bik, Bad, Bcl2L11, Noxa and Puma. These share sequence homology only in the BH3 domain.
- iii. Anti-apoptotic members such as Bcl-2, Bcl-XL and Bcl2L2, all of which exert anti-cell death activity and share sequence conservation within all four BH domains.

I.1.4.4 TNF family and receptors

Tumour Necrosis Factor (TNF) is a soluble inflammatory cytokine produced by macrophages/monocytes during acute inflammation and is responsible for a diverse range of signaling events within cells, leading to apoptosis, cell proliferation, inflammation, allergy or autoimmune disease. The protein is also important for resistance to infection and cancer treatment. TNF exerts many of its effects by binding to the cognate membrane receptors

termed TNFR-1(CD120a) or a TNFR-2 (CD120b). Both of these receptors belong to the TNF receptor superfamily. The signal transduction of cell death from TNFR-1 is via its cytoplasmic death domain (DD) by the activation of caspase 8 alone to activate caspase 3 or by the activation of the mitochondria-dependent amplification loop to cause apoptosis. TNFR2 directly recruits TNF receptor-associated factors (TRAF), induces gene expression and intensively cross-talks with TNFR-1 (Idriss and Naismith, 2000; He and Ting, 2002; Micheau and Tschopp, 2003; Wajant *et al.*, 2003). Death domains are also found in a further subgroup of the TNF receptor family members (Singh *et al.*, 1998). These death receptors (DR) include the p55 receptor for TNF (TNF-R55), the CD95 molecule (Fas, Apo-1), DR3, DR6, and the two receptors for the TNF related apoptosis-inducing ligand (TRAIL), DR4 (Apo2, TRAIL-R1) and DR5 (KILLER, TRAIL-R2), although Fas ligand and TRAIL, mainly induce apoptosis on cells expressing their receptors (Luschen *et al.*, 2000).

I.2 Cancer

Cancer is a highly complex and heterogeneous disease. According to estimations by the World Health Organization (WHO), more than 100 different types of cancers and respective subtypes have been described. Each type is a clinically distinct disease, but they share the ability to grow in an uncontrolled way, resulting in the formation of an unstructured tissue mass called a tumor. The fact that not all developed tumors are dangerous is used to distinguish two classes: benign and malignant cancers. Benign cancers are those which proliferate, but do not invade the adjacent tissue. They are rarely life-threatening if they can be removed surgically. On the other hand, malignant cancers grow and penetrate adjacent tissues. When infiltrating into the blood stream, they can form new tumors in areas very distant from their place of origin. This behavior is called metastatic potential and describes the aggressiveness of the corresponding cancer. Worldwide, metastasizing cancers are responsible for 90% of cancer associated deaths. Among them, carcinomas (epithelial cancer) are the most common and aggressive types accounting for 80% of cancer-related deaths (Parkin *et al.*, 2001).

Hanahan and Weinberg reviewed in 2000 six crucial steps in the transformation process of a normal to a malignant cell (Hanahan and Weinberg, 2000). The ‘hallmarks of cancer’ are alterations in cell physiology that constitutively influence malignant cell growth (Figure 2). All of these physiological changes are novel capabilities acquired during tumor development. They represent the successful suppression of an anticancer defence mechanism tightly

connected to cells and tissues. The mechanistic pathways vary from cell to cell, and not all six hallmarks have to be fulfilled in each malignant cellular transformation.

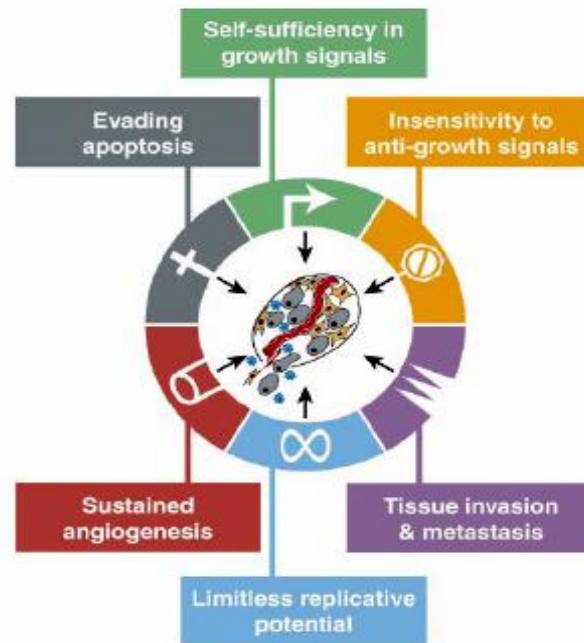


Figure 2- **Acquired capabilities of cancer** (Hanahan and Weinberg, 2000).

I.2.1 Apoptosis and Cancer

Cancer is a disorder that can be characterized by uncontrolled cell division and/or the cellular resistance to apoptosis. Apoptosis is a physiological process that occurs in all tissues and under a variety of circumstances. The balance between normal cell division, differentiation and apoptosis is tightly regulated in order to ensure the integrity of organs and tissues. The inactivation of programmed cell death has profound effects, not only on the development but also on the overall integrity of multicellular organisms. Beside developmental abnormalities, it may lead to tumorigenesis and other serious health problems. The idea that tumor development and progression could be influenced by apoptosis goes back to Kerr, Wyllie and Currie's original 1972 paper, in which they showed that the observed growth rate of tumors was less than the predicted rate as a result of a high level of endogenous tumor cell apoptosis (Crawford *et al.*, 1972; Kerr *et al.*, 1972). Subsequent studies showed that apoptosis played an integral part in tumor growth, progression and resistance to therapy (Kerr *et al.*, 1994). The average adult human body generated approximately 6×10^9 cells per day, and, consequently,

an equal number of cells must die by apoptosis in order to maintain cellular homeostasis. Therefore, it was not surprising that deregulation of apoptosis could lead to an accumulation of living cells and contribute to tumor development (Cotter, 2009). Members of the Bcl-2 family and many other oncogenes and tumor suppressor genes, such as *Myc* and *TP53*, were implicated in the regulation of apoptosis in different types of cancers, including breast cancer. Deregulated apoptosis may also be the leading cause of cancer therapy chemoresistance.

I.2.2 Breast cancer

Different types of cancers are named based on the part of the body from which they originate. Thus, breast cancer is a pathological condition in which this uncontrolled cell division has started in breast tissue (Figure 3). Breast cancer is, in turn, classified into different types based on the cellular location of the tumor.

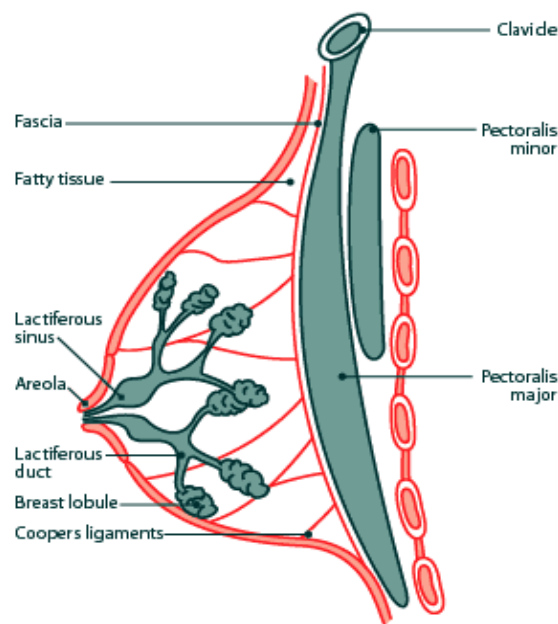


Figure 3- **The anatomy of breast tissue.** (www.breastcancersource.com)

Breast cancer is the most common malignant tumor in women, both worldwide and in the high-income countries, as defined by the World Bank. According to estimations by the WHO, breast cancer leads to more than 500,000 deaths per year in the world, and belongs to the top ten mortal diseases. Besides the large number of cases, breast carcinoma is also among the most heterogeneous types of cancer: first, in terms of the clinical course and classification; second, in terms of the cellular and genetic background of the actual tumor mass. Successful treatment of patients with primary breast carcinoma is therefore highly dependent on an in-

depth characterization of each individual case. A more profound examination, e.g. concerning the local spread, the tissue of origin (ductal, lobular, and others), the estrogen and progesterone hormone receptor status, as well as a detailed histochemical characterization of expressed proteins like Her2/Neu, P53, Bcl-2 (apoptosis marker) or the proliferation marker Ki67, is today's clinical standard (Urruticoechea *et al.*, 2005). Several genes such as *BRCA1/2*, *PTEN*, *LKB1*, *ATM*, *PALB2* and *CHEK2* are also proposed to contribute to breast cancer (Domchek and Weber, 2006; Renwick *et al.*, 2006; Rahman *et al.*, 2007).

I.2.2.1 Breast cancer and apoptosis

Since 1990, death rates from breast cancer have decreased by over 25%. This is at least in part due to the improved use of adjuvant chemotherapy. Apoptosis plays a key role in the development of the normal breast. Normal breast development is controlled by a balance between cell proliferation and apoptosis, and there is strong evidence that tumor growth is not just a result of uncontrolled proliferation, but also of reduced apoptosis. Dysregulation overrides many of the normal checkpoint pathways and leads to expansion of neoplastic cells. The balance between proliferation and apoptosis is also crucial in determining the overall growth or regression of the tumor in response to chemotherapy, radiotherapy and, more recently, hormone treatments (Reed, 1999; Tamm *et al.*, 2001). Apoptosis is induced by chemotherapy, endocrine treatment, and radiotherapy. When these treatments fail, dysregulation of apoptosis may be a cause for cancer development. Genes and proteins that control apoptosis have become targets for manipulation in order to enhance the cancer cell death. Understanding these relations could allow individually tailored treatments to maximize tumor regression and increase the efficacy of treatment. It could also help answer why some tumors fail to respond, thereby indicating new routes of drug development (Parton *et al.*, 2001).

I.3 RNA interference

RNA interference (RNAi) is a universal and evolutionary conserved post-translational regulatory system within living cells that helps to control which, and in what way, genes are active. RNAi has been discovered as a mechanism that can be exploited as a valuable experimental tool, leading to efficient sequence-specific gene silencing, thus allowing functional gene analysis (Fire *et al.*, 1998). In the RNAi process, double-stranded RNA (dsRNA), homologous to the target locus, can specifically inactivate gene function (Hannon,

2002). RNA interference can be experimentally achieved by delivery of a synthetic small interfering RNA (siRNA) (Elbashir *et al.*, 2001a) or by a plasmid DNA vector containing sequence coding for a small hairpin RNA (shRNA) (Brummelkamp *et al.*, 2002; Elbashir *et al.*, 2002; Paddison *et al.*, 2002). Both siRNAs and shRNAs are currently being tested in clinical trials against conditions in which an overactive gene needs to be silenced (Check, 2007).

I.3.1 RNA interference mechanism

The RNAi mechanism is the disruption of a gene's expression by a double stranded RNA (dsRNA) in which one strand is complementary to a section of the gene's mRNA. Figure 4 presents an overview of the RNAi pathway. In an RNAi assay, dsRNAs are introduced into the cell. In the cytoplasm, they are processed by an enzyme of the Dicer family into 21-23 bp fragments called small interfering RNAs (siRNAs) (Elbashir *et al.*, 2001b). Next, the siRNAs are used as targeting co-factors by RISC, which binds to and destroys complementary mRNAs catalytically. In fruit flies and mammals, the antisense strand is directly incorporated into the RISC and activates it. In worms and plants the antisense strand might first be used in an amplification process, in which new long dsRNAs are synthesized, which are again cleaved by Dicer. Finally, antisense siRNA strands guide the RISCs to complementary RNA molecules, where they cleave and destroy the cognate target RNA. This process leaves the genomic DNA intact but suppresses gene expression by RNA degradation. Key components of the RNAi pathway have also been implicated in the processing of the novel class of molecules called microRNAs (miRNAs), which are emerging as key endogenous regulators of gene expression during development (Elbashir *et al.*, 2001b). MicroRNAs are initially transcribed as long RNAs, and are processed in the nucleus by the RNase III enzyme Drosha into a pre-miRNA of about 70 nucleotides (nt). The pre-miRNA, which forms an imperfect hairpin structure, is bound by Exportin-5 and exported into the cytoplasm where Dicer further processes it into a mature, single-stranded miRNA. MiRNAs from animals appear to regulate gene expression by binding to partially complementary sequences in the 3' untranslated regions (UTRs) of target mRNAs and suppressing translation (Lund *et al.*, 2004).

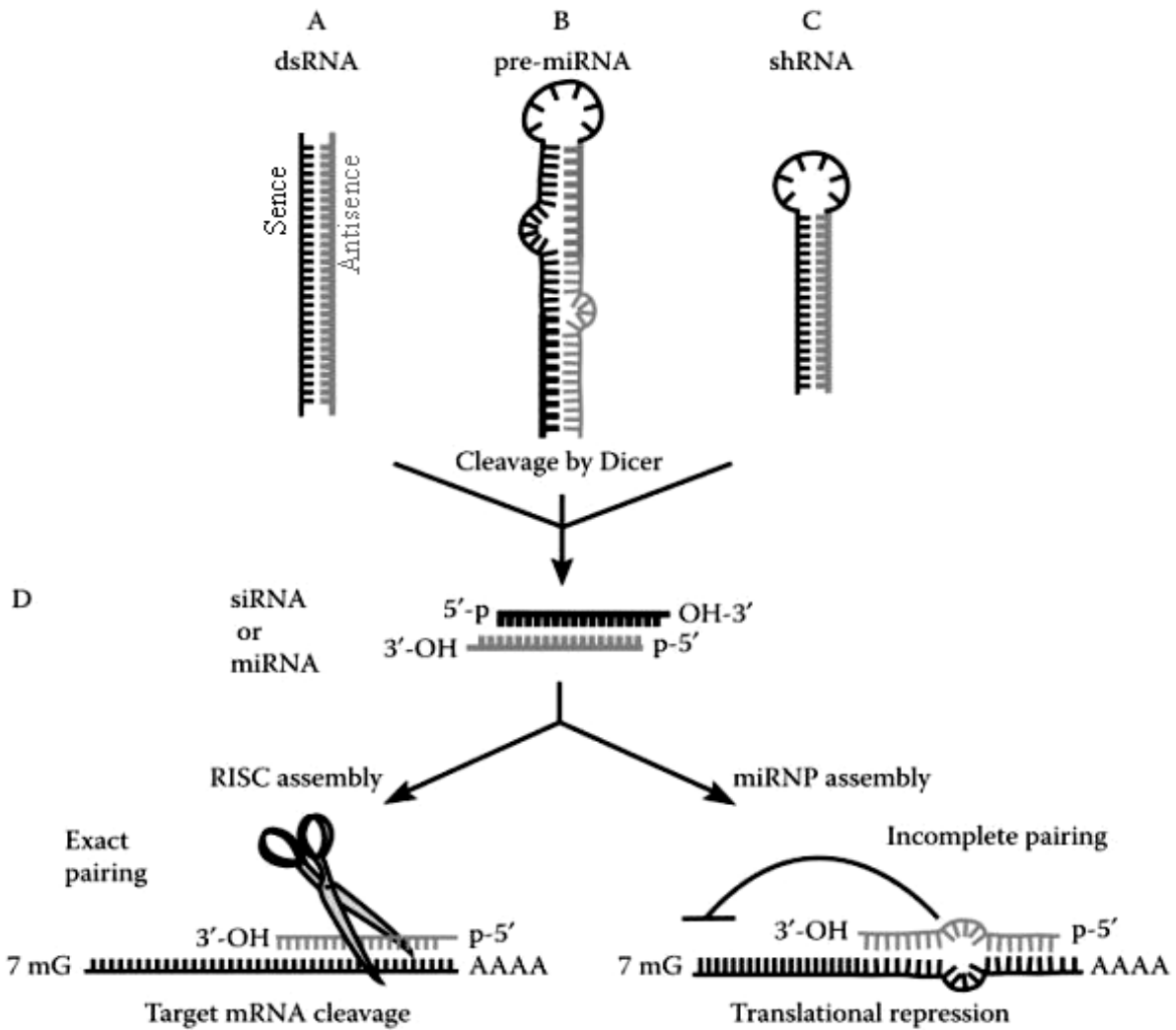


Figure 4- **The RNAi pathway.** Sources for RNA-induced gene silencing include (a) dsRNAs, (b) miRNAs, (c) shRNAs and (d) chemically synthesized siRNAs. Dicer processes dsRNAs, pre-miRNAs and shRNAs into siRNA/miRNA duplexes containing 5' monophosphate groups and 2-nt 3' overhangs. Next, these duplexes are unwound and incorporated into the appropriate effector complex (RISC/miRNP). The degree of pairing between the siRNA/miRNA and the target mRNA appears to determine whether silencing occurs via mRNA degradation or translational repression. 7 mG, 7-methyl guanine; AAAAA, poly-adenosine tail (Kittler and Moss, 2006).

I.3.2 Applications of RNA interference

The success of this basic methodology has led to the rapid, widespread adoption of RNAi as the new method for targeted gene silencing in a wide variety of experimental systems from *C. elegans* to human cells. RNAi is prominent in functional genomics research for two reasons. The first one is the physiological role of RNAi in gene regulation. The second reason is that screens resulting in the inhibition of target genes by RNAi can be applied on a broader scale, thus allowing the rapid identification of genes whose modulation contributes to changes in

cellular processes and pathways (Mello and Conte, 2004). RNAi has become widely used for knocking-down the expression of a specific target gene by a posttranscriptional silencing mechanism, thereby allowing phenotypic analysis of gene function in cells of different organisms (Kamath and Ahringer, 2003; Kiger *et al.*, 2003; Lettre *et al.*, 2004). Unfortunately, the high cost of genome-wide libraries of chemically synthesized 21mers necessary for RNAi (Figure 5a, b) in human cells (Elbashir *et al.*, 2001b) has, so far, limited screens to small targeted libraries of several hundred genes, at most (Aza-Blanc *et al.*, 2003). The alternative technology of short hairpin RNAi (Figure 5e, f) has been applied in different assays, such as luminescence assays (Zheng *et al.*, 2004).

The high activity, long protein half-life and high endogenous expression of some genes might make it difficult to generate detectable loss-of-function phenotypes by RNAi, especially in the case of certain enzymes, as residual activity might be sufficient for the enzymes to fulfil their cellular roles (Boutros and Ahringer, 2008). Importantly, using multiple siRNAs for the same target gene theoretically increases silencing from 70% to 95%. Although the concept of using such a pool of siRNAs (Figure 5c-d) is attractive for achieving a higher probability of strong silencing in fewer experimental samples, it is assumed that the silencing performance of the pool is at least as good as the individual siRNAs (Echeverri and Perrimon, 2006).

Previous studies have shown that RNAi screening studies are powerful approaches to identify genes involved in biological processes, such as cell division, proteasome- and p53 function (Lettre *et al.*, 2004; Nollen *et al.*, 2004; Kittler *et al.*, 2007; Rines *et al.*, 2008). Recently, RNAi techniques have been used to study entire sets of kinases and phosphatases that regulate various signaling pathways involved in cell survival and apoptosis (MacKeigan *et al.*, 2005; Mattila *et al.*, 2008). In addition, RNAi screening by time-lapse imaging of living cells provides a great advantage in discriminating the primary immediate phenotype caused by gene suppression from a secondary cellular response (Neumann *et al.*, 2006). The beneficial or detrimental effects of siRNA or shRNA inhibition of specific genes and the induction of phenotypic changes in affected cells are analyzed using various means, including pharmacological, histological and biochemical assays.

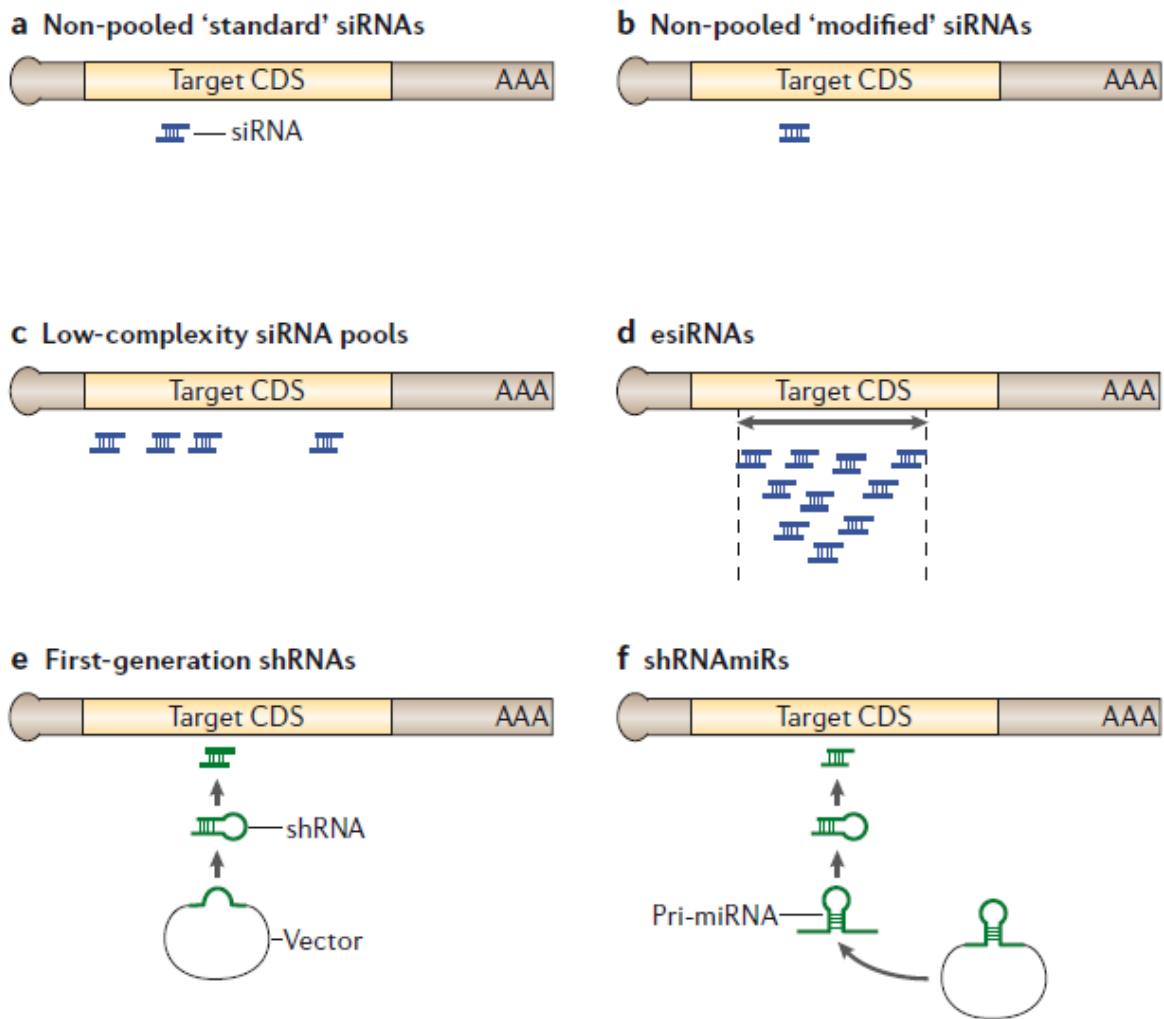


Figure 5- **Silencing reagents for RNAi screens in mammalian cells.** Publicly available libraries of silencing reagents enable genome-scale RNAi screens in mammalian cells using the following types of molecules. (a) The most widely used small interfering RNAs (siRNAs) are synthetic molecules with a canonical structure that consists of a 19-bp duplex with 2-base overhangs at the 3' ends and an unmodified RNA backbone (these are supplied by various companies, for example Ambion, Dharmacon and Qiagen). (b) Alternatively, synthetic siRNAs with non-canonical siRNA structures (an siRNA with no overhangs is shown) and/or a modified RNA backbone are also available (for example, the Stealth siRNAs from invitrogen) (c) siRNAs can also be used as low-complexity pools of <10 molecules that target the same transcript (for example, SmartPools from Dharmacon). (d) High-complexity pools of siRNA-like molecules (esiRNAs) can be synthesized by *in vitro* digestion of long dsRNAs using bacterial RNase III or Dicer. (e) As an alternative to these synthetic molecules, vector-based library reagents are also available, all expressing short hairpin RNA (shRNA) constructs, which are usually delivered virally. Most vector-based shRNA libraries carry a single RNase III-driven shRNA insert. (f) A new vector design now offers an RNase II- or RNase III-driven shRNA insert within a backbone from a known miR, producing so-called 'shRNAmiRs' that enter the RNAi pathway as pri-miRNAs, upstream from conventional shRNAs. CDS, coding sequence (Echeverri and Perrimon, 2006).

I.4 Reverse transfection cell array

The application of microarray-based technology for molecule genetic analysis has revolutionized the study of certain aspects of gene function. DNA microarrays allow high-throughput analysis of gene expression, and thus a technology for identifying genes whose modulation are potentially involved in particular cellular processes. However, DNA microarrays do not provide a direct analysis of gene product function within the living cell, and such functional analyses are often performed singly, on a one by one basis.

In 2001, Ziauddin and Sabatini established a method for miniaturization of cell-based functional studies called “reverse transfection cell microarray” (Figure 6) (Ziauddin and Sabatini, 2001). The term *reverse* was used because the order of addition of the target cells and DNA to the surface is reversed compared to conventional transfections. This technology allows spatially restricted transfection without the use of wells by immobilizing nucleic acids complexed together with a transfection reagent in a gel matrix spot. Adherent cells growing on top of such printed spots will take up the nucleic acids deposited in the spot, while cells growing between the spots will not be transfected. As contact between DNA and the target cells is a requirement for successful transfection, immobilizing DNA particles prior to the attachment of target cells can lead to higher transfection efficiencies (Webb *et al.*, 2003).

Merging of surface-mediated transfection technology with DNA microarray technology provided a method for simultaneously screening large numbers of genes using surface-mediated transfection of arrayed libraries of cDNAs, siRNAs and shRNAs (Ziauddin and Sabatini, 2001; Mousses *et al.*, 2003; Wheeler *et al.*, 2005; Mannherz *et al.*, 2006; Moffat *et al.*, 2006).

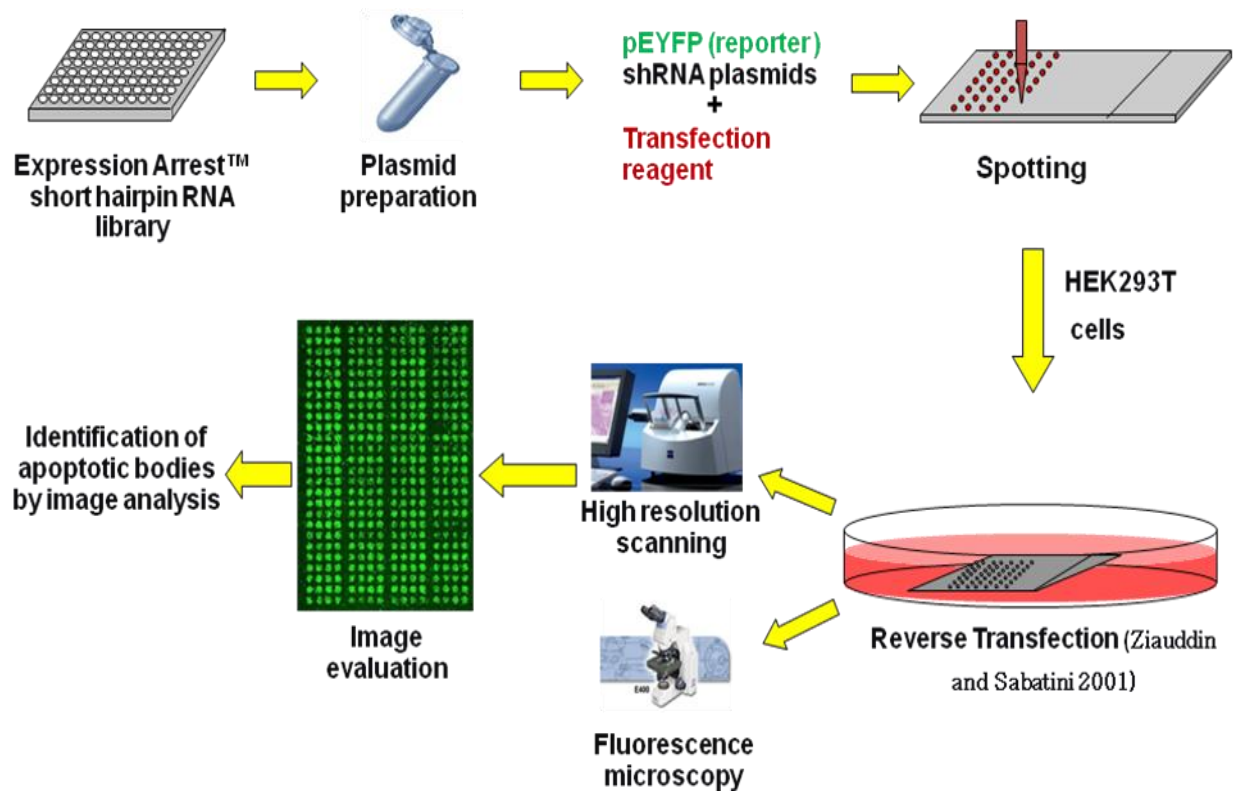


Figure 6- **Reverse transfection cell array scheme.** This method involves spotting of siRNAs, shRNAs or cDNA vectors, complexed with a transfection reagent and a reporter plasmid such as pEYFP on standard glass slides. These slides are then exposed to cells in culture, allowing transfection of the nucleic acids into the cells in contact with the spots. Thereafter, a cell-based assay, for example the presence of apoptotic bodies, is used to monitor the effects caused by the transfected molecule.

I.5 Aim of this project

The aim of this project was the identification and characterization of human genes with possible capability to inhibit apoptosis in normal and tumorigenic cell lines.

In the first part of the study, in order to identify novel human anti-apoptotic factors in non-tumorigenic human embryonic kidney (HEK293T) cells, a loss-of-function screen through transient transfection of shRNA-coding plasmids targeting a set of poorly characterized genes, was the method of choice. In the second part of the study, an RNA interference approach using siRNAs was used to identify anti-apoptotic candidates among genes which were over-expressed in human breast cancer patients who were resistant to chemotherapy. In this study, MCF7 breast cancer cells were selected as a cancer model to study the effect of silencing of the genes.

Loss of function screen in HEK293T cells would help to uncover novel factors involved in apoptosis pathways while screen of candidate genes in the second part may lead to identification of genes important for survival and proliferation of cancer cells leading to possible new strategies for treatment of breast cancer.

II Materials and methods

II.1 Materials

II.1.1 Instruments

| <i>REAGENT</i> | <i>PURCHASED FROM</i> |
|---|--|
| 7900 HT Fast Real Time PCR Systems | Applied Biosystems, Forster city, USA |
| ABI PRISM 3100 Genetic Analyzer, 16 Capillary DNA Sequencer | Applied Biosystems, Forster city, USA |
| ABI PRISM 7900 Sequence Detection System | Applied Biosystems, Forster city, USA |
| Automatic developing machine | Amersham, Freiburg, Germany |
| BD FACS Array™ Bioanalyzer System | BD Bioscience, San Jose, USA |
| BD FACSCanto II workstation | BD Bioscience, San Jose, USA |
| BD FACSCalibur workstation | BD Bioscience, San Jose, USA |
| Beckman GS-6KR centrifuge | Beckmann, Wiesloch, Germany |
| Biofuge 13R, Biofuge Fresco, Biofuge pico | Heraeus, Kendro, Hanau, Germany |
| Centrifuge 5810 R | Eppendorf, Hamburg, Germany |
| Bacterial incubator | Heraeus, Kendro, Hanau, Germany |
| Cell culture incubator | Köttermann, Hänigsen, Germany |
| Cell culture microscope | Carl Zeiss, Jena, Germany |
| Centrifuge 580R | Eppendorf, Hamburg, Germany |
| Coverslip | R. Langenbrinck, Teningen, Germany |
| CCD camera ORCA-ER-1394 | Hamamatsu Photonics K.K, Japan |
| EL800 Universal Microplate Reader | BIO-TEK, VT, USA |
| Electrophoresis power supply | E-C Apparatus Corporation, USA |
| Fluorescence Microscope Axioplan | Carl Zeiss, Jena, Germany |
| GenePix 4000A microarray scanner | Axon Instruments, CA, USA |
| GSA- and SS34- Rotor | DuPont, Boston, USA |
| Heat Block QBT2 | Grant Instruments/CLF, Emersacker |
| Incubation chamber Hybri-Well | Sigma-Aldrich, Munich, Germany |
| LB-940 Mithras Multilabel Reader | Berthold Technologies, Bad Wildbach, Germany |
| Mastercycler PCR-Maschine | Eppendorf, Cologne, Germany |
| Micro-centrifuge | NeoLab Laborbedarf, Heidelberg, Germany |
| Mini-Protein 3 gel and electrophoresis system | Bio-Rad Laboratories, Munich, Germany |
| Multifuge 3SR | Heraeus, Kendro, Hanau, Germany |
| NanoDrop ND-100 Spectrophotometer | NanoDrop Technologies, San Diego, USA |
| Omnigrid Microarrayer | GeneMachines, San Carlos, USA |
| Poly-L-lysine-coated Poly-Prep Slides | Sigma-Aldrich, Munich, Germany |
| QuadriPERM plates | Vivascience, Hannover, Germany |
| Speedvac concentrator apparatus | Eppendorf, Cologne, Germany |
| Spotting pins | TeleChem International, Sunnyvale, USA |
| Thermomixer compact | Eppendorf, Cologne, Germany |
| Unimax 1010 Shaker | Heidolph Instruments, Schwabach, Germany |
| Vortex | Scientific Industries Genie-2, New York, USA |
| Water bath SW22 | Julabo Labortechnik, Seelbach, Germany |

II.1.2 Chemical reagents and general materials

| REAGENT | PURCHASED FROM |
|---|--|
| Acrylamide (30% w/v)/Bisacrylamide (29/1 0.8%) | Bio-Rad Laboratories, Munich, Germany |
| Agarose | Sigma-Aldrich, Munich, Germany |
| Ammonium peroxydisulfate (APS) | Sigma-Aldrich, Munich, Germany |
| Ampicillin | Sigma-Aldrich, Munich, Germany |
| Bacto-agar | Difco Laboratories, Detroit, USA |
| Bovine serum albumin (BSA) | Sigma-Aldrich, Munich, Germany |
| Bacto-trypton | Difco Laboratories, Detroit, USA |
| Bacto-yeast -extract | Difco Laboratories, Detroit, USA |
| Bromphenol blue | Sigma-Aldrich, Munich, Germany |
| Blocking-Reagent | Roche Diagnostics, Mannheim, Germany |
| 2-Mercaptoethanol | Roche Diagnostics, Mannheim, Germany |
| Chloroform | Merk, Darmstadt, Germany |
| Cy3-streptavidin | Amersham Bioscience, Buckinghamshire, UK |
| Chloramphenicol | Sigma-Aldrich, Munich, Germany |
| Desoxynucleotide –Set (dATP, dGTP, dCTP, dATP) | Roche Diagnostics, Mannheim, Germany |
| Dithiothreitol (DTT) | Sigma-Aldrich, Munich, Germany |
| Dimethylsulfoxide (DMSO) | Sigma-Aldrich, Munich, Germany |
| Ethylenediaminetetraacetic acid-disodium salt (EDTA) | Merk, Darmstadt, Germany |
| Ethanol | Merk, Darmstadt, Germany |
| Ethidiumbromide | Sigma-Aldrich, Munich, Germany |
| Etoposide | Sigma-Aldrich, Munich, Germany |
| Formamide | Merk, Darmstadt, Germany |
| FasL | BD Bioscience, Heidelberg, Germany |
| Gelatin | Sigma-Aldrich, Munich, Germany |
| Glycerin | Roth, Karlsruhe, Germany |
| Halt™ protease and phosphatase inhibitor single-use cocktail, EDTA-free | Thermo Scientific, Rockford, USA |
| Kanamycin | Roche Diagnostic, Mannheim, Germany |
| Magnesiumchloride | Merk, Darmstadt, Germany |
| Methanol | Merk, Darmstadt, Germany |
| Milk powder | Sigma-Aldrich, Munich, Germany |
| Na ₂ HPO ₄ | Merk, Darmstadt, Germany |
| NaH ₂ PO ₄ | Merk, Darmstadt, Germany |
| NaOH | Merk, Darmstadt, Germany |
| Natriumacetat | Merk, Darmstadt, Germany |
| Natriumchloride | Merk, Darmstadt, Germany |
| Natriumcitrate | Merk, Darmstadt, Germany |
| Methanol | Merk, Darmstadt, Germany |
| Nuclease free water | Ambion, Austin, USA |

| | |
|---|--|
| Propidium iodide (PI) | Invitrogen, Karlsruhe, Germany |
| QIAzol | Qiagen, Hilden, Germany |
| Rainbow Molecular Weight Marker | Amersham, Freiburg, Germany |
| SDS | Sigma-Aldrich, Munich, Germany |
| TEMED | Bio-Rad Laboratories, Munich, Germany |
| Tris-(hydroxymethyl)-aminomethane (Tris) | Sigma-Aldrich, Munich, Germany |
| Tris-Base | Sigma-Aldrich, Munich, Germany |
| Triton-X100 | Sigma-Aldrich, Munich, Germany |
| Tween 20 (Polyoxy-ethylen-sorbitan-monolaurate) | Sigma-Aldrich, Munich, Germany |
| TNF α | Calbiochem, Darmstadt, Germany |
| Vectashield mounting medium containing DAPI | Vector Laboratories, Burlingame, CA, USA |
| z-VAD-FMK | Calbiochem, Darmstadt, Germany |

II.1.3 Cell Culture

| REAGENT | SOURCE |
|--|---|
| DMEM | Gibco BRL/ Invitrogen, Karlsruhe, Germany |
| Foetal calf serum (FCS) | Biochrom, Berlin, Germany |
| Phosphate buffered saline (PBS) | Gibco BRL/ Invitrogen Karlsruhe, Germany |
| Penicillin 1000u/ml Streptomycin 100 μ g/ml | Gibco BRL/ Invitrogen Karlsruhe, Germany |

II.1.4 Kits

| ITEMS | SOURCE |
|---|--|
| Absolute qPCR Green Mixes | ABgene, Epsome, UK |
| All Prep RNA Protein Kit | Qiagen, Hilden, Germany |
| Caspase-Glo3/7 assay | Promega, Karlsruhe, Germany |
| Caspase-Glo8 assay | Promega, Karlsruhe, Germany |
| Caspase-Glo9 assay | Promega, Karlsruhe, Germany |
| Big Dye Terminator Sequencing Kit | Applied Biosystems, Forster City, USA |
| Effectene Transfection Reagent | Qiagen, Hilden, Germany |
| ECL + Western Blot Detection Kit | GE Healthcare Europe GmbH, Freiburg, Germany |
| ECL Hyperfilm | GE Healthcare Europe GmbH, Freiburg, Germany |
| Plasmid Mini Kit | Qiagen, Hilden, Germany |
| Dual-Luciferase Assay Reporter System | Promega, Karlsruhe, Germany |
| RNeasy mini Kit | Qiagen, Hilden, Germany |
| siPORT™ NeoFX™ | Ambion, Austin, USA |
| Pierce BCA Protein Assay Kit – Reducing Agent Compatible Kit. | Thermo Scientific, Rockford, USA |

II.1.5 Antibodies

| <i>ANTIBODIES</i> | <i>SOURCE</i> | <i>DILUTIONS</i> |
|--|--|------------------|
| APC anti-human TNF receptor 1 | BD Bioscience, Heidelberg, Germany | 1:200 |
| Mouse IgG1 antibody | BD Bioscience, Heidelberg, Germany | 1:1000 |
| PE anti-human CD95 | BD Bioscience, Heidelberg, Germany | 1:1000 |
| Rabbit anti-human PPP1R15B | Sigma-Aldrich, Munich, Germany | 1:500 |
| Mouse anti-human P53 | Prof. Dr. H. Zentgraf DKFZ, Heidelberg | 1:2000 |
| Mouse anti-human Lamin B1 | Santa Cruz Biotechnology, CA, USA | 1:1000 |
| Mouse anti-human GAPDH | Calbiochem, Darmstadt, Germany | 1:5000 |
| Anti-rabbit IgG, HRP-linked Antibody | Cell Signaling Inc, Danvers, USA | 1:5000 |
| Anti-mouse IgG, HRP-linked Antibody | Cell Signaling Inc, Danvers, USA | 1:5000 |
| SAv-APC (Streptavidin-Allophycocyanin) | BD Bioscience, Heidelberg, Germany | 1:200 |

II.1.6 sh-RNAs and plasmid DNA

| <i>SH-RNAS AND PLASMID DNA</i> | <i>SOURCE</i> |
|----------------------------------|--|
| Expression Arrest™ shRNA library | Open Biosystems, Huntsville, USA. Table5 (supplementary) |
| sh-Birc4 (1) | Open Biosystems, Huntsville, USA. V2HS_94574 |
| sh-Birc4 (2) | Open Biosystems, Huntsville, USA. V2HS_94579 |
| sh-Birc5(1) | Open Biosystems, Huntsville, USA. V2HS_94583 |
| sh-Birc5(2) | Open Biosystems, Huntsville, USA. V2HS_94582 |
| sh-Birc7(1) | Open Biosystems, Huntsville, USA. V2HS_200958 |
| sh-Birc7(2) | Open Biosystems, Huntsville, USA. V2HS_5714 |
| sh-TP53 | Open Biosystems, Huntsville, USA. V2HS_93615 |
| sh-LMNB1 | Open Biosystems, Huntsville, USA. V2HS_62672 |
| sh-GFP | Open Biosystems, Huntsville, USA. RHS4459 |
| pCMV6-XL5-CHMP5 | OriGene, Technologies Inc, Rockville, USA |
| pCMV6-XL5-Birc4 | OriGene, Technologies Inc, Rockville, USA |

| | |
|----------------------|---|
| pCMV6-XL5 | OriGene, Technologies Inc, Rockville, USA |
| NFκB-luc pGL3 | Dr. Min Li-Weber DKFZ, Heidelberg (Li-Weber <i>et al.</i> , 1998) |
| pTK-RL | Dr. Stefanie Heck DKFZ, Heidelberg |
| pSUPEdL | Pscherer <i>et al.</i> , 2006 (Pscherer <i>et al.</i> , 2006) |
| FLIP cDNA expression | Dr. Ina Lavrik Division of Immunogenetics, DKFZ Heidelberg |
| pEYFP-C1 | BD Biosciences Clontech, Palo Alto, CA, USA |

II.1.7 Oligonucleotides Primers

| PRIMER NAME | SEQUENCE |
|----------------------|--|
| PGK1 forward | 5'-AAGTGAAGCTCGGAAAGCTTCTAT-3' |
| PGK1 reverse | 5'-TGGGAAAAGATGCTTCTGGG-3' |
| LAMINB1 forward | 5'-CTGGAAATGTTT GCATCGAAGA-3' |
| LAMINB1 reverse | 5'-GCCTCCCATGGTTGATCC-3' |
| GAPDH | Qiagen, Hilden, Germany (no sequence available) (Cat. #: QT00079247) |
| CHMP5 forward | 5'-GGAAAGCGAAACCCAAGG-3', |
| CHMP5 reverse | 5'-TGGATTCTGCTCTACTGTCCAC-3' |
| BIRC4 forward | 5'-GGCGCGAAAAGGTGGACAAGTCCT-3' |
| BIRC4 reverse | 5'-CCTTATTGATGTCTGCAGGTACAC-3' |
| FLIP forward | 5'-GCTCACCATCCCTGTACCTG-3' |
| FLIP reverse | 5'-CAGGAGTGGGCGTTTTCTT-3' |
| PPP1R15B forward | 5'-TCGGTACAGCGTGACGTTTC-3' |
| PPP1R15B reverse | 5'-GCGATCCTCATCACCCTTAT-3' |
| U6 sequencing primer | 5'-GACTATCATATGCTTACCGT-3' |

II.1.8 siRNAs

| SI-RNA NAME | SOURCE |
|------------------------------|-------------------------------------|
| CHMP5-siRNA 1 | Qiagen, Hilden, Germany, SI00728098 |
| CHMP5-siRNA 2 | Qiagen, Hilden, Germany, SI03187905 |
| Birc4-siRNA | Qiagen, Hilden, Germany, SI00299446 |
| Birc5-siRNA | Qiagen, Hilden, Germany, SI00299453 |
| Birc7-siRNA | Qiagen, Hilden, Germany, SI02645111 |
| GFP-siRNA | Ambion, Austin, USA, AM4626 |
| GFP-siRNA | Qiagen, Hilden, Germany, SI3650346 |
| “All stars“ negative control | Qiagen, Hilden, Germany, SI1027280 |
| FLIP-siRNA | Qiagen, Hilden, Germany, SI00057218 |
| PPP1R15B-siRNA 1 | Qiagen, Hilden, Germany, SI03045462 |

| | |
|------------------------------|---|
| PPP1R15B-siRNA 2 | Qiagen, Hilden, Germany, SI03050257 |
| PPP1R15B-siRNA 3 | Qiagen, Hilden, Germany, SI03087245 |
| PPP1R15B-siRNA 4 | Qiagen, Hilden, Germany, SI03079923 |
| 107 siRNA pool for screening | Qiagen, Hilden, Germany, Hilden, Germany. Prof. Michael Boutros, DKFZ, Germany (Table 6 Supplementary) |

II.1.9 Cell lines

| <i>CELL LINES</i> | <i>CELLULAR ORIGIN</i> | <i>SOURCE</i> |
|-------------------|------------------------|---|
| HEK293T | embryonic kidney | HEK293T cells transformed with the SV40 Large T Antigen (ATCC CRL-1573) |
| MCF7 | breast | Human breast cancer cell line (ATCC HTB-22) |
| EVSAT | breast | Prof. Peter Altevogt DKFZ, Germany |
| MDA-MB231 | breast | Prof. Peter Altevogt DKFZ, Germany |
| MDA-MB435 | breast | Prof. Peter Altevogt DKFZ, Germany |
| SKBR3 | breast | Prof. Peter Altevogt DKFZ, Germany |
| T47D | breast | Prof. Peter Altevogt DKFZ, Germany |
| HDQP1 | breast | Prof. Peter Altevogt DKFZ, Germany |

II.1.10 Media, Solutions and Buffers

| <i>MEDIA, SOLUTIONS AND BUFFERS</i> | <i>COMPONENTS</i> |
|-------------------------------------|---|
| APS | 10% APS w/v in ddH ₂ O |
| LB Medium | 1 % (W/V) Bacto-Trypton 0.5 % (W/V) Bacto-Yeast –Extract 1 % (W/V) NaCl In H ₂ O, pH = 7.5 Autoclave at 121°C and 1000hPa for 20 min |
| S.O.C. Medium | 2% trypton 0.5% yeast extract 10 mM NaCl 2.5 mM KCL 10 mM MgCL ₂ 10 mM MgSO ₄ 20 mM glucose |

Materials and methods

| | |
|-------------------------------------|--|
| 10x PBS | 137 mM NaCl 27 mM KCl 100 mM NaH ₂ PO ₄ 17 mM KH ₂ PO ₄ dissolve in ddH ₂ O |
| 1x TBS-T | 20 mM Tris-Base 137 mM NaCl 3.8 ml 1M HCl 0.1% (v/v) Tween 20 dissolve in 1l ddH ₂ O |
| 5x Loading buffer | 100 mM EDTA 30% (v/v) glycerine 0.25% (w/v) bromophenolblue dissolve in ddH ₂ O |
| 20% SDS | 20% SDS (w/v) dissolve in ddH ₂ O |
| 2x Laemmli buffer | 50 mM Tris/HCl pH=8.0 2.4% w/v SDS 8% glycine 0.2% w/v bromphenol blue 2.5% v/v β-mercaptoethanol |
| 5x SDS-PAGE running buffer | 25 mM Tris-Base 200 mM glycine 10% (w/v) SDS ddH ₂ O |
| 10x Western blot buffer | 25 mM Tris-Base 192 mM Glycine 20% v/v methanol (added when preparing 1x buffer) ddH ₂ O |
| BSA- blocking buffer | 3% BSA in PBS |
| FACS staining buffer (DNA staining) | 0.1% (w/v) sodium citrate, pH 7.4 0.1% (v/v) Triton X-100 50 µg/ml propidium iodide in PBS |
| FACS buffer (Receptor staining) | 5%FBS 0.1% sodium azide in PBS |
| Resolving gel buffer | 1.5M Tris-Base 10% (w/v) SDS ddH ₂ O PH= 8.8 |
| Stacking gel buffer | 0,5M Tris-Base 10% (w/v) SDS ddH ₂ O PH=6.8 |

Materials and methods

| | |
|----------------------|--|
| Milk-blocking buffer | 10% Milk powder in TBS-Tween (0.1%) |
| Stripping buffer | 100 nM β -Mercaptoethanol 2% SDS 62.5 nM Tris-HCl, pH=6.7 ddH ₂ O |
| RIPA buffer | 0.5% natrium deoxycholate (w/v) 1% Nonidet P-40(v/v) 0.1% SDS(w/v) ddH ₂ O |

II.1.11 Antibiotics

| <i>NAME</i> | <i>STOCK CONCENTRATION</i> | <i>SOLVED IN</i> | <i>CONCENTRATION IN MEDIUM</i> |
|-----------------|----------------------------|------------------|--------------------------------|
| Ampicillin | 100 mg/ml | H ₂ O | 100 μ g/ml |
| Chloramphenicol | 100 mg/ml | Ethanol | 100 μ g/ml |
| Kanamycin | 100 mg/ml | H ₂ O | 100 μ g/ml |

II.2 Methods

II.2.1 General molecular biology methods

II.2.1.1 Transformation in competent bacteria

One Shot® TOP10 chemically competent *E.coli* DH10B (Invitrogen, Karlsruhe, Germany) were used to amplify plasmid DNA. 50µl of electro-competent *E.coli* were thawed on ice, mixed with the complete ligation reaction and incubated on ice for 30 minutes. Thereafter, the bacteria were shifted to 42°C for 60 s and briefly equilibrated on ice. 250-300µl of SOC medium was then added and cells were incubated for 1 h at 37°C with shaking (800 rpm). The suspension was plated onto LB-agar plates containing the respective antibiotic and incubated overnight at 37°C. In order to propagate the cultures, either single colonies were picked or frozen glycerol stocks were thawed and inoculated into 10ml LB medium with antibiotic, and shaken overnight at 37°C. For storage of bacteria, a bacterial culture was grown in culture medium to an OD of 0.8 (measured at 600nm). Thereafter, 500µl of the bacterial culture was combined together with 500µl glycerol and subsequently frozen at -80°C.

II.2.1.2 Mini-preparation of plasmid DNA

E.coli containing the plasmid of interest was inoculated in 8ml LB medium, including the appropriate antibiotics, and grown overnight at 37°C in a shaking incubator (200 rpm). Plasmid DNA was extracted using the Qiagen Plasmid Mini Kit. First, the bacteria was harvested by centrifugation for 15 min at 3500 rpm and re-suspended in 250µl buffer P1 containing 0.1mg/ml RNase A. Thereafter, 250µl of lysis buffer P2 was added and the tube inverted gently 4–6 times. 350µl neutralization buffer N3 was then added to the tube and mixed again by inversion. The resulting lysate was centrifuged for 10 minutes at maximum speed in a tabletop microcentrifuge (13,000 rpm). The supernatant from this centrifugation was added to a QIAprep spin column containing 2ml collection tube and centrifuged for one minute by 13,000 rpm. The flow-through was discarded and the column bound plasmid DNA was washed using 500µl of buffer PB, followed by centrifuging for one minute (13,000 rpm). After discarding the flow-through, the column was washed with 750µl of PE-buffer, followed by centrifuging for 1 minute (13,000 rpm). Thereafter, the column was placed into a clean 1.5ml microcentrifuge tube, 50 µl of water was added and incubated at room temperature for

one minute. The DNA was then eluted by centrifugation for 1 minute (13,000 RPM). Quantification of the DNA samples were carried out on a Nanodrop spectrophotometer using the DNA measurement setting.

II.2.1.3 RNA isolation and quality assessment

Total RNA was extracted from cells (1×10^6) in culture. The cells were harvested, washed with PBS and centrifuged for 5 minutes at 3000 rpm. The cell pellet was lysed in 1ml lysis reagent reagent (QIAzol), incubated for 5 minutes at RT, then 300 μ l chloroform was added. The mixture was mixed thoroughly and incubated for another 5 minutes at RT. Thereafter the cell lysate was centrifuged for 15 minutes in a pre-cooled centrifuge at 4°C at 13,000 rpm. The aqueous phase was placed into a fresh tube and mixed with an equal volume of 70% ethanol, transferred to a RNeasy spin column and centrifuged for one minute at 13,000rpm. The flow-through was discarded and 700 μ l of wash buffer RW1 was added, and the centrifugation and flow through removal procedure repeated. The same procedure was repeated using 500 μ l RPE wash buffer. In the end, the RNeasy spin column was placed in a new collection tube and the RNA eluted in 50 μ l nuclease free water by centrifugation at 13,000 rpm for one minute. Quantification of the RNA sample was carried out using the Nanodrop spectrophotometer using the RNA measurement settings (A260 / A280 ratio).

II.2.1.4 Protein isolation with RIPA buffer

RIPA buffer enables the extraction of cytoplasmic, membrane and nuclear proteins and is used many applications, including reporter assays, protein assays, immunoassays and protein purification. RIPA buffer does not contain protease or phosphatase inhibitors. However, if desired, protease and phosphatase inhibitors (Halt™ Protease and phosphatase inhibitor) can be added to the RIPA buffer (10 μ l/ml) just before use, in order to prevent proteolysis and to maintain the phosphorylation state of the proteins. For protein extraction, cultured cells were harvested, washed in PBS, and centrifuged (800 rpm, 10 min, RT) in order to isolate the pelleted cells. These cells were then lysed in 100 μ l of RIPA buffer incubated for 20 minutes on ice and centrifuged at 13,000 rpm for 15 minutes to remove particulate material. The supernatant containing the extracted protein was transferred to a new microcentrifuge tube and stored at -20 °C.

II.2.1.5 Protein quantification (BCA Protein Quantification)

Total protein concentration was measured using the Pierce BCA Protein Assay. The BCA assay is based on the reduction of Cu⁺² to Cu⁺¹ by protein in an alkaline medium followed by colorimetric detection of the cuprous cation using bicinchoninic acid (BCA).

BCA working reagent was prepared by mixing 50 parts of BCA Reagent A to 1 part of BCA Reagent B. 20µl of the BSA standards or samples were plated into single wells of a 96 well microtiter plate well. Thereafter, 100µl of BCA working reagent was added, the plate shaken for 30 seconds and then placed in a 37°C incubator for 30 minutes. The plate was then cooled to room temperature and the absorbance read at 562nm. A standard curve of absorbance versus micrograms of standard protein was prepared, and the protein concentration of the samples was determined from this graph.

II.2.1.6 DNA sequencing

Sequencing of DNA was performed according to the modified dideoxy-sequencing method of Sanger (Sanger *et al.*, 1977). The reaction mix (Big Dye Terminator Cycle Sequencing Kit) contained fluorescent labelled dideoxy-derivates for all of the four nucleotides (Rosenblum *et al.*, 1997), dNTPs, a specific oligonucleotide primer for the DNA to be sequenced and a thermostable DNA polymerase. Due to the initial denaturation step during the reaction, sequencing of dsDNA is possible. In this assay, 250ng of plasmid DNA and 100pmol DNA sequencing primer was mixed with 3µl of Big Dye and adjust to 10µl with water. DNA cycle sequencing was then performed using a thermocycler. The cycling conditions for the PCR amplification were: 2 minutes at 96°C, followed by 25 cycles of 5 s at 96°C, 10 s at 55°C, and 4 minutes at 60°C. After PCR amplification, the samples were precipitated at RT with 2.5 Vol. 100% ethanol and 1/10 Vol. 3M natrium-acetate, washed once with 70% ethanol, dried and resuspended in 10µl formamide. An ABI3100 Capillary DNA Sequencing Apparatus was used for DNA separation and sequence detection.

II.2.1.7 Quantitative real time -PCR primer design

PCR primers for quantitative real-time (qRT)-PCR experiments were designed with the primer design tool from Roche Applied Science: 'Universal probe library' (<https://www.roche-applied-science.com/sis/rtpcr/upl/index.jsp?id=UP030000>). Primer pairs were chosen which included at least one intron sequence in the PCR product in order to

distinguish between contaminating genomic DNA amplicons, and those resulting from amplification of the correct cDNA template.

II.2.1.8 cDNA synthesis

Reverse transcription (RT) is the transcription of RNA into single strand complementary DNA (cDNA). For the RT reaction, in a final volume of 20 μ l, 1 μ g of total RNA (in 8 μ l RNase-free water) was used together with 2 μ l of 5x 1st strand buffer (250 mM Tris-HCl, pH 8.3, 375 mM KCl, 15 mM MgCl₂) and 1 μ l (10 units) DNaseI, and incubated for 20 minutes at RT to allow digestion of genomic DNA. Thereafter, 3 μ l of Master Mix1, which contained equal parts of 25mM EDTA, dNTP mix (10mM dNTP's each), and 300ng/ μ l random hexamer primers, was added to the mix and incubated in a thermocycler, first for 10 minutes at 65°C and then for 10 minutes at 25°C. This step removed secondary structures; heat inactivated the DNaseI and allowed the annealing of primers to the RNA. 5 μ l of master mix 2 containing 5x 1st strand buffer, 0.1 M DTT and nuclease free water at a ratio of 2:2:1 was then added. The mixture was incubated initially at 42°C for 2 minutes, then 1 μ l of reverse transcriptase and 0.2 μ l of T4 gene P32 protein were added to the mixture and further incubated for 50 minutes at 42°C. Thereafter, the reaction was heat inactivated for 10 minutes at 95°C.

II.2.1.9 Real-Time PCR analysis

The PCR reaction mixture consisted of 6 μ l SYBR Green PCR mixture, 100nM forward and reverse primer and 2 μ l cDNA templates in a reaction volume of 12 μ l. A standard curve consisting of a dilution series of the Stratagene qPCR Human Reference cDNA (1:1, 1:2, 1:4, 1:8, 1:16, 1:32, 1:64, 1:128), was used to determine the efficiency of the PCR reaction. To quantify cDNA templates obtained from RNA samples, real-time PCR was performed in a 7900 HT Fast Real-Time PCR System (Applied Biosystems, Foster City, USA) with the following settings: 2 minutes at 50°C, 95°C for 15 minutes, then 40 cycles of 15 seconds at 95°C, 1 minute at 60°C. Final steps comprised 15 seconds at 95°C, 15 seconds of 60°C, and 15 seconds at 95°C. The heating ramp between the last two steps was increased to 20 minutes to obtain a melting curve of the final qRT-PCR products. This was necessary because SYBR Green fluorescence products may also be derived from side products such as primer dimers. Calculation of efficiency and relative quantification was performed using the housekeeping genes (phosphoglycerate kinase 1 (*PGKI*), lamin B1 (*LMNB1*) and Glyceraldehyde 3-phosphate dehydrogenase (*GAPDH*) as reference.

II.2.1.10 Western blot analysis

For 10% SDS-PAGE gel 10% acrylamide/bisacrylamide in resolving buffer for the resolving part and 5% acrylamide in stacking buffer for the stacking part were prepared. 0.06%(w/v) ammoniumpersulphate and 0.1%(v/v) N,N,N',N'-tetramethylethyldiamine (TEMED) were added to the gel solution to induce polymerization. Transfected cells were harvested by centrifugation (800 rpm, 10 minutes, room temperature (RT)). 6µg of the protein samples (see II.2.1.4 and II.2.1.5) were boiled in Laemmli buffer (1:1) for 5 minutes and subsequently loaded onto the slots of the gel. In addition, a protein size maker was also included. Electrophoresis of the protein gel was applied for 45 minutes at 160V and 70mA. The electrophoretic transfer of polypeptides from the polyacrylamide (PAA) gel to a polyvinylidene fluoride (PVDF) membrane was performed by using a wet gel transfer apparatus. The PVDF membrane was briefly activated in 100% methanol and soaked for 5 minutes in Western blot buffer for 10 minutes. The PAA gels were carefully removed from the electrophoresis chamber, the stacking gel was cut and the gel was soaked 3 minutes in Western blot buffer. The Western blot 'sandwich' was assembled and the transfer was carried out for 2h at 100V and 250mA in ice-cold Western blot buffer. For protein detection with antibodies, the membrane containing the separated polypeptides were placed in a tank and washed with washing buffer (15 minutes) followed by milk-blocking buffer for 1h at RT. After blocking, the membrane was incubated with diluted primary antibody over night at 4°C. After washing (3x10 minutes), the membrane was incubated with the secondary antibody conjugated with horse radish peroxidase for 1h at RT. After a further set of membrane washings (3x10 minutes), the blots were ready for enhanced chemiluminescence (ECL) protein detection (ECL Western Blot Detection Kit). The ECL substrate was prepared and the blot incubated with the solution for 1 minute in the dark at RT. The solution was then drained off, the membrane placed in a plastic foil to prevent drying, placed in a X-ray cassette and exposed to ECL film (Hyperfilm-ECL™). The exposure time of the film was between 10 seconds and 5 minutes.

II.2.1.11 Immunostaining of fixed cells

At 72 hours after transfection (see II.2.3.3), cells which had been grown on slides were washed in PBS (5 minutes) and fixed with 4% para-formaldehyde in PBS. Thereafter, the samples were permeabilized and blocked in 0.2% Triton X-100/PBS with 10% blocking serum for 1hour, then incubated with mouse monoclonal anti-P53 (1:2000) or mouse

monoclonal anti-Lamin B (1:1000;) antibodies diluted in 1% blocking serum/PBS by 37°C for 1h. After three washes (each time 5 minutes) with PBS, the cells were incubated with secondary antibody (1:5000), then washed again in PBS and air-dried. One drop of Vectashield mounting medium containing DAPI (staining of nuclei) was added and the slides were covered by coverslips. Fluorescence images were acquired by fluorescence microscopy using a CCD camera.

II.2.2 Cell culture

II.2.2.1 Cell maintenance

Cell lines were maintained at 37°C and 5% CO₂ in the following media: HEK293T, MCF-7, SKBR3, MDA-MB 231 in DMEM with 1g/l D-glucose (Invitrogen) supplemented with 10% fetal bovine serum (FBS), 100 units/ml penicillin and 100µg/ml streptomycin. All cells were routinely passaged every 2-3 days cells and diluted 1:6 in fresh medium.

II.2.2.2 Reverse transfection cell array

Reverse transfection was based on the protocol published by Ziauddin et al. (Ziauddin and Sabatini, 2001; Mannherz *et al.*, 2006). Genes of interest were targeted using shRNA plasmids from the Expression Arrest™ shRNA library. Expression Arrest™ shRNA was cloned into the pSHAG-MAGIC2 (pSM2) retroviral vector. This vector has a Murine Stem Cell Virus (MSCV) backbone and can be used for transient transfection. The vector contains different element such as U6 promoter and chloramphenicol/kanamycin bacterial selection marker. “Expression Arrest™ short hairpin” RNA constructs are expressed as human microRNA-30 (miR-30) primary transcripts. The “Expression Arrest™ Human” shRNA collection is provided in 96-well microtiter plates containing frozen stock cultures of *E. coli* (DH10bpir116) in LB broth with 8% glycerol and chloramphenicol (50µg/ml). After preparing the plasmids (II.2.1.2), 0.6µg pEYFP plasmid, Bax overexpression plasmid and 0.6µg of each shRNA plasmids (Expression Arrest™ shRNA) (II.1.6), and 1.5µl Enhancer (included in Effectene Transfection Kit) were added to 15µl EC buffer (included in Effectene Transfection Kit) containing 0.1 M sucrose. The mixture was incubated for 5 min at room temperature. Subsequently, 5µl Effectene was added and, again, incubated for 10 min at room temperature. A 1× volume of 0.4% (w/v) gelatin was mixed with the solution in order to complete the transfection master mix. The DNA–gelatin solution was arrayed in quadruplicate onto poly-L-

lysine-coated Poly-Prep slides using the Omnigrid microarrayer and SMP15B spotting pins. Dot spacing was 1000 μ m, mean spot diameter was 600 μ m for all experiments. Slides were stored at room temperature for up to four weeks in a dry and sterile atmosphere until further processing. For transfection, slides were placed in QuadriPERM plates, overlaid with 2.2×10^6 HEK293T cells, and cultured in DMEM supplemented with 10% (v/v) fetal bovine serum, 100 U/ml penicillin, and 100 μ g/ml streptomycin for 48 hrs. Cells were then fixed for 60 min at room temperature in 3.7% (w/v) paraformaldehyde in phosphate buffered saline (PBS). Fixed cells were permeabilized (0.1% sodium citrate (w/v), 0.1% (v/v) Triton X-100) in PBS for 5 min, washed two times for 5 min in PBS, overlaid with Vectashield mounting medium containing DAPI and covered with a coverslip (24 \times 40 mm). The slides were scanned with a GenePix 4000A microarray scanner in order to evaluate transfection efficiency and EYFP expression. Morphologic and nuclear changes were assessed using an Axioplan fluorescence microscope. Fluorescence images were acquired on the fluorescence microscope by using the CCD camera ORCA-ER-1394 (Mannherz *et al.*, 2006) (Figure 6, see section I.4).

II.2.2.3 Standard transfection of HEK293T cells

Chemical transient transfections using Effectene transfection reagent (Qiagen), siPORTTM NeoFXTM (Ambion) and respective amounts of plasmid DNA or siRNA were performed in 24 or 96 well plates. Effectene-based transfections were carried out in 24 well plates using 4×10^4 cells per well and 100ng/ μ l plasmid DNA in a final volume of 400 μ l culture medium. Plasmids expressing sequence verified short hairpin RNAs against 288 human poorly characterized genes were selected from the Expression ArrestTM shRNA library (Open Biosystems, see Table 5 Supplementary). Plasmids were isolated using the QIAprep Spin Miniprep Kit and quantified by spectrometry. In shRNA experiments, a plasmid coding for a shRNA against *firefly* Luciferase (Pscherer *et al.*, 2006), GFP and an expression vector containing pEYFP, were used as negative control, whereas shRNAs targeting *Birc4*, *Birc5*, *Birc7* (II.1.6) were used as positive controls. Ectopic expression was performed for CHMP5, *Birc4* using a pCMV6- expression vectors with pCMV6-XL used as negative control.

Reverse transfection using siPORTTM NeoFX involves the simultaneous transfecting and plating of cells. siPORTTM NeoFX transfection agent and siRNA are mixed, incubated, distributed to culture wells, and overlaid with cells. Transfection complexes are active and stable in the presence of serum; therefore, in the absence of a cellular stress response, there is no need to remove or replace media after transfection. In the this study, siPORTTM NeoFXTM-

based transfections were carried out in 96 well plate using 6×10^3 cells per well in a final volume of 100 μ l culture medium or 24 well plate using 4×10^4 cells per well and 50nM siRNA in a final volume of 500 μ l culture medium. Different siRNAs targeting *GFP* were used as negative control whereas siRNAs against *Birc4*, *Birc5*, *Birc7* or *FLIP* were used as positive controls (II.1.8). Two different siRNAs targeting the coding region (siRNA1-CHMP5) or the 3' UTR-region (siRNA2-CHMP5) of *CHMP5* were used for CHMP5 knock-down experiments.

II.2.2.4 Transfection of MCF7 and other breast cancer cells

For screening in breast cancer cells, 107 siRNAs ((II.1.8) Qiagen, human siRNA library) were used for transfection. Transient transfections of MCF7 cells were carried out in 96-well plates, using 6×10^3 cells per well, siPORT™ *NeoFX*™ transfection reagent and respective amounts of si-RNAs (50nM) in a final volume of 100 μ l culture medium; or 24 well plate using 4×10^4 cells per well and 50nM siRNA in a final volume of 500 μ l culture medium. Different siRNAs targeting *GFP*, luciferase and All Star Negative siRNA Control (Qiagen) were used as negative controls, whereas siRNAs against *Birc4*, *Birc5*, and *Birc7* were used as positive controls. Four different siRNAs targeting the coding region of *PPP1R15B* (siRNA-1-PPP1R15B, siRNA-2-PPP1R15B, siRNA-3-PPP1R15B, siRNA-4-PPP1R15B) were used for validation experiments (II.1.8).

II.2.3 Expression arrays

II.2.3.1 Illumina expression array

Three major expression profiling platforms (Affymetrix, Agilent, Illumina) are commercially available. In this study the Illumina platform for expression profiling has been used (service is available at core facility of DKFZ). Illumina's BeadArray technology is based on 3 μ m silica beads that self assemble in microwells on either of two substrates: fiber optic bundles or planar silica slides. When randomly assembled on one of these two substrates, the beads have a uniform spacing of ~ 5.7 μ m. Each bead is covered with hundreds of thousands of copies of a specific oligonucleotide representing one unique cDNA sequence that act as the capture sequences in the Illumina assay. Characteristics of the BeadArray technology are quality control of every single array and the high feature- redundancy (>20 x average) providing high-confidence results. The BeadChip array format used by Illumina utilizes either 6, 8, or 12

different arrays on a glass slide, which are processed simultaneously. In the current study, we applied 6 arrays/chip, each representing > 48,000 probe sequences.

II.2.3.1.1 RNA preparation and quality analysis

Total RNA from HEK293T cells at 24h, 48h, or 72h after transfection with pSM2-sh-CHMP5, pCMV6-CHMP5, sh-Luc or pCMVX plasmids were isolated using an RNeasy kit as described in (II.2.1.3). The quality of total RNA was tested on an Agilent 2100 Bioanalyzer using the total RNA Nano Chip Assay (Agilent Technologies GmbH, Germany).

II.2.3.1.2 cRNA synthesis, purification and labeling

In this step, 250 ng of total RNA was used for complementary DNA (cDNA) synthesis (II.2.1.8), followed by an amplification/ labelling step (in vitro transcription) to synthesize biotin-labeled cRNA according to the MessageAmp II aRNA Amplification kit (Ambion Inc., Austin, TX). Biotin-16-UTP was purchased from Roche Applied Science (Penzberg, Germany). The cRNA was column-purified according to TotalPrep RNA Amplification Kit's manual (Ambion, Austin, USA) and eluted in 60µl of water. The quality of cRNA was controlled using the RNA Nano Chip Assay on an Agilent 2100 Bioanalyzer and spectrophotometrically quantified using a NanoDrop spectrophotometer.

II.2.3.1.3 Probe labeling and Illumina Sentrix BeadChip array hybridization

Biotin-labelled cRNA samples for hybridization on Illumina Human Sentrix-6 BeadChip arrays (Illumina, Inc.) were prepared according to the protocol of Illumina's recommended sample labeling procedure (Eberwine et al., 1992). Hybridization was performed at 58°C, in GEX-HCB buffer (Illumina Inc., San Diego, USA) at a concentration of 50 ng cRNA/µl, unsealed in a wet chamber for 20h. Spike-in controls for low, medium and highly abundant RNAs were added, as well as mismatch control and biotinylation control oligonucleotides. The microarrays were washed twice in E1BC buffer (Ambion Inc., Austin, TX) at room temperature for 5 minutes. After blocking for 5 minutes in 4 ml of 1% (w/v) Blocker Casein in phosphate buffered saline Hammarsten grade (Pierce Biotechnology Inc., Rockford, IL), array signals were developed by a 10-minutes incubation in 2 ml of 1µg/ml Cy3-streptavidin solution and 1% blocking solution. After a final wash in E1BC buffer, the arrays were dried and scanned.

II.2.3.1.4 Scanning and data analysis

Microarray scanning was done using a Beadstation array scanner, setting adjusted to a scaling factor of 1 and PMT settings at 430. Raw data extraction was performed using the Beadarray R package (svn release 1.7.0) from bioconductor.org. Next, outliers were removed when their expression value dropped below a threshold: the median + *MAD (median absolute deviation) expression of all negative control beads. Individual bead types were also flagged as filtered when their bead replicate count dropped below 17. All data were then used for the mean expression value calculations within Beadarray. Finally, a bead type was discarded when the bead type's filter flag was set across all samples. Data analysis was carried out by variance stabilizing and robust spline normalization of the remaining signals using the algorithms from the Lumi R package (release 1.1.0 from bioconductor.org). Subsequently, values of different time points were subtracted from values of the time point zero and related negative controls. The thresholds for individual samples were determined by calculating the median value of all values within one sample and subtracting or adding the 1.5-fold standard deviation from each median value. Values higher (up-regulated) or lower (down-regulated) than each threshold defined differentially regulated genes.

II.2.3.2 Pathway analysis

II.2.3.2.1 Comprehensive gene pathway analysis

Analysis of the experimental results in the wide context of gene pathways or gene groups is an important step during data analysis. It helps to identify significant trends or changes in the data in a level above that of a single gene. Microarray data for gene expression patterns are mapped into gene or metabolic pathways with the help of the software Comprehensive Gene Pathway Analysis (CGPA) (Engel et al. *in preparation*). Pathway analysis with CGPA aims to identify the most discriminating gene pathways between two groups. For example, it helps to differentiate between two time points of equally treated samples in terms of relevant general biological processes or functions.

After performing the analysis using R, the statistical programming language, and PHP (hypertext reprocessor programming), a scored pathway list is presented to the user. The scoring procedure includes significance tests, random permutations and multiple testing adjustments. Here, pathways are scored for the relevance as well as for their degree of modulation from the most activated pathway to the most inactivated pathway, discriminating

the two groups. The visualization takes shape in a webpage (Table 7, Supplementary data).

II.2.3.2.2 Ingenuity pathway analysis

For Ingenuity Pathways Analysis (IPA, www.ingenuity.com), three lists of fold change values for the genes (24h, 48h, and 72h) differentially regulated by CHMP5 silencing were used. Up- and down-regulated genes, whose values were above a threshold of two fold standard deviations, were included in this analysis. More than 95% of these genes mapped to the Ingenuity software. The identified genes were sorted by the mapped genetic networks found in the Ingenuity database. Each potential network was given a score, which was a probabilistic fit between the number of affected genes in a given network and a list of biological functions stored in the Ingenuity Pathways Knowledge Base (IPKB). These scores were used to rank the networks. We restricted our analysis to those networks that had the highest rank.

II.2.4 Functional analysis

II.2.4.1 Apoptosis assay

Apoptosis was assayed by flow cytometry using propidium iodide (PI) staining (Nicoletti *et al.*, 1991). Cells from a 24-well microtiter plate were harvested, washed once with (PBS), resuspended in 100µl FACS staining buffer and incubated at 4°C for 6h in darkness. Finally, the DNA content present in the stained nuclei was determined by flow cytometry using the FACSArray Bioanalyzer System.

In over-expression and rescue assays, apoptosis was induced in HEK293T cells by etoposide at a concentration of 25µg/ml and measured by PI staining using the FACSArray Bioanalyzer System.

For the caspase inhibition assay, cells were transfected with shRNA expressing vectors and 24h later were treated with the caspase inhibitor Z-VAD-FMK at a final concentration of 20µM, which was administered every 24h due to its instability. The cells were analyzed for apoptosis 72h after transfection by FACS analysis after PI staining of the nuclei.

II.2.4.2 Cell viability assay

The CellTiter-Glo[®] Luminescent cell viability assay is a method of determining the number of viable cells in culture based on quantitation of the ATP present, an indicator of metabolically active cells. The Cell Titer Glo Luminescent Cell Viability Assay was used to verify the

viability of the transfected MCF7 cells in opaque-walled multiwell plates (Costar, Baar, Germany). 72h after transfection, 100µl of CellTiter-Glo[®] Reagent (Promega) was added to each well in order to measure the ATP content of the well. 100µl or 400 µl of the reagent was used to measure cell viability of transfected cells in the 96 or 24 well plate formats, respectively. After 10 minutes incubation at RT on a shaker (350rpm), fluorescence intensity was measured using a luminometer. Each assay was performed in triplicate. An integration time of 0.25 seconds per read was applied.

II.2.4.3 Cell cycle analysis

Fluorescence-activated cell sorter (FACS) analysis was performed to determine cell cycle kinetics. Transfected cells in each well, were stained with 400µl of FACS staining buffer and cellular DNA content of 10,000 events per sample was determined by flow cytometry using the FACS Canto II flow cytometer and was analyzed using the CellQuest[™] software (Becton, Dickinson and Company).

II.2.4.4 Proliferation assay

The effect of a single gene knock-down on the proliferation of breast cancer cell line MCF7 was assessed using the Click-iT[™] EdU Flow Cytometry Assay Kit. EdU5-ethynyl-2'-deoxyuridine is a nucleoside analogue to thymidine and is incorporated into DNA during active DNA synthesis. Briefly, 48h after transfection of cells with siRNAs (II.1.8), EdU was added to the medium and, after incubation for an additional 2h, the number of EdU-positive cells were measured for each experimental condition. Detection was based on a click reaction, a copper catalyzed covalent reaction between an azide and an alkyne. In this application, the EdU contained the alkyne, while the Alexa Fluor[®] 488 dye, Alexa Fluor[®] 647 dye, or Pacific Blue[™]dye contained the azide. Flow cytometry method was used for determining the percentage of the cells population that are in S-phase.

II.2.4.5 Caspase activity measurement using the Caspase-Glo[®] Assay

The Caspase-Glo[®] Assay is a luminescent assay that measures caspase activity. Different types of caspases can be measured using the Caspase-Glo 3/7, Caspase-Glo 8 or Caspase-Glo 9 Assay kits (Promega). The assay provides a proluminescent caspase-8, 9 and 3/7 substrate in a buffer system optimized for caspase activity, luciferase activity and cell lysis.

Luminescence is proportional to the amount of caspase activity present. Caspase activity assays were performed in 96 well plates. HEK293T and MCF7 cells were seeded (5×10^3 cells/well) and transfected with the respective siRNAs (II.1.8). After incubation for 24h or 48h, 100 μ l of Caspase-Glo reagents for different caspases (caspase-8, -9 and -3/7) were added to each well, incubated for 30 minutes, and the luminescent signal was measured using a luminometer.

II.2.4.6 NF- κ B luciferase reporter assay (dual-luciferase reporter assay)

Genetic reporter systems are widely used to study regulation of eukaryotic gene expression. The term 'dual' refers to the simultaneous expression and measurement of two individual reporter enzymes within a single system. The experimental reporter (*firefly*-luciferase) correlates with specific experimental conditions, while the activity of the co-transfected 'control' (*renilla*-luciferase) provides an internal control that serves as a baseline for transfection efficiency. Normalizing the activity of *firefly*-luciferase to the activity of *Renilla*-luciferase minimizes experimental variability caused by differences in cell viability or transfection efficiency.

The *firefly*-luciferase plasmid, containing four binding sites for NF- κ B (Li-Weber et al., 1998), and the *renilla*-luciferase plasmid (pTK-RL pGL4.74, Promega) were used for transfection of cells. HEK293T cells (4×10^4 per well) were seeded in 48-well plates. After 24h, the cells were transiently co-transfected with 100ng of NF- κ B *firefly*- luciferase reporter vector and 2ng of *renilla*-luciferase reporter plasmid. After additional 24 h incubation, *firefly* and *renilla*-luciferase activities were assayed using the Dual-Luciferase Reporter System (Promega) and the luminescent signal was measured using a luminometer. Transfected cells grown in a 24-well plate were lysed with 50 μ l of 1x passive lysis buffer (Promega) for 15 minutes at RT on a shaker (310 rpm). 120 μ l of each lysate were pipetted into a reader plate of the luminometer in triplicate. The *firefly*-luciferase activity was measured by adding 100 μ l of LAR II reagent (Promega) to generate a stabilized luminescent signal. After quantifying the *firefly* luminescence, this reaction was quenched and the *renilla*-luciferase reaction was initiated by adding 100 μ l of Stop- and Glo reagent to the same tube. The Stop- and Glo reagent (Promega) produces a stabilized signal of the *renilla*-luciferase, which was measured in the luminometer. After normalizing the *firefly*-luciferase activity to the *renilla*-luciferase activity, a direct comparison of samples regarding NF- κ B activity in the nucleus was possible.

II.2.4.7 Flow cytometric analysis of cell surface death receptor

To detect expression levels of the cell surface receptors CD95 and TNFR1, 1×10^6 cells were exposed to fluorochrome-conjugated antibodies against these proteins and analyzed by flow cytometry. Briefly, cells were harvested 24h after transfection and incubated in FACS buffer containing biotin-labeled anti-human CD120a, a monoclonal antibody against TNFR1 (1×10^6 cells, clone mAb TNFR1-B1), followed by SAV-APC (Streptavidin-Allophycocyanin, 1×10^6 cells), or PE-conjugated anti-human CD95 monoclonal antibody (1×10^6 cells, clone DX2) for 30 min at 4°C in the dark. Isotope-matched antibodies were used as negative controls. After washing with FACS buffer, 10,000 cells were analyzed using a FACS Calibur flow cytometer equipped with CellQuest software. Results were expressed as median fluorescence intensities.

II.2.5 Statistical analysis

Data were expressed as mean values \pm SD from two to five independent experiments.

Statistical significance was determined using T-test to compare groups of data. *P*-values < 0.05 were considered as statistically significant.

III Results

In order to identify novel genes involved in apoptosis and cell viability, two sets of transient RNAi screens were performed; one screening in normal cells (HEK293T) (III.1) and another one in tumor cells (MCF7) (III.2). Loss-of-function screens applied in this study aimed to uncover the potential anti-apoptotic function of studied genes. To this aim, as the read-out of the screening experiments apoptosis and cell viability were measured. Further functional assays on candidates, including gene expression profiling and reporter gene assays, as well as receptor staining and cell cycle analysis were used to identify the pathway context of the candidate genes (III.1 and III.2).

III.1 Short hairpin RNAi screen to in normal cells

To screen for novel regulators of apoptosis, we performed an in vitro screen of 288 poorly characterized human genes using apoptosis as a read-out in HEK293T cells. Cells were transfected with single shRNA-coding plasmids targeting specifically the respective genes. After 72h, apoptosis was measured using fluorescent microscopy in the reverse transfection array method or PI staining and FACS analysis in direct transfection.

III.1.1 Reverse transfection cell array technology

In order to identify late apoptotic markers such as apoptotic bodies as a phenotype, reverse transfection was performed. In this study, pEYFP plasmid was used as a reporter for transfection efficiency of each individual shRNA (II.2.3.1). Knock-down efficiency was also examined using shRNAs against *P53* and *Lamin B1* followed by immunostaining (Figure 7).

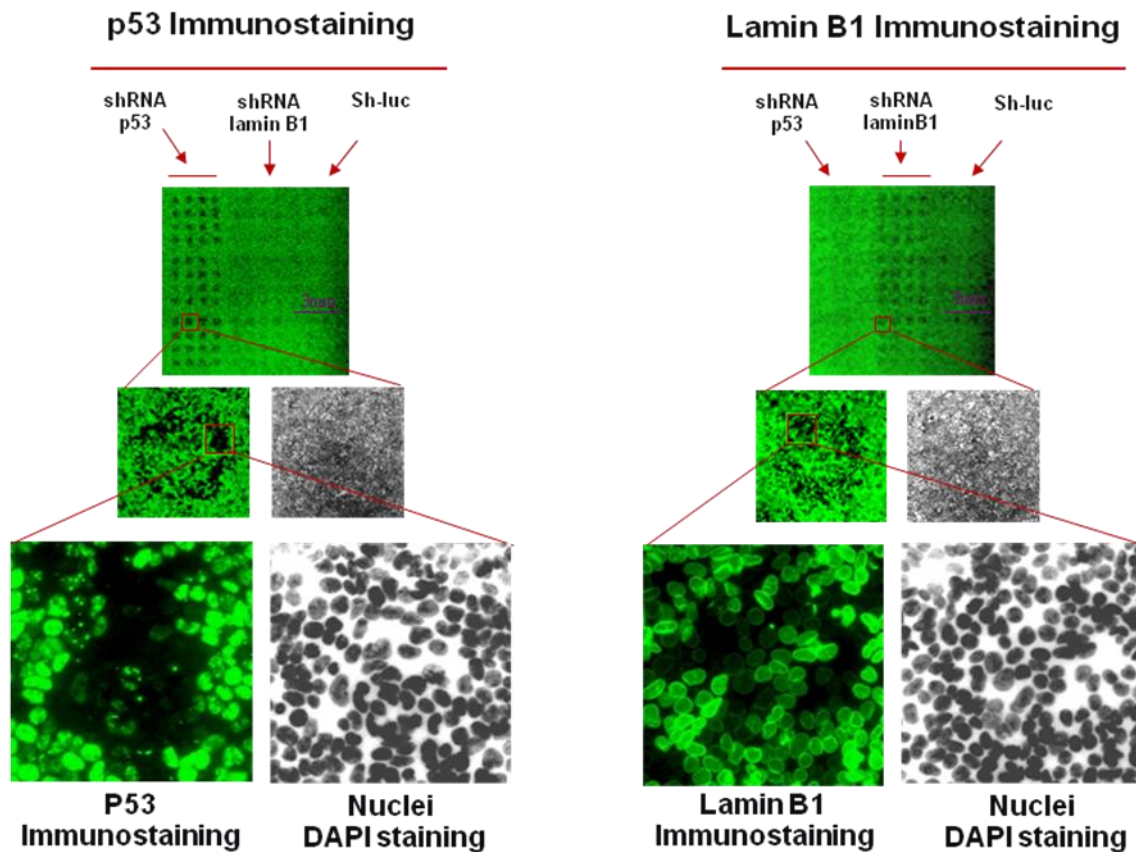


Figure 7- **Immunostaining of P53 and Lamin B1**. HEK293T cells transfected by pEYFP expression vector, sh-Luciferas (sh-Luc, negative control), sh-P53 and sh-LaminB1, were stained by P53 and Lamin B1 antibodies 72h after transfection. DAPI was used to visualize the nuclei. P53 and Lamin B silenced cells are in dark areas upon immunostaining.

In the initial attempt, which was a array-based assay to identify potential anti-apoptotic genes, 288 shRNA coding plasmids were transfected into HEK293T cells and an apoptotic phenotype, was evaluated by fluorescent microscopy 72h after transfection. In this assay, pEYFP and Bax expressing vectors were used as negative and positive controls, respectively and apoptotic bodies were considered as a specific late phenotype of apoptosis pathway activation (Figure 8).

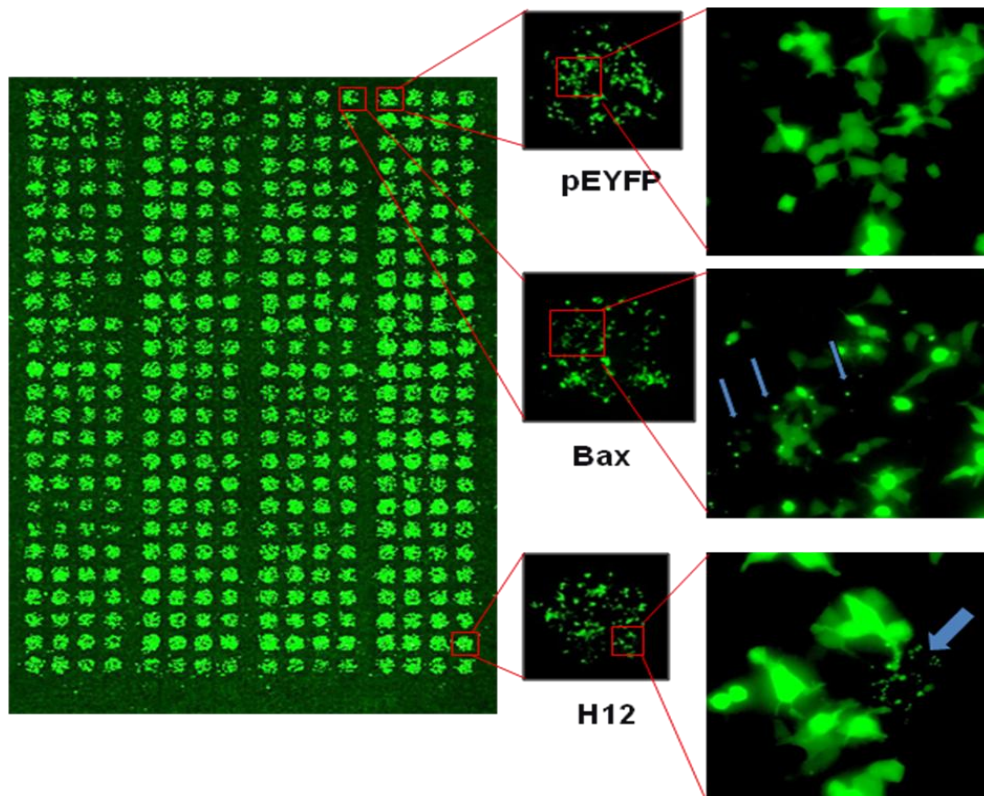


Figure 8- **Identification of apoptotic cells by reverse transfection cell arrays.** An example of 96 shRNA out of 288. HEK293T cells transfected by shRNAs in 4 replicas. Negative and positive controls (pEYFP and Bax) are spotted in first and last rows of each slide. Apoptotic bodies are shown in Bax over-expressed and one of the shRNAs (H12) transfected cells by arrows.

In these array-based set of screens, due to the lack of enough apoptotic cells that could be observed under the microscope, no significant difference in the amount of dead cells was detected following silencing of genes. For example, only in one cluster of the shRNA transfected cells (shRNA clone H12) could a few apoptotic cells be detected, and only in a single spot out of four replicas. Therefore, due to these technical problems, screening of all 288 shRNAs using the reverse transfection method did not result in the identification of a candidate that could be involved in apoptosis. It was observed that many dead cells, which were not tightly attached to the slides, were removed during the fixation procedures prior to microscopy for detection of apoptotic cells, making it difficult to compare the low number of apoptotic cells within different spots. Such observations led us to measure apoptosis as a read out by a more reliable method to consider larger amount of dead cells, which might appear following the silencing of individual genes.

III.1.2 Direct transfection and FACS analysis

In this experiment, HEK293T cells cultured in microwells were directly transfected with shRNA-coding plasmids targeting specifically the genes of interest using effectene transfection reagent. About 72 hours after transfection, apoptosis was measured using PI staining and FACS analysis (Figure 9 B). Based on the reduced DNA content compared to the normal G1 population, sub-G1 cells were considered as apoptotic cells. The efficiency and reliability of transfection were determined by transfection of pEYFP expressing vector and the green fluorescent signal produced from this vector was visualized by-fluorescent microscopy.

III.1.2.1 Optimization of the screening set-up

An essential step for each screening is the definition of the best window, in which strong signals could be obtained with high sensitivity and low variability. Reproducibility is also an important factor that should be considered in each optimization procedure.

In a particular assay, the dynamic range of the read-out is represented by difference between ‘baseline values’, which are acquired by negative control genes and ‘positive hit values’, which are obtained by positive control genes. The normalization of all data subsets from different plates into a single coherent data set is a great advantage of negative control included assays. Positive controls provide a quality control to ensure that the experiment was working properly.

In the current study, several well-known apoptotic inhibitors such as Birc4, Birc5, and Birc7, and negative controls including pEYFP, pSuper- *firefly* luciferase (sh-Luc), pSM2-GFP (sh-GFP) were examined in order to establish the experimental conditions. Different shRNA sequences targeting the above-mentioned positive control genes were tested for their silencing efficiency. The percentage of apoptotic cells observed upon silencing of putative apoptosis inhibitor genes is shown in Figure 9 A and B.

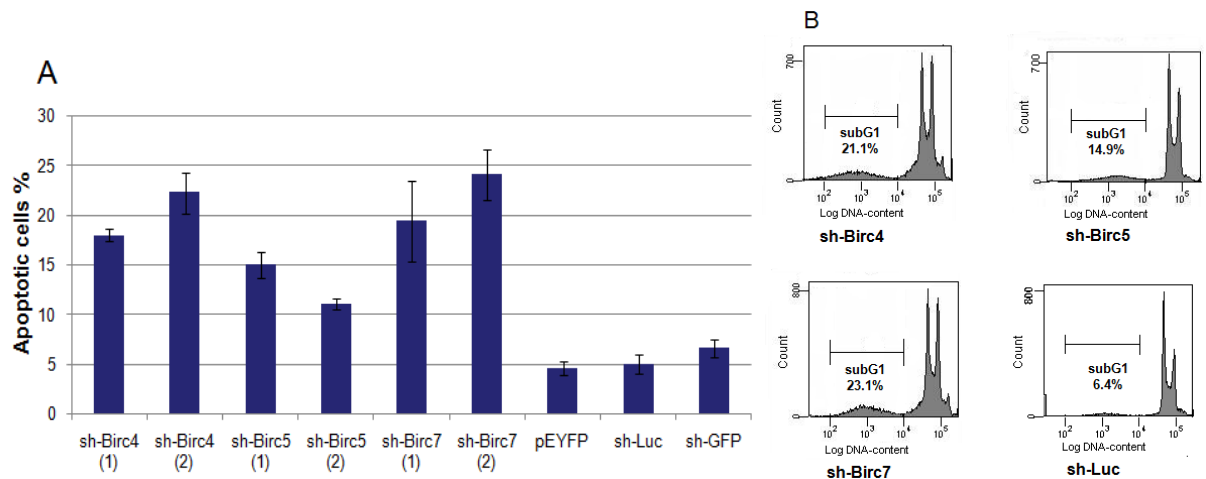


Figure 9- **Apoptosis mediated by IAP genes silencing.** (A) Percentage of apoptosis mediated by shRNAs targeting different sequences of positive controls *Birc4* (1,2), *Birc5* (1,2) and *Birc7* (1,2) and negative controls pEYFP expression vector and shRNAs targeting luciferase and GFP. (B) Percentage of apoptotic cells (sub- G1 cells) of a single experiment measured by FACS analysis is shown. *Birc 4, 5, 7* were used as positive controls and *firefly Luciferase* was negative control.

Based on fold change increase in apoptosis obtained following silencing of the above mentioned positive controls, sh-Birc4(2) sh-Birc5(1) and sh-Birc7(2) were selected as proper positive controls and sh-Luc was selected as negative control to be used in the screening procedure.

III.1.3 Short hairpin RNA (shRNA) screen to identify putative anti apoptotic genes

The set of 288 shRNAs coding plasmids were transfected into HEK293T cells, and apoptosis was measured using PI staining and FACS analysis 72h after transfection. The relevant targets of those shRNAs that increased the level of apoptotic cells by more than 2.0 fold compared to the negative control (shRNA-luciferase), were defined as anti-apoptotic candidates (Figure 10A). Four of the tested shRNA-clones, C6 (*Opsin-1*), F12 (*CHMP5*), H8 (*EPAS2*) and D9 (termed “similar to *KIAA1466*”), fulfilled this demand. The identity of these shRNA-coding inserts for clones F12, H8 and D9 was verified by sequence analysis. Unfortunately, the C6-shRNA sequence was found to be non-specific for *Opsin-1*. This sequence did not match with any known human gene or transcript sequence when compared to genome databases. Therefore, it was excluded from the validation assays. Moreover, replicate analysis of the shRNAs F12, H8 and D9 revealed a reproducible specific apoptotic effect only for clone F12 clone (which targets *CHMP5*), such that about a two fold increase in the amount of apoptotic

cells (compared to the negative control sh-Luc) was observed after transfection, which was similar to the effect seen by the positive controls, (Figure 10 B). Transfection of cells with plasmids coding shRNAs against known anti-apoptotic genes (*Birc4*, *Birc5* and *Birc7*), resulted in a change of more than two fold in the amount of apoptotic cells when compared to the negative control sh-Luc. To test the specificity of the observed anti-apoptotic phenotype of CHMP5, further validation and functional characterization experiments were carried out including i. shRNA-knock-down, ii. over-expression, iii. rescue assays, and iv. measurement of caspase activities.

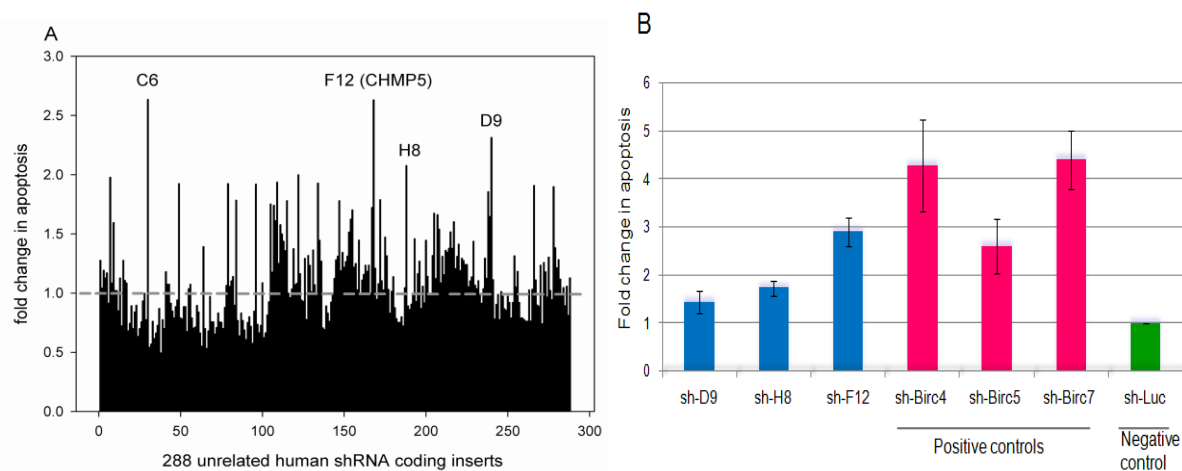


Figure 10- Loss-of-function screening identifies *CHMP5* as an anti-apoptotic candidate gene. (A) By screening 288 shRNAs targeting genes with unknown or poorly characterized function, *CHMP5* was identified as an anti-apoptotic candidate. HEK293T cells were transfected with individual shRNA coding plasmids. 72h later, apoptosis was measured by PI staining and FACS analysis. Dashed line marks the value of the negative control (shRNA targeting *firefly* luciferase, used for normalization). (B) Fold change in apoptosis was confirmed by transfection of cells with individual shRNA coding plasmids targeting D9, H8 and F12 (*CHMP5*), as well as *Birc 4*, *5*, *7* (positive controls) and *firefly* luciferase (negative control). Error bars represent the standard deviation (SD) based on three independent experiments.

III.1.4 Validation studies confirm the specificity of *CHMP5* anti-apoptotic function

III.1.4.1 siRNAs targeting different segment of *CHMP5* RNA

One major concern regarding RNAi is the proof of target specificity. Recent reports have demonstrated a possible risk for RNAi-induced off-target effects (Jackson *et al.*, 2003). This phenomenon, potentially mediated by both the sense and antisense strands of siRNA or

shRNA duplexes, may lead to unspecific knock-down of genes (Snove and Holen, 2004; Tschuch *et al.*, 2008).

To exclude that possible off-target effects initiated the CHMP5-phenotype, we confirmed the shRNA-mediated CHMP5-phenotype by using two siRNAs directed against different segments of the *CHMP5*-mRNA. Both siRNAs increased the percentage of apoptotic cells (11% *CHMP5*-siRNA1 and 8.4 % *CHMP5*-siRNA2) when compared to a negative control (GFP-siRNA, 5.4 % Figure 11).

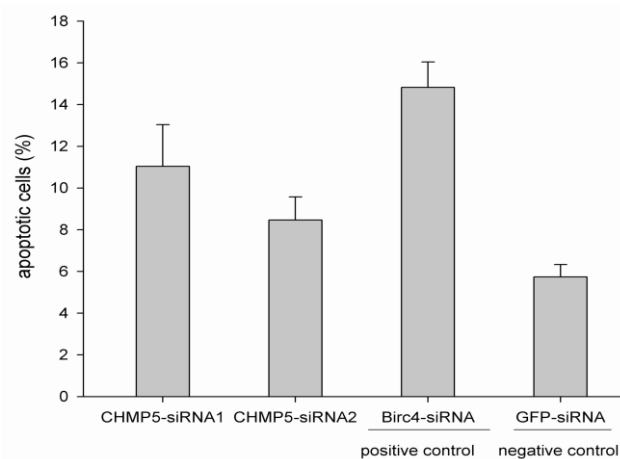


Figure 11- Specificity of CHMP5 silencing effect. Induction of apoptosis in HEK293T cells was confirmed by transfection of two different *CHMP5*-siRNAs (1 and 2) targeting different sites in the *CHMP5* mRNA-sequence. *Birc4*-siRNA was used as positive control and GFP-siRNA as negative control. Apoptosis was measured 72h after transfection by PI staining and FACS analysis. Error bars represent the SD based on three independent experiments.

In addition, the silencing efficiency of shRNAs and siRNAs directed against *CHMP5* was validated by quantitative real-time PCR measuring *CHMP5* mRNA levels. Both shRNA-coding plasmid and the two different siRNAs targeting *CHMP5*, reduced target mRNA levels by about 50% (Figure 12). Thus, the induced apoptotic phenotype seems to be resulted from specific silencing of *CHMP5*.

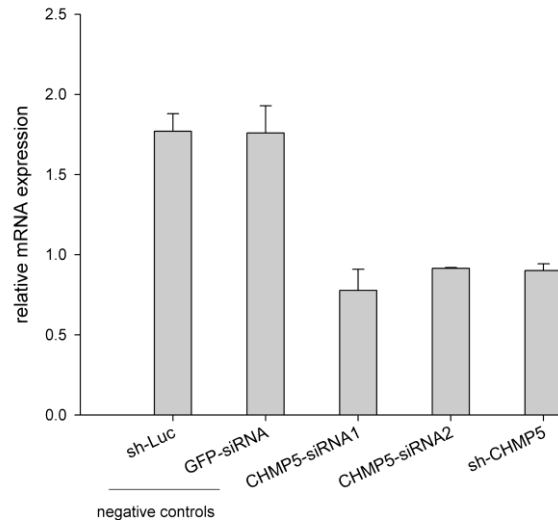


Figure 12- **Expression of *CHMP5* in transfected HEK293T cells.** The level of *CHMP5* mRNA was measured by qRT-PCR 48h after transfection and values were normalized to *laminB1* and *PGK* mRNA levels, which were used as loading controls. Error bars represent the SD based on two independent experiments.

III.1.4.2 Over expression and rescue assays

To validate the anti-apoptotic function of CHMP5, we sought to perform over-expression and rescue assays. Ectopic expression of CHMP5 was carried out by transfecting CHMP5 expression plasmid (pCMV6-CHMP5) into HEK293T cells. A chemical induction of apoptosis was done using etoposide (25 $\mu\text{g/ml}$) and apoptosis was measured (Figure 13A).

72 hours after transfection, transfection of cells with pCMV6-CHMP5 (human or murine) or pCMV6-Birc4 reduced the number of apoptotic cells to about 50% for Birc4 and 40% for human CHMP5 and murine CHMP5 when compared to the negative control experiments (cells transfected with empty pCMV6 expression vector). Therefore, the over-expression of CHMP5 increased the survivability the cells emphasizing that CHMP5 plays a role in modulating apoptosis.

Rescue assays were performed by co-transfection of cells with either the human or the murine CHMP5-cDNA expression vector with the CHMP5 sh-RNA coding plasmid (see Figure 13B). The shRNA sequence targets human *CHMP5* mRNA with perfect complementary, whereas in case of the murine CHMP5, three mismatches in base-pairing are present (Supplementary Figure 30) which disturb the targeting effect of the sh-RNA. The anti-apoptotic effect observed after transfection of the human CHMP5 expression vector could be rescued by co-transfection of shRNA-CHMP5. However, in case of the transfection with murine CHMP5

expression vector, the human CHMP5-shRNA was not able to revert the decreased apoptotic phenotype. Taken together, these experiments define a specific anti-apoptotic function for CHMP5.

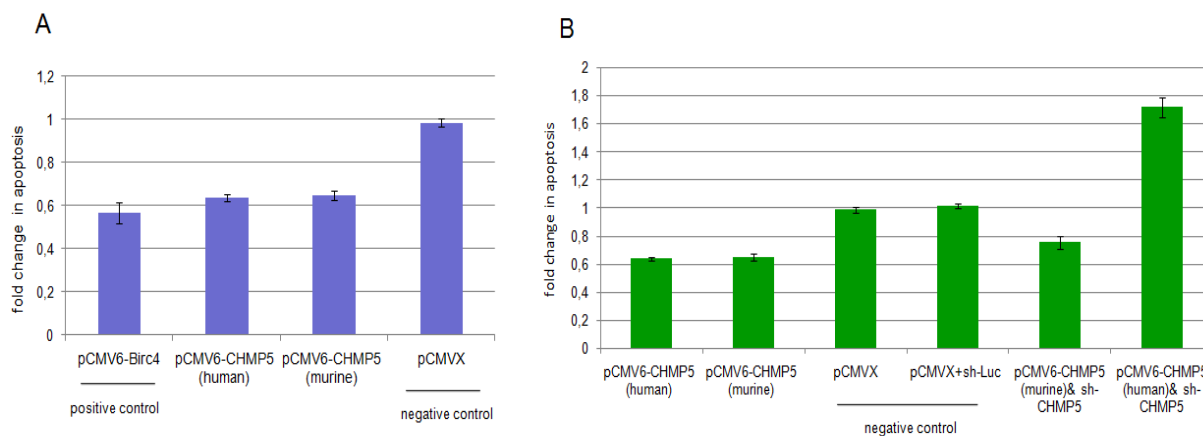


Figure 13- Validation of CHMP5 function in apoptosis by overexpression and rescue studies. Over-expression of human and murine CHMP5 (pCMV6-CHMP5) as well as Birc4 (positive control) reduce apoptosis induced by etoposide. HEK293T cells, seeded in 24 well plates, were transfected with cDNA-expressing vectors: pCMV6 (negative control), *Birc4* (positive control), human or murine CHMP5 (pCMV6-CHMP5). For rescue experiments, cells were co-transfected with human shRNA-CHMP5 and cDNA vectors for human or murine CHMP5 (pCMV6-CHMP5), and co-transfection of pCMV6 and sh-Luc as negative control. 24h after transfection, cells were treated with 25 μ /ml etoposide. Apoptosis was measured 72h after transfection by FACS analysis after PI staining. Error bars represent the SD based on two independent experiments.

III.1.5 Functional characterization of CHMP5

III.1.5.1 CHMP5-silencing induces caspase activation

In order to confirm induction of apoptosis after silencing of CHMP5, downstream factors such as caspase-3/-7 were studied. In this experiment, HEK293T cells were transfected with shRNA-coding plasmids targeting *Birc4*, *CHMP5*, or *firefly-luciferase* and the activity of caspases-3/-7, key mediators of apoptosis, was measured by the caspase-Glo3/7 assay (Promega). Compared to the negative control (sh-Luc), the activity of caspase-3/7 was considerably higher in *Birc4*- (positive control) and *CHMP5*-silenced samples (2.95 and 2.75 folds, respectively) (Figure 14 A). In addition, inhibition of caspase activity was examined by incubating transfected cells either in the presence or absence of the pan-caspase inhibitor Z-VAD-FMK. The inhibition of caspase activity by Z-VAD-FMK led to a clearly reduced percentage of apoptotic cells in *CHMP5*-shRNA transfected cells (6 % versus 12 %) (Figure

14 B), as well as in the positive control cells transfected with sh-Birc4 (9 % versus 17 %). These data demonstrate that the observed apoptotic phenotype mediated by CHMP5-silencing is dependent on caspase activity, supporting the conclusion that CHMP5 plays a role in apoptotic pathways through caspase-3/7.

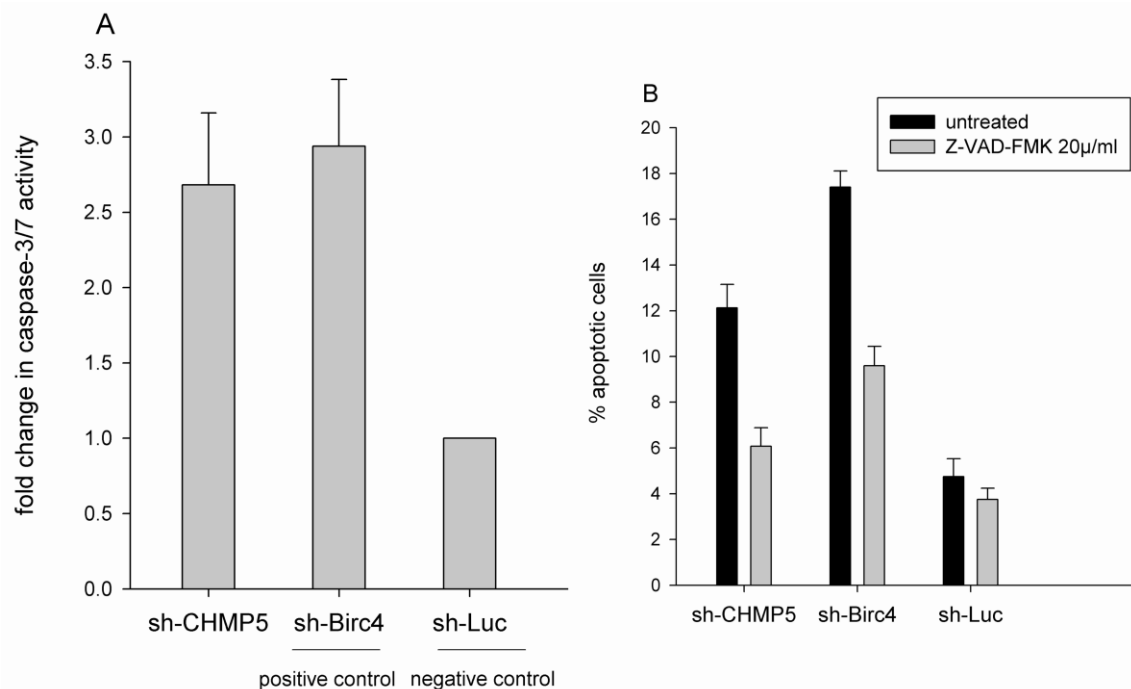


Figure 14- **Involvement of caspase activity in CHMP5 RNAi mediated apoptosis.** (A) Caspases-3/7 activation obtained by CHMP5 silencing. Cells were transfected with shRNA targeting luciferase (sh-Luc as negative control), CHMP5 (sh-CHMP5) or Birc4 (sh-Birc4 as positive control) and activity of caspase-3/7 was determined by the caspase-Glo 3/7 luminescence assay. Results are displayed as fold changes in caspase activity relative to sh-Luc related value, which was set to one. (B) Inhibition of apoptosis by pan-caspase inhibitor Z-VAD-FMK. Transfected cells were treated with 20 µg/ml pan-caspase inhibitor Z-VAD-FMK 12h after transfection and incubated for 72h. Thereafter apoptosis was measured by PI staining and FACS analysis. Error bars represent the SD based on three independent experiments.

To verify whether the activation of caspase-3/7 in CHMP5-silenced cells is a result of the extrinsic apoptotic pathway, specific caspase-8 activity was assayed. As shown in Figure 15A, caspase-8 activity in HEK293T cells transfected with siRNAs, which target either CHMP5 or the well known caspase-8 inhibitor FLIP, was about 1.6 fold higher than the negative control. These data clearly indicate an involvement of caspase-8 activation in the apoptotic effect induced by CHMP5 silencing. In contrast, caspase-9 activation after CHMP5 siRNA transfection was only 1.2 fold higher when compared to the activity observed after transfection of the GFP-specific negative control. In addition, caspase-9 activity initiated by

the silenced positive control (Birc4) showed a 1.4 fold increase over the negative control (Figure 15B). Knock-down efficiency in each experiments was measured by qRT-PCR (Figure 31 supplementary).

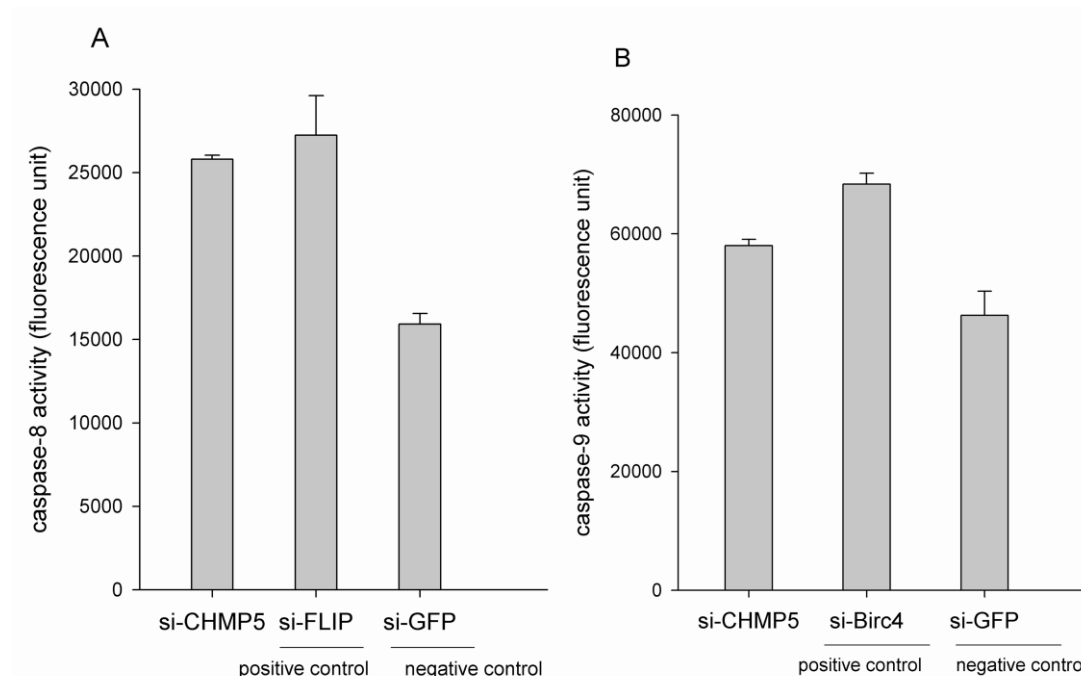


Figure 15- **Activation of caspase-8 and-9 by CHMP5 silencing.** Caspase-8 (A) and 9 (B) activities (fluorescence units) were measured in HEK293T cells 24h after transfection with si-CHMP5, si-FLIP and si-Birc4 (positive controls) or si-GFP (negative control). Error bars represent the SD of two independent experiments each based on triplicate raw data.

Taken together, these observations suggest that CHMP5 silencing induces apoptotic pathway by caspase cascade activation mainly through caspase-8 initiated caspase-3/7 activation leading to the apoptosis phenotype.

III.1.6 Expression array analysis

A DNA microarray experiment shows the expression levels of thousands of genes at a single time point and this provides a snapshot view of genome-wide expression patterns.

To investigate the potential regulatory effects of CHMP5 upon a broad spectrum of signaling pathways, the effect of CHMP5 knock-down or overexpression 24h, 48h and 72h after transfection were examined by genome wide expression array profiling using Illumina Human Sentrix-6 BeadChip arrays. Gene expression profiles of HEK293T cells after CHMP5 silencing or overexpression were compared to the expression profiles of relevant negative

Results

controls (sh-Luciferase and pCMV6). Quantitative real time PCR of the RNA used for gene expression profiling was performed to measure the *CHMP5* RNA level at 24h, 48h and 72h after transfection both by sh-CHMP5 and by sh-luc or pCMV6-CHMP5 and pCMV6 empty vector. Lists of regulated gene transcripts for different time points (24h, 48h, and 72h) after CHMP5 modulation were generated following processing of the array raw data. All information about expression array analysis are available in in the Gene Expression Omnibus (GEO) dataset (<http://www.ncbi.nlm.nih.gov/geo/query/acc.cgi?acc=GSE17003>). Regulated transcripts, which were potentially affected by CHMP5 silencing, were selected if they were ranked within the first 100 most affected genes in at least two of the three time points measured, based on their fold change. Down-regulated genes are listed in Table 1 and up-regulated genes are shown in Table 2. Similar analysis, performed in HEK293T cells over expressing CHMP5, are shown in Table 8 (see supplement). In all individual time-point comparisons, we identified *CHMP5* itself among the most affected transcripts: down-regulated-rank 1 for loss-of-function-24h, down-regulated-rank 2 for loss-of-function-48h, down-regulated-rank 5 for loss-of-function-72h, as well as up-regulated-rank 1 for gain of function-48h and 72h.

Table 1- Down-regulated genes revealed by expression array analysis following CHMP5 silencing at different time points.

| A | | | | | |
|----------------------|--------------------|------|---------------------|--------------------|------|
| Down-regulated genes | | | | | |
| CHMP5 silencing-24h | | | CHMP5 silencing-48h | | |
| gene name | fold change (log2) | rank | gene name | fold change (log2) | rank |
| CHMP5 | -0.61 | 1 | CHMP5 | -1.08 | 2 |
| SMS | -0.57 | 2 | THEM2 | -0.64 | 4 |
| MT1X | -0.47 | 5 | GTF2H5 | -0.56 | 6 |
| GTF2H5 | -0.45 | 6 | CPT1C | -0.47 | 15 |
| APBB3 | -0.43 | 10 | SFRS7 | -0.46 | 18 |
| MSRB2 | -0.41 | 14 | SMS | -0.41 | 47 |
| NSMCE1 | -0.33 | 45 | TYBN | -0.41 | 49 |
| SFRS7 | -0.32 | 54 | C9orf46 | -0.39 | 56 |
| CPT1C | -0.32 | 56 | MSRB2 | -0.39 | 61 |
| TYBN | -0.32 | 60 | APBB3 | -0.38 | 70 |
| C9orf46 | -0.31 | 77 | MT1X | -0.37 | 77 |
| THEM2 | -0.31 | 78 | CCDC71 | -0.36 | 90 |
| CCDC71 | -0.3 | 80 | NSMCE1 | -0.36 | 97 |

| B | | | | | |
|----------------------|--------------------|------|---------------------|------|--|
| Down-regulated genes | | | | | |
| CHMP5 silencing-24h | | | CHMP5 silencing-72h | | |
| gene name | fold change (log2) | rank | fold change (log2) | rank | |
| CHMP5 | -0.61 | 1 | -1.43 | 5 | |
| DNAJB1 | -0.34 | 33 | 0.7 | 35 | |

| C | | | | | |
|----------------------|--------------------|------|---------------------|------|--|
| Down-regulated genes | | | | | |
| CHMP5 silencing-48h | | | CHMP5 silencing-72h | | |
| gene name | fold change (log2) | rank | fold change (log2) | rank | |
| CHMP5 | -1.08 | 2 | -1.43 | 5 | |

* Genes belonged to the list of 100 most affected genes in more than one time point. Regulated genes in both 24h and 48h (A), 24h and 72h (B), 48h and 72h(C) time points are shown.

Table 2- Up-regulated genes upon CHMP5 silencing at different time points.

| A | | | | | | B | | | | | |
|---------------------|--------------------|------|---------------------|--------------------|------|---------------------|--------------------|------|---------------------|--------------------|------|
| Up-regulated genes | | | | | | Up-regulated genes | | | | | |
| CHMP5 silencing-24h | | | CHMP5 silencing-48h | | | CHMP5 silencing-24h | | | CHMP5 silencing-72h | | |
| gene name | fold change (log2) | rank | gene name | fold change (log2) | rank | gene name | fold change (log2) | rank | gene name | fold change (log2) | rank |
| TMEM43 | 2.05 | 1 | PPP1R15A | 1.5 | 1 | TMEM43 | 2.05 | 1 | TMEM43 | 0.75 | 4 |
| ATF3 | 1.36 | 2 | ATF3 | 1.44 | 2 | DUSP1 | 1.06 | 4 | GADD45B | 0.59 | 15 |
| KIAA0101 | 1.32 | 3 | GADD45A | 1.43 | 3 | GADD45A | 1.05 | 5 | DUSP1 | 0.57 | 22 |
| DUSP1 | 1.06 | 4 | DUSP1 | 1.41 | 4 | PPP1R15A | 0.97 | 6 | GADD45A | 0.57 | 23 |
| GADD45A | 1.05 | 5 | GADD45B | 1.33 | 5 | HNRPDL | 0.76 | 14 | MAFB | 0.61 | 33 |
| PPP1R15A | 0.97 | 6 | iSLC3A2 | 1.03 | 8 | GADD45B | 0.54 | 24 | PPP1R15A | 0.52 | 48 |
| DNAJB9 | 0.95 | 7 | AXUD1 | 1.09 | 7 | MAFB | 0.49 | 33 | KIAA0907 | 0.5 | 53 |
| AXUD1 | 0.92 | 8 | ADM | 0.99 | 9 | KIAA0907 | 0.38 | 82 | HNRPDL | 0.46 | 73 |
| MYC | 0.82 | 11 | TMEM43 | 0.94 | 10 | | | | | | |
| HNRPDL | 0.76 | 14 | HNRPDL | 0.91 | 11 | | | | | | |
| HERPUD1 | 0.7 | 15 | DNAJB9 | 0.79 | 14 | | | | | | |
| DDIT3 | 0.67 | 16 | RASSF1 | 0.73 | 15 | | | | | | |
| RND3 | 0.67 | 17 | MAFB | 0.72 | 16 | | | | | | |
| SLC3A2 | 0.62 | 19 | RND3 | 0.72 | 17 | | | | | | |
| SAT | 0.57 | 22 | KIAA0101 | 0.7 | 20 | | | | | | |
| GADD45B | 0.54 | 24 | HERPUD1 | 0.69 | 22 | | | | | | |
| RASSF1 | 0.53 | 26 | NFKBIA | 0.68 | 23 | | | | | | |
| IFRD1 | 0.52 | 28 | AMD1 | 0.66 | 25 | | | | | | |
| iSLC3A2 | 0.5 | 31 | PIM1 | 0.62 | 31 | | | | | | |
| CYR61 | 0.49 | 32 | SAT | 0.61 | 35 | | | | | | |
| MAFB | 0.49 | 33 | SLC3A2 | 0.6 | 36 | | | | | | |
| EMILIN2 | 0.45 | 43 | CYR61 | 0.57 | 39 | | | | | | |
| NDRG1 | 0.45 | 44 | ARC | 0.54 | 46 | | | | | | |
| SYVN1 | 0.43 | 53 | SLC25A25 | 0.54 | 52 | | | | | | |
| AMD1 | 0.42 | 56 | OTUD1 | 0.52 | 56 | | | | | | |
| SLC25A25 | 0.41 | 58 | ATP1B3 | 0.51 | 63 | | | | | | |
| ATP1B3 | 0.41 | 62 | CCNC | 0.51 | 61 | | | | | | |
| XBP1 | 0.41 | 63 | NDRG1 | 0.51 | 64 | | | | | | |
| OTUD1 | 0.4 | 69 | IFRD1 | 0.49 | 66 | | | | | | |
| PIM1 | 0.39 | 72 | EMILIN2 | 0.49 | 68 | | | | | | |
| ADM | 0.39 | 77 | MYC | 0.49 | 69 | | | | | | |
| DSCR1 | 0.39 | 78 | DDIT3 | 0.47 | 77 | | | | | | |
| ARC | 0.38 | 79 | KIAA0907 | 0.46 | 79 | | | | | | |
| KIAA0907 | 0.38 | 82 | SYVN1 | 0.44 | 83 | | | | | | |
| NFKBIA | 0.37 | 90 | MOAP1 | 0.44 | 87 | | | | | | |
| CCNC | 0.36 | 97 | XBP1 | 0.42 | 94 | | | | | | |
| MOAP1 | 0.36 | 99 | DSCR1 | 0.42 | 99 | | | | | | |

| C | | | | | |
|---------------------|--------------------|------|---------------------|--------------------|------|
| Up-regulated genes | | | | | |
| CHMP5 silencing-48h | | | CHMP5 silencing-72h | | |
| gene name | fold change (log2) | rank | gene name | fold change (log2) | rank |
| PPP1R15A | 1.5 | 1 | ID1 | 0.81 | 2 |
| GADD45A | 1.43 | 3 | TMEM43 | 0.75 | 4 |
| DUSP1 | 1.41 | 4 | P2RY11 | 0.66 | 8 |
| GADD45B | 1.33 | 5 | GADD45B | 0.59 | 15 |
| TMEM43 | 0.94 | 10 | DUSP1 | 0.57 | 22 |
| HNRPDL | 0.91 | 11 | GADD45A | 0.57 | 23 |
| ZCCHC12 | 0.64 | 30 | SON | 0.52 | 41 |
| P2RY11 | 0.47 | 75 | PPP1R15A | 0.52 | 48 |
| KIAA0907 | 0.46 | 79 | KIAA0907 | 0.5 | 53 |
| ID1 | 0.45 | 81 | ZCCHC12 | 0.47 | 68 |
| SON | 0.43 | 92 | HNRPDL | 0.46 | 73 |

*Genes belonged to the list of 100 most affected genes in more than one time point. Regulated genes in both 24h and 48h (A), 24h and 72h (B), 48h and 72h(C) time points are shown.

Gene ontology analysis of all selected genes upon revealed a high frequency of apoptosis-associated factors (*SMS*, *APBB3*, *MSRB2*, *DNAJB1*, *GADD45B*, *DDIT3*, *GADD45A*, *ATF3*, *PPP1R15A*, *CYR61*, *AXUD1*, *RND3*, *ADM*, *NFKBIA* and *MOAP1*).

III.1.7 Pathway analysis

III.1.7.1 Comprehensive gene pathway analysis after CHMP5 modulation identifies relevant signaling cascades

To identify CHMP5-affected signaling pathways, comprehensive gene pathway analysis (CGPA) software (II.2.3.2.1) was applied to the expression array data (III.1.6). The high-ranked pathways affected in both silenced and over-expressed cells, were grouped into the following categories: cancer, protein degradation, metabolism and signaling (Table 3 and Table 7 (A, B) Supplementary).

Table 3- Processes affected by the modulation of CHMP5 expression

| Cancer | Protein degradation | Metabolism | Signaling |
|-----------------------------|---------------------------------------|---------------------------------|-------------------------|
| Thyroid | Caprolactam degradation | Propanoate metabolism | PPAR signaling pathway |
| Acute Myloid Leukemia (AML) | Proteasome | Fatty acid metabolism | Notch signaling pathway |
| Prostate | Limonene and pinene degradation | Butanoate metabolism | mTOR signaling |
| Endometrial | Benzoate degradation via CoA ligation | Arginine and proline metabolism | |
| Small cell lung | | | |
| Colorectal | | | |
| Renal cell | | | |

III.1.7.2 Ingenuity pathway analysis and relevant NF- κ B factors

Ingenuity Pathway Analysis (IPA) is a powerful tool to elucidate pathways and networks connected to a gene of interest, based on the expression profiling data (see methods). A more detailed analysis using IPA revealed that several regulated genes are mainly implicated in the NF- κ B network (Figure 16). Most of these genes are involved in cellular processes such as apoptosis. Several of these genes, such as *TSC22D3*, *TNFRSF12A*, *SGK*, *DDIT3*, *GADD45B* can function as regulators of NF- κ B and others such as *TRIB3*, *ADM*, *SMAD7*, *SLIT2*, *PEA15*, *SLC7A1* and *RGS16*, can be regulated by NF- κ B.

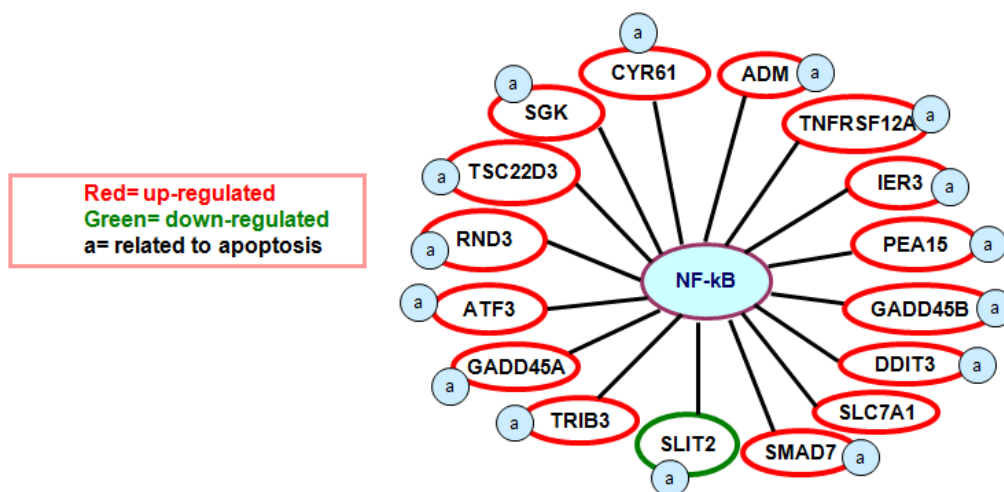


Figure 16- **NF-κB network related factors affected by CHMP5 silencing.** Related genes were identified by Ingenuity pathway analysis (IPA).

Based on these findings, we assessed the ability of CHMP5 to modulate NF-κB activity using NF-κB-luciferase reporter construct assays. Figure 17 shows that NF-κB activity is inhibited by CHMP5 over-expression (luciferase reporter activity value = 0.7) compared to the pCMV6-empty vector control (luciferase reporter activity value = 1.6), whereas silencing of CHMP5 resulted in an increased NF-κB activity (luciferase reporter activity values of 2.3 and 1.6 for sh-Luc and sh-CHMP5 transfected cells, respectively).

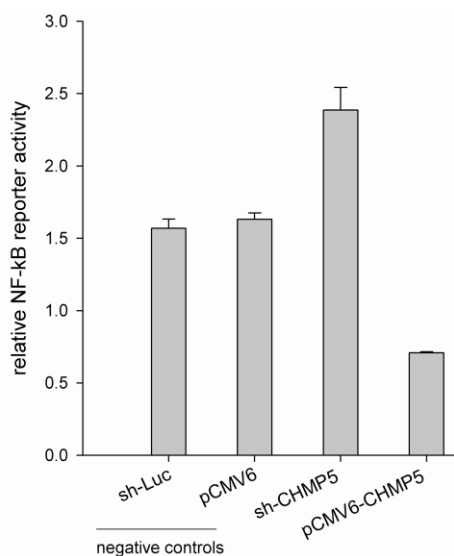


Figure 17- **NF-κB reporter assay.** NF-κB-*firefly* luciferase activity relative to renilla luciferase is shown in normalized light units (Rlu). HEK293T cells were transfected with shRNA CHMP5 plasmid or pCMV6-expression plasmid for . pCMV6 empty vector and sh-luciferase were used as negative controls. Relative luciferase activity was measured 24h after transfection. Error bars represent the SD of two independent experiments, each based on triplicate raw data.

III.1.8 Death receptor expression is influenced by CHMP5

Our expression array and pathway analyses showed that NF- κ B-associated genes and apoptotic related genes are regulated upon CHMP5-silencing. In addition, previous studies showed that CHMP5 deficiency induces up-regulation of multiple signaling pathways that are related to the lack of internalized receptor degradation (Shim et al., 2006). Likewise, caspase activity data in this study indicated that the loss of CHMP5 is inducing apoptosis by the extrinsic pathway. Therefore, we investigated the expression of the two death receptors TNFR1 and CD95, both known to be upstream regulators of the NF- κ B signaling pathway and also involved in extrinsic apoptosis activation. Surface expression of death receptor TNFR1 on the cell membrane was measured by FACS analysis of HEK293T cells in which the CHMP5 gene activity had been modulated. Surface expression of TNFR1 was significantly increased (p-value = 0.0002) upon CHMP5 silencing, whereas it was reduced compared to negative controls (p-value = 0.005) following overexpression of CHMP5 (Figure 18 A, B). In contrast, surface expression of the CD95 (Apo-1/Fas) receptor, another cell death receptor of the TNFR family, was not significantly changed by silencing or overexpression of CHMP5 (Figure 18 C). Our results suggested that CHMP5 might specifically influence the expression of TNFR1, but not that of CD95 receptor on the cell membrane surface.

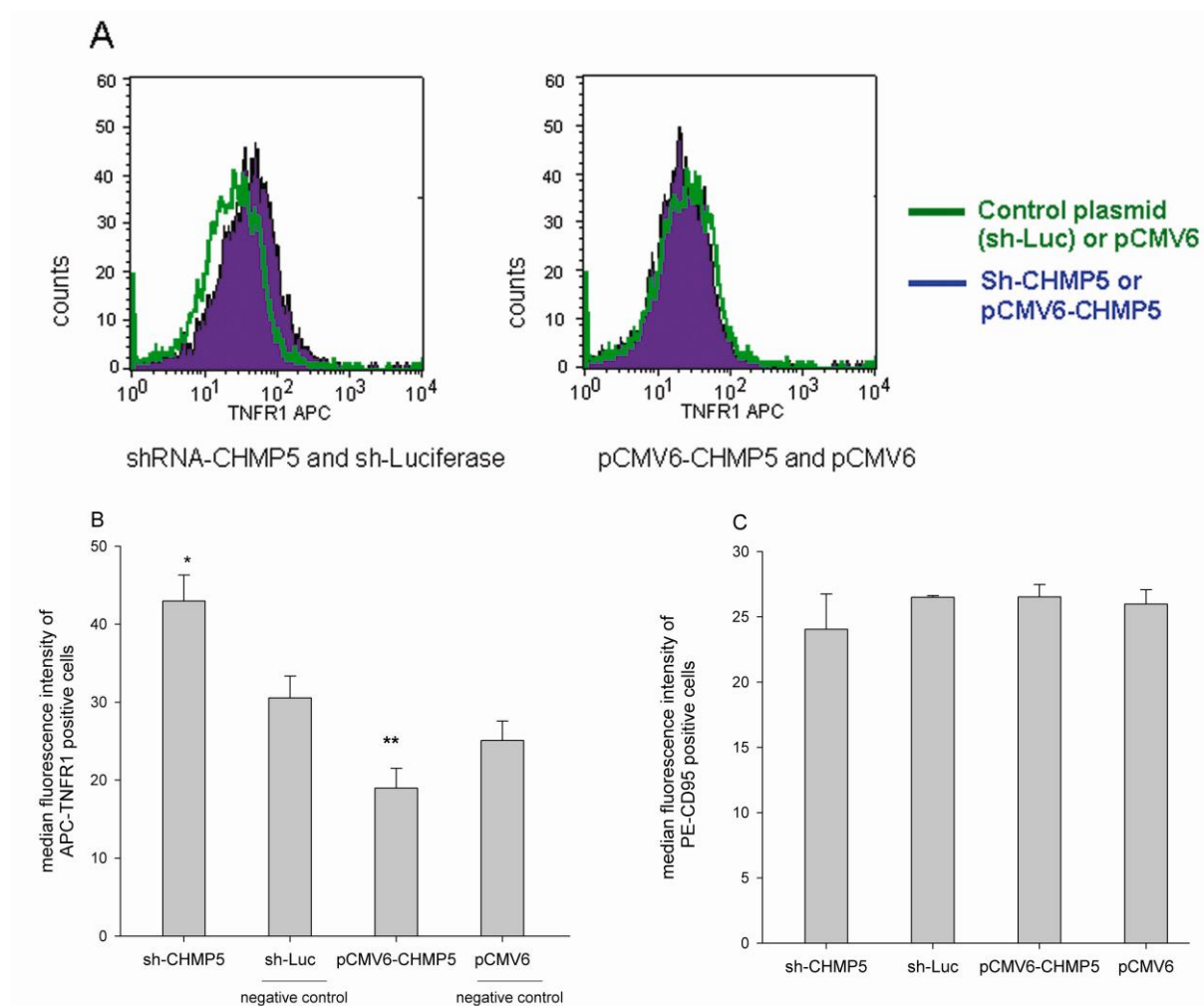


Figure 18- Cell surface expression of death receptors TNFR1 and CD95 . HEK293T cells were transfected with shRNA-or overexpression-plasmids for CHMP5. ShRNA-luciferase and empty vectors (pCMV6) were used as negative controls. Cells labelled by fluorescent antibodies detecting TNFR1 or CD95 were counted by flow cytometry 24h after transfection. Flow cytometry analysis (one out of five experiments is exemplified in A) shows differences in median values of surface expression of TNFR1 by silencing (*, $P < 0.0002$ versus sh-Luc) or overexpression of CHMP5 (**, $P < 0.005$ versus pCMV6) (A, B) and (C) no difference in CD95 surface expression. Error bars represent the SD based on five independent experiments.

III.2 SiRNA screen in breast cancer cells

In order to identify novel regulators of cell death in breast cancer cells, we performed an in vitro screening in MCF7 cells using siRNAs against 107 transcripts that had been found over-expressed in breast cancer patients resistant to chemotherapy. Cell viability was used as read-out in this project.

III.2.1 Background of selected genes for RNAi screening

Recently a comprehensive study investigated the potential of a gene expression signature, to predict the response of patients to the triple chemotherapy with GEDoc (gemcitabine, epirubicin and docetaxel) (Thuerigen *et al.*, 2006). Gene expression analysis performed in this study was based on RNA samples from small tissue biopsies, obtained from primary breast tumor tissue. Breast cancer patients were classified based on their response to the therapy. According to the clinical behavior, patients were considered as responders only if they had a pathological complete remission (pCR) after primary systemic chemotherapy. Patients with residual tumor cells at surgery, either resulting in pathological partial remission (pPR) or pathologically no change (pNC), were considered as non-responders.

It had been hypothesized that among genes, which are up-regulated in pNC compared to pCR, cell death inhibitors can be found that might be responsible for proliferation and survival of cancer cells and cause a negative response to therapy. For this purpose, Significant Analysis of Microarray (SAM) analysis was performed between series of gene expression data of nine pCR and six pNC samples to identify significantly differentially expressed genes between the two patients' groups. Out of 376 differentially expressed genes, 151 were up-regulated in the pNC group. Based on available siRNAs against these transcripts, we performed a loss-of-function screen of 107 up-regulated genes in pNC to identify those that have an impact on the reduction of cell viability and proliferation upon silencing. Our ultimate goal was to identify genes, which are potentially involved in survival pathways responsible for resistance to therapy in patients, who were classified as exhibiting no change (pNC) after chemotherapy.

III.2.2 Optimization of the screening set-up

Screening in breast cancer MCF7 cells was performed using siRNAs. The reason for using siRNAs in this screen was because of the availability of a genome-wide siRNA library (Qiagen) in house, which provided the opportunity to pick up the siRNAs targeting the

candidate genes of this library. For optimization procedures, different negative controls, such as “Allstar siRNAs”, and siRNAs directed against *firefly* luciferase and *GFP* were tested to obtain the baseline of the assay read-out. SiRNAs targeting *Birc4*, *5* and *7* were also tested to optimize the best condition for screening. In this experiment, MCF7 cells were cultivated in white 96 well plates and transfected directly using the above-mentioned siRNAs. At 24, 48 and 72h after transfection, Cell Titer Glo reagent (Promega) was added to each well and the luminescence signal representing cell viability (ATP content) was measured using a luminometer. The best results were obtained at 72 hours after transfection (Figure 19). In this experiment, lower light unit signal meant less ATP content and less viability. Upon optimization of the set up, si-Birc5 was selected as the proper positive and si-GFP as the negative control, and 50% reduction in cell viability (compared to negative control value) was used as a threshold for selection of candidates in screening procedures.

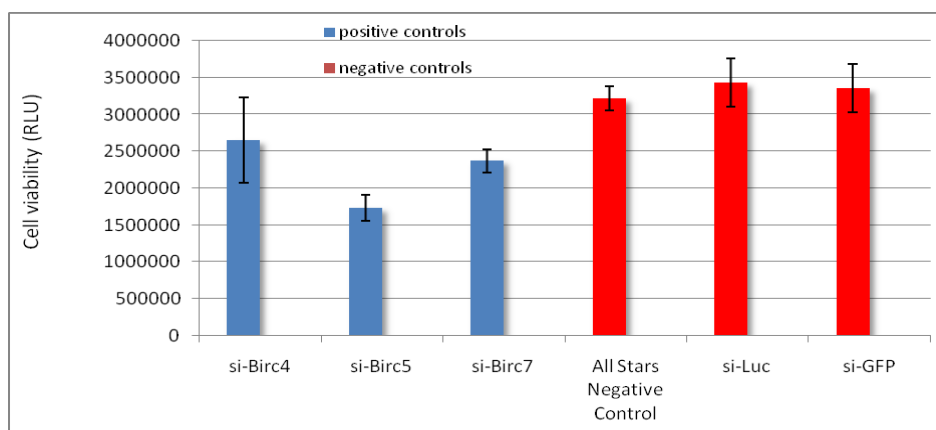


Figure 19- **Cell viability assay for control optimization.** SiRNAs pools against *Birc4*, *5* and *7* were transfected to MCF7 cells as positive controls, and “Allstars negative control” siRNA, *firefly* luciferase and *GFP* siRNA were used as negative controls. Cell viability was measured using CTGlo assay about 72h after transfection. cell viability is shown as related light unit (RLU). Error bars represent the SD based on five independent experiments.

III.2.3 SiRNA screen to identify genes involved in survival of breast cancer cells

One major application of RNAi is loss-of-function screens to identify and characterize genes of interest based on changes in the observed phenotype. In this study, a set of 107 siRNAs (pools of four siRNAs each targeting a single mRNA) were transfected into MCF7 cells and cell viability (as a phenotype read-out) was measured using an ATP-dependent luminescent

Results

cell viability assay 72h after transfection. The relevant targets of those siRNAs that decreased the level of viability by at least 50% compared to the negative control (si-GFP) were defined as candidate genes contributing to cell survival (Figure 20).

Three biological replicates of each siRNA knock-down were performed and positive ‘hits’ were selected according to the criteria defined based on reaching the threshold value and reproducibility of the read-out in different replicates. Following these criteria, functional screening of 107 siRNAs resulted in the identification of *PPP1R15B* as a candidate gene with an profound impact on cell viability. This gene was selected for further validation experiments. Moreover, to avoid missing additional candidates that showed a 20-50% reduction in the cell viability read-out in this set of siRNA screen, eight genes including (*PPP1R15B*, *EPHA3*, *PCTK2*, *HHLA2*, *TBC1D13*, *TTC19*, *ZNF436*, *SYTL4*) were re-examined (Figure 20).

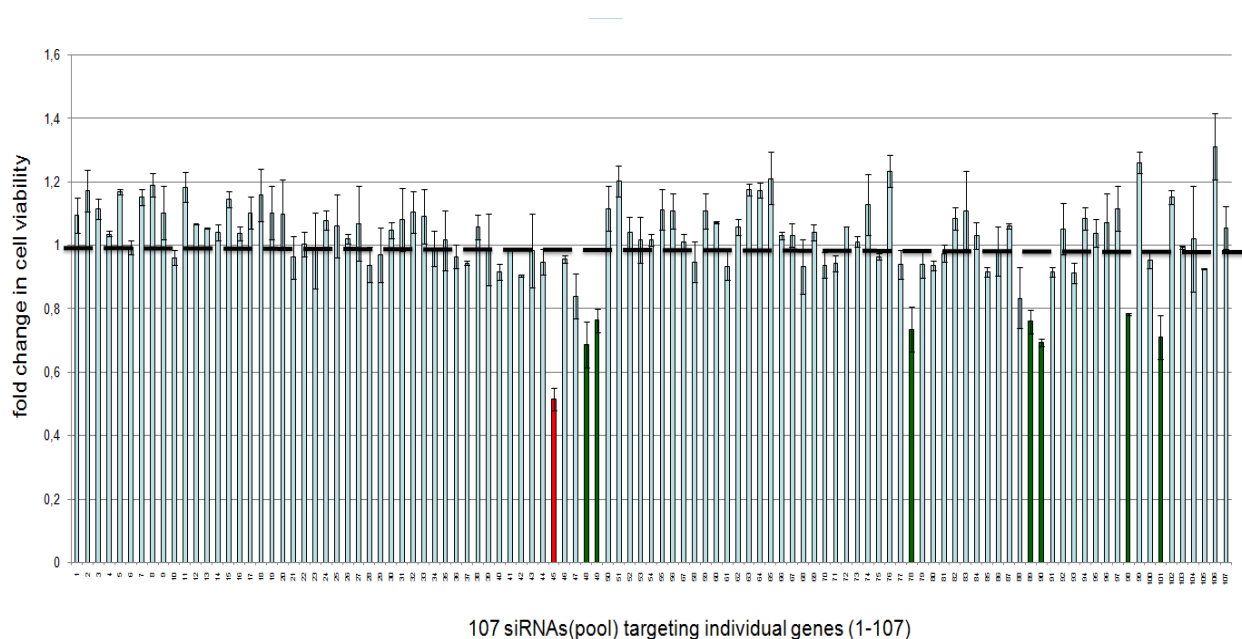


Figure 20 - Loss-of-function screen identified *PPP1R15B* as a candidate gene involved in survival. Upon screening of 107 siRNAs, *PPP1R15B* (shown in red bar number 45) and 7 more genes (green bars, numbers: 48, 49, 78, 89, 90, 101) were selected for re-analysis. MCF7 cells were transfected with individual siRNAs. 72h later, cell viability was measured by CTGlo assay. Dashed line shows the value of the negative control (siRNA targeting GFP, used for normalization). Error bars represent the standard deviation (SD) based on three experiments.

III.2.4 Accuracy of screening readout

Knock-down and cell viability assays were performed for seven genes (*EPHA3* [48], *PCTK2* [49], *HHLA2* [78], *TBC1D13* [89], *TTC19* [90], *ZNF436* [98], *SYTL4* [101]) in addition to *PPP1R15B* [45]. By replicate analysis of all eight genes, hit value (50% reduction of cell viability compared to negative control si-GFP value) for cell viability was observed specifically by silencing of the *PPP1R15B* (Figure 21). Therefore, *PPP1R15B* gene was selected as the only promising candidate for more detailed validation and functional assays.

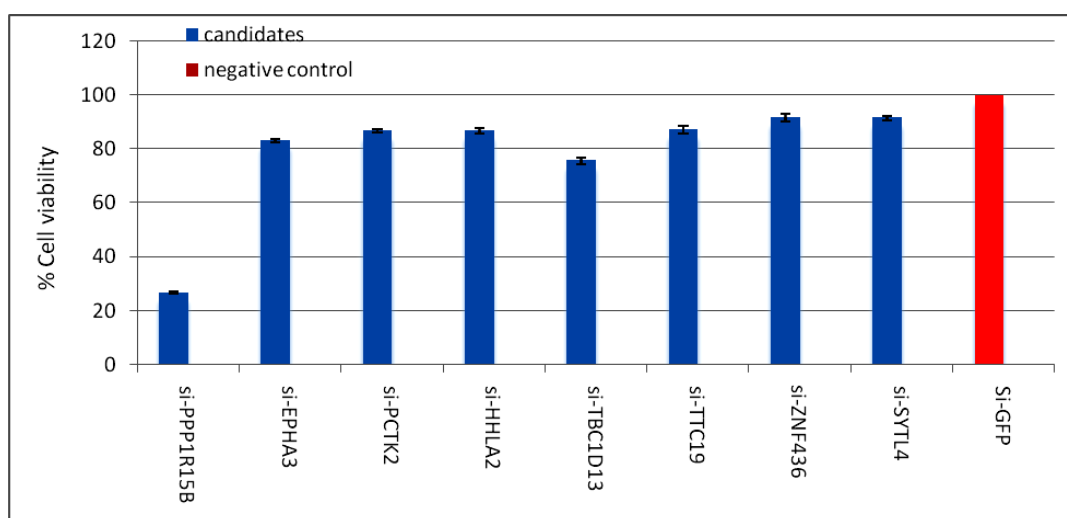


Figure 21- **Cell viability assay for candidate genes.** Cell viability assay shows the change for ATP levels produced by cells after silencing of the candidate genes *PPP1R15B*, *EPHA3*, *PCTK2*, *HHLA2*, *TBC1D13*, *TTC19*, *ZNF436* and *SYTL4* compared to the negative control siGFP (red bar). Error bars represent the standard deviation (SD) based on three experiments.

III.2.5 Validation of the cell death inhibitory function for candidate gene *PPP1R15B*

To test the specificity of the cell death inhibitory phenotype observed by the cell viability assay for PPP1R15B, further validation and characterization experiments were carried out including: i. knock-down using different single siRNAs and measuring RNA expression level and cell viability, ii. measuring the PPP1R15B protein level to evaluate knock down efficiency and iii. validation of an apoptosis phenotype readout using FACS analysis and PI staining.

III.2.5.1 Efficacy of the PPP1R15B silencing phenotype

Four single siRNAs targeting different sequences of the *PPP1R15* gene were tested for knock-down efficacy and specificity of the cell viability phenotype readout. To determine the efficacy of siRNAs with respect to their target genes, degradation of targeted mRNA after the application of siRNA needed to be tested. The RNA expression levels were evaluated by quantitative real time PCR. MCF7 cells were transfected with different siRNAs against *PPP1R15B* mRNA (si-ppp 1,2,3 and 4) and 48h after transfection, the target mRNA level was measured by qRT-PCR.

Two siRNAs of four showed a similar efficacy, reaching a maximum knock-down of *PPP1R15B* RNA compared to si-GFP non-silencing control in this experiment. *Lamin B* and *PGK* were used for the normalization of expression data (Figure 22A).

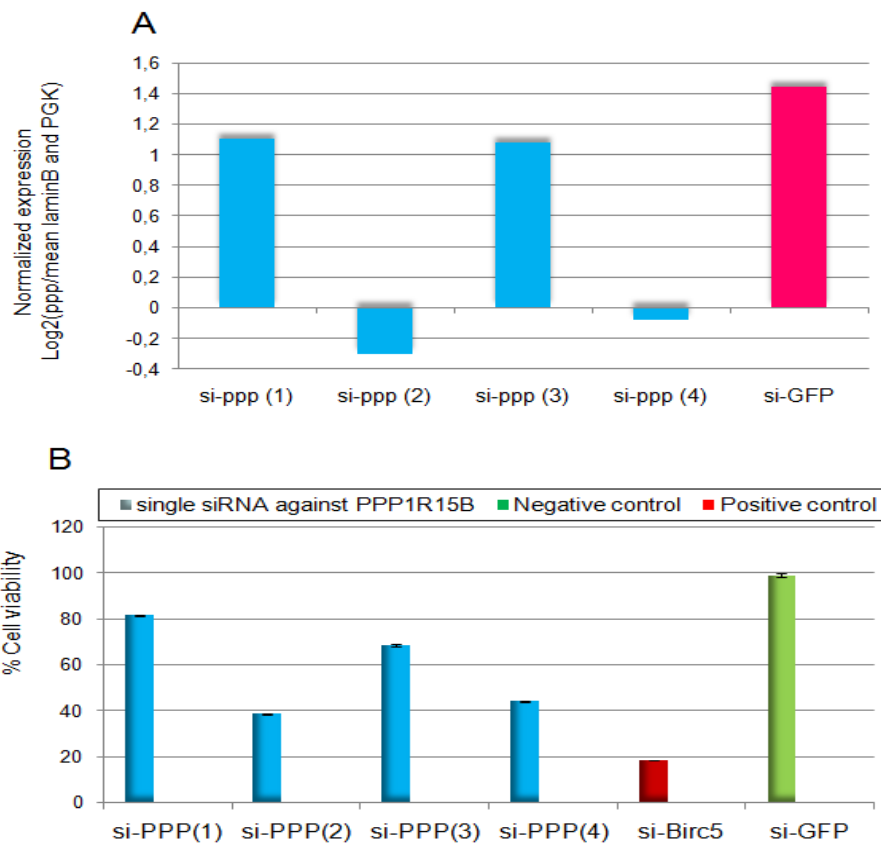


Figure 22- The silencing efficacy of four si-PPP1R15B (si-ppp) monitored by qRT-PCR and cell viability assay. (A) Expression of *PPP1R15B* was measured by qRT-PCR in MCF7 cells transfected by different siRNAs targeting its mRNA. Transfection of si-ppp sequence 2 and 4 (blue) resulted in a profound reduction of *PPP1R15B* RNA level compared to a non-targeting siRNA (pink bar si-GFP). (B) Measurement of cell viability at 72h after transfection with siRNAs-PPP (1-4), si-Birc5 (red bar) as positive control and si-GFP (green bar) as negative control.

To evaluate the correlation of knock down efficiency with phenotype readout, cell viability was tested 72 hours after the transfection of MCF7 cells using all four single siRNAs targeting *PPP1R15B*, si-Birc5 as positive and si-GFP as negative controls (Figure 22B).

In this experiment, cell viability was reduced to less than 50% when compared to the negative control (si-GFP) after transfection of cells with si-PPP(2) and si-PPP(4) and si-Birc5 (positive control). The observed phenotype following silencing of *PPP1R15B* was strongly correlated with the profound knock-down mediated by the two siRNAs shown in Figure 22A.

III.2.5.2 The impact of *PPP1R15B* knock-down at the protein level

The specific knock-down of *PPP1R15B* RNA is expected to show a corresponding effect at the protein level. To investigate the knock-down efficiency of si-ppp(2) at the protein level,

MCF-7 cells were transfected with the siRNA at a concentration of 50nM. After 48h, the cells were lysed and PPP1R15B protein levels were assayed by Western blot using a PPP1R15B-specific monoclonal antibody. As a negative control, cells were also transfected with siRNA directed against GFP at a final concentration of 50nM in parallel. The housekeeping protein GAPDH was used as a loading control. The same amount of proteins for si-PPP and si-GFP transfected cells, were loaded onto gel. Transfection with si-PPP caused reduction in the PPP1R15B protein level when compared to si-GFP negative control. As it is shown in Figure 23, the amount of the control protein was also slightly reduced by PPP1R15B deficiency. This might be due to the role of PPP1R15B in global protein biosynthesis (IV.2.5). Evaluating protein levels of other housekeeping genes in this experiment may help to verify this effect.

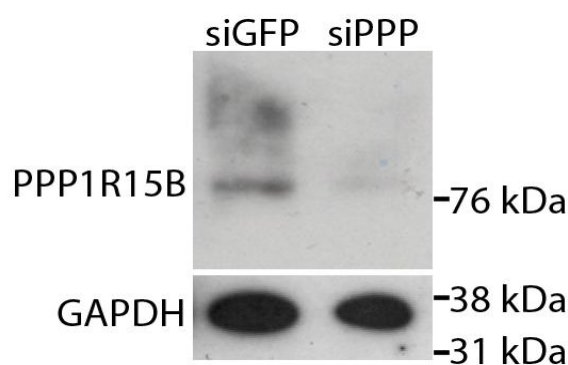


Figure 23- **Western blot analysis of PPP1R15B protein expression.** siRNAs were transfected into MCF-7 cells. After 48 h, cells were lysed and protein expression was analyzed by western blot. GAPDH and PPP1R15B were detected with specific antibodies. Protein analysis 48 h after transfection showed reduction of PPP1R15B levels in si-PPP2-transfected MCF-7 cells.

III.2.5.3 Apoptosis induction upon PPP1R15B knock-down cells

An apoptosis assay was applied to determine the consequences of PPP1R15B knock-down in MCF7 cells (Figure 24). After transfection with different siRNAs against PPP1R15B, the transfected cells were stained with propidium iodide and analyzed by flow cytometry. Our results demonstrated that an increase of apoptotic cell number can be achieved in the presence of efficient PPP1R15B siRNA knock-down compared to negative control experiments. Based on reduced DNA content compared to the normal G1 population, sub-G1 cells were considered as apoptotic cells. The siRNAs targeting PPP1R15B, Birc5 (positive control) and GFP (negative control) were transfected into MCF-7 cells at a concentration of 50nM. The percentage of subG1 cells was increased more than 4 fold by deficiency of PPP1R15B and

Results

Birc5 when compared to si-GFP (Figure 24A). Thus, apoptosis was induced efficiently by silencing of PPP1R15B (si-PPP2, si-PPP4) and positive control Birc5 in MCF7 cells (Figure 24 B).

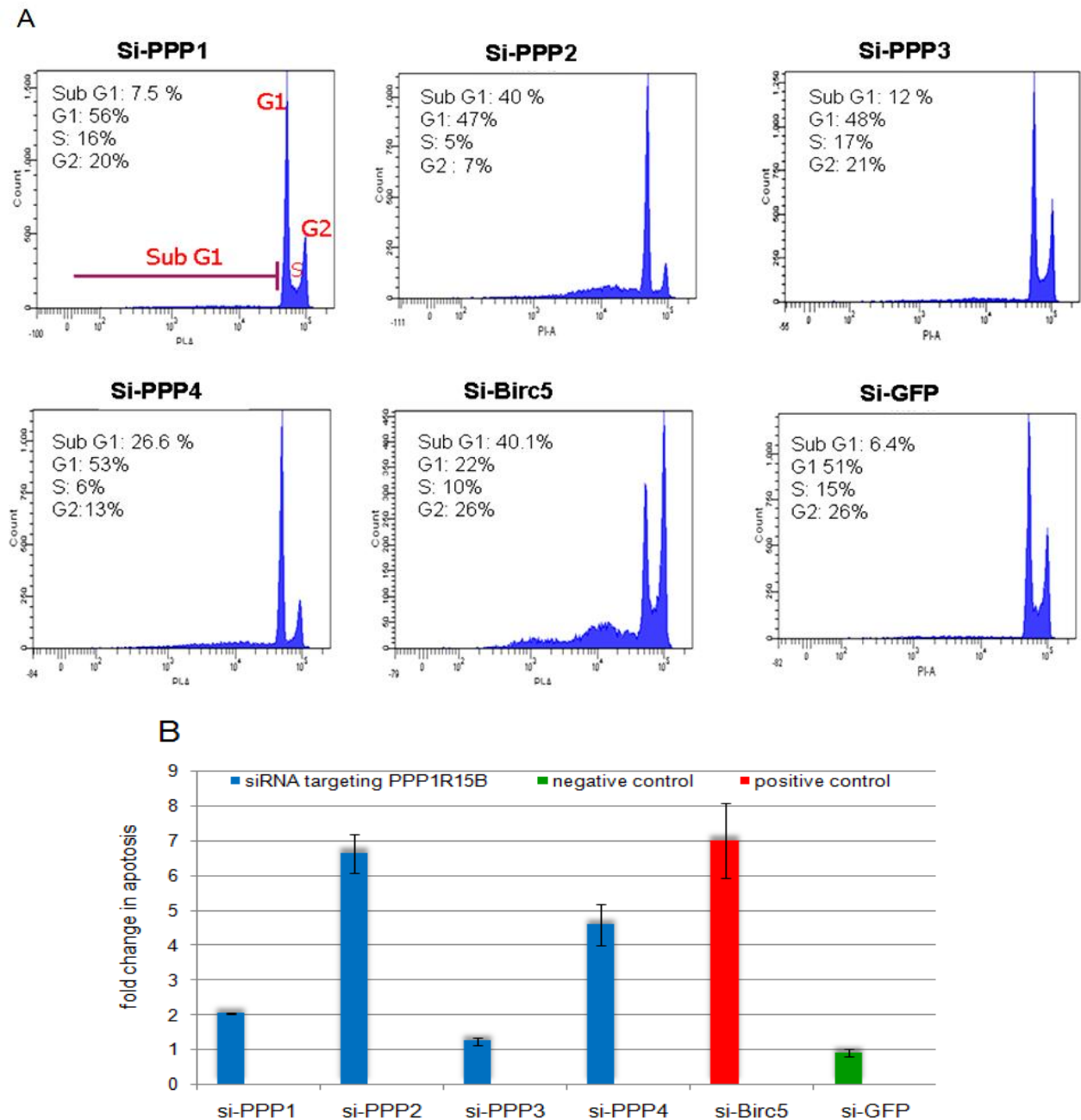


Figure 24- Apoptotic phenotype mediated by PPP1R15B silencing. (A) The percentage of apoptotic cells (sub-G1 cells) of a single experiment measured by FACS analysis is shown. Birc5 and GFP were positive and negative controls, respectively. (B) The fold change in apoptosis induction was confirmed by individual siRNAs transfection targeting different sequences of *PPP1R15B* as well as *Birc5* and *GFP*. Error bars represent the standard deviation (SD) based on three independent experiments.

III.2.6 Effect of PPP1R15B deficiency on caspase activation

In order to confirm induction of apoptosis after silencing of PPP1R15B, MCF7 cells were transfected with siRNAs targeting *Birc5*, *PPP1R15B* or *GFP* and the activity of caspases-3/7, as key mediators of apoptosis, was measured by the caspase-Glo3/7 assay (Promega). Compared to the negative control (si-GFP), the activity of caspase-3/7 was considerably higher in *Birc5*-silenced cells (positive control, 6 fold) whereas it was slightly higher in PPP1R15B-silenced cells (2.2 fold by siPPP2) (Figure 25).

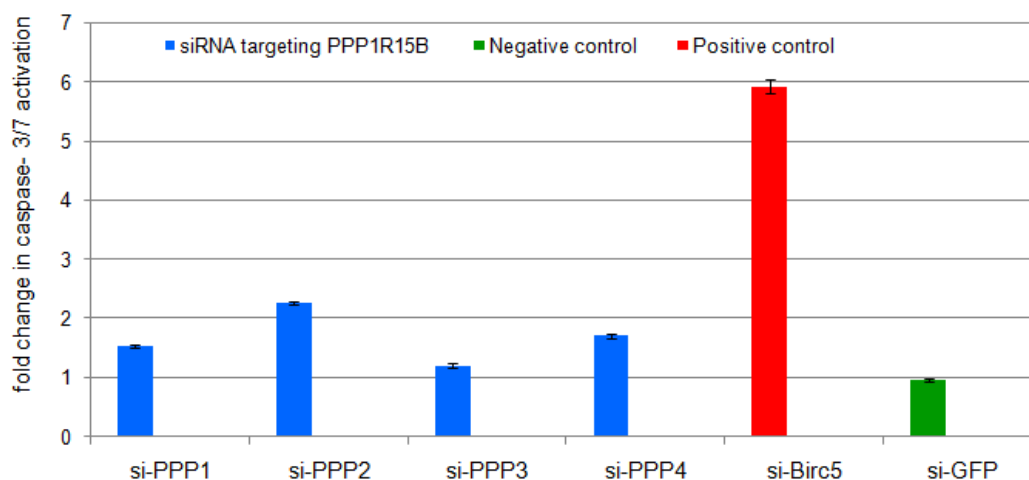


Figure 25- **Caspases-3/7 activation upon PPP1R15B silencing.** MCF7 cells were transfected with siRNA targeting *GFP* (si-GFP as negative control), *PPP1R15B* (si-PPP 1-4) or *Birc5* (si-Birc5 as positive control) and the activity of caspase-3/7 was determined by caspase-Glo 3/7 luminescent assay. The results are displayed as fold changes in caspase activity relative to si-GFP value. Error bars represent the standard deviation based on three experiments.

III.2.7 Apparent involvement of PPP1R15B in cell cycle regulation

We further analyzed functional properties of PPP1R15B by investigating cell cycle distribution patterns using FACS analysis following PPP1R15B silencing. As shown in Figure 24, PPP1R15B knock-down by si-PPP(2) strongly induced apoptosis (40%) when compared to the negative control si-GFP. Moreover, the proportion of S-phase cells was found to be reduced in the PPP1R15B silenced cell population compared to the control cells (si-GFP transfected) 72 hours after transfection (Figure 26). The frequency of cells distributed in S and G2 phases are significantly reduced ($p < 0.0002$, $p < 0.005$ respectively) upon silencing of PPP1R15B in comparison to the control transfection (Table 4). Taken together, based on this

Results

observation, the cell cycle was arrested in the G1 phase and progression of cell cycle toward phase S and G2 was inhibited by PPP1R15B deficiency. Subsequently arrested cells undergo apoptosis as revealed by their accumulation in subG1 (Figure 26).

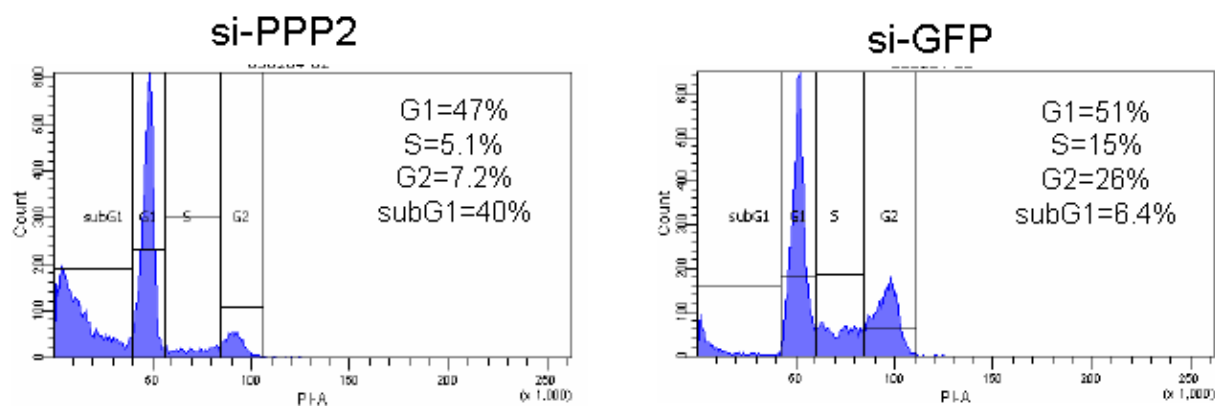


Figure 26- **Cell cycle analysis of PPP1R15B knocked-down cells.** Cell cycle distribution of a single experiment is shown. MCF7 cells were transfected by si-PPP targeting PPP1R15B and with si-GFP as negative control. Cell cycle distribution was analyzed 72h after transfection by PI staining and FACS analysis.

Table 4- **Cell cycle profile upon PPP1R15B and GFP (negative control) knock-down.**

| Cell cycle Phases | Si-PPP2 (three independent experiments) | | | Si-GFP (three independent experiments) | | | P-value |
|-------------------|---|------|-------|--|-------|-------|----------|
| G1% | 40% | 47% | 43% | 51% | 62% | 62.8% | |
| S% | 5% | 5.1% | 5.2% | 15% | 12.9% | 13.9% | $p<0002$ |
| G2% | 7% | 7.2% | 7.1% | 26% | 17.5% | 17.8% | $P<005$ |
| subG1% | 47.4% | 40% | 44.2% | 6.4 | 6.9% | 5.5% | |

III.2.8 Inhibition of proliferation by PPP1R15B silencing

One of the most accurate method to measure proliferation is to measure DNA synthesis directly. The effect of PPP1R15B deficiency on cell proliferation was examined using the ClickiT™ (an antibody-based detection of the nucleoside) and FACS assay. At 72h after transfection of MCF7 cells with siRNA targeting, PPP1R15B and si-GFP (negative control), cell proliferation was measured by FACS. In this assay, cell proliferation was considerably reduced (50%) by PPP1R15B deficiency (Figure 27).

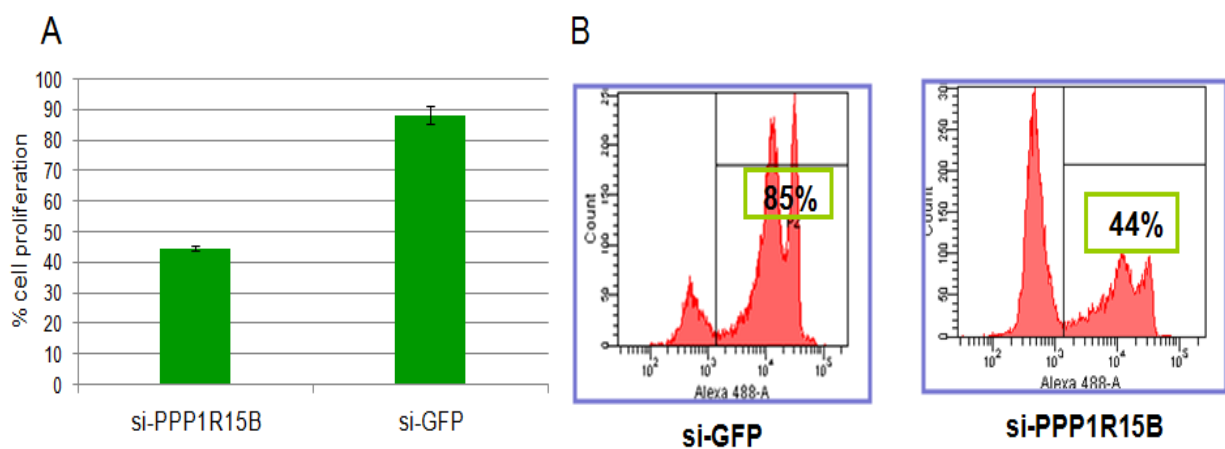


Figure 27- **Cell proliferation assay following silencing of PPP1R15B.** (A) Decrease in percentage of proliferating cells confirmed by individual siRNA transfection targeting *PPP1R15B*, as well as *GFP* (negative control). Error bars represent the standard deviation (SD) based on three independent experiments. B) Percentage of proliferating cells of a single experiment measured by FACS analysis is shown.

III.2.9 *PPP1R15B* expression in different breast cancer cell lines

In order to determine the expression level of *PPP1R15B* in different breast cell lines qRT-PCR was performed to measure the RNA level in breast cancer cell lines. Available breast cancer cell lines MCF7, MDA-MB231, SKBR3, EVSAT, MDA-MB435, T47D and HDQP1 were included in the measurements. Various levels of *PPP1R15B* RNA expression were observed in different cell lines by qRT-PCR. The highest values were obtained in MCF7, MDA-MD231, T47D cells. In contrast, SKBR3, MDA-MB435 and HDQP1 cell lines showed a low level of *PPP1R15B* expression (Figure 28). Therefore, highly *PPP1R15B* expressed cell lines, MDA-MB231, T47D and one of low expressing cell lines (SKBR3), were selected for further investigation of *PPP1R15B* deficiency on cell viability.

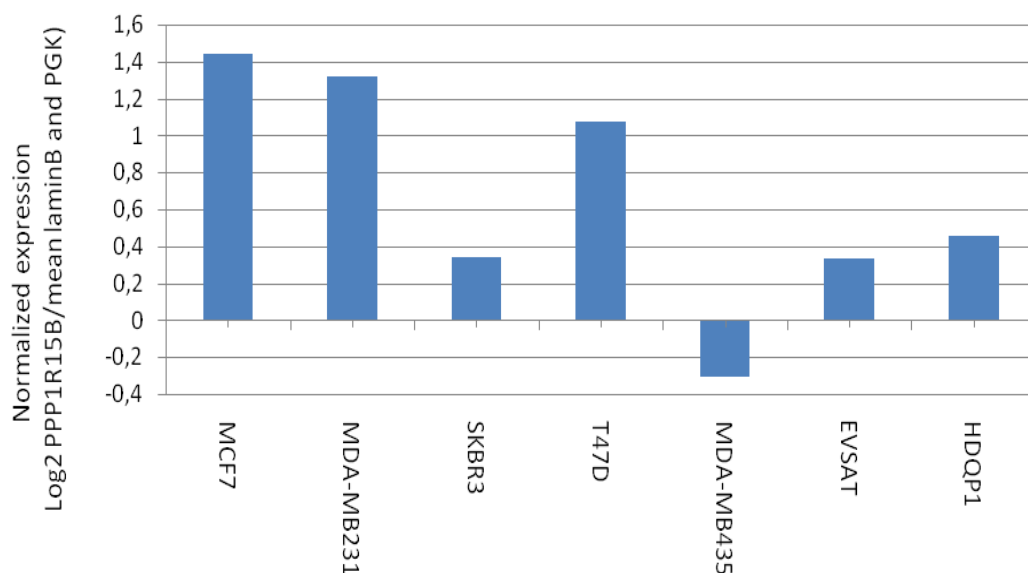


Figure 28- **Expression level of *PPP1R15B* in different breast cell lines monitored by qRT-PCR.** mRNA expression level of *PPP1R15B* was measured in 6 breast cancer cell lines by qRT-PCR. Expression values were normalized to the expression levels of *PGK* and *Lamin B* housekeeping mRNAs.

III.2.10 Investigation of *PPP1R15B* deficiency effect on cell viability in other breast cancer cell lines

To investigate the contribution of *PPP1R15B* to the viability of other breast cancer cell lines, in addition to MCF7, cell lines including MDA-MB231, SKBR3 and T47D were examined. Knock-down efficiency of siRNA against *PPP1R15B* was tested by qRT PCR. The set up

Results

using standard transfection (II.2.2.4) was efficient for MCF7, MDA-MB231 and SKBR3 (Figure 29 A). Cell viability was measured 72h after transfection of the above-mentioned cell lines with siRNA targeting *PPP1R15B* and siRNA-GFP (negative control). Significant reduction of cell viability was obtained upon silencing of *PPP1R15B* only in MCF7 (45%) cells when compared to the negative control (Figure 29 B) (see section IV.2.6).

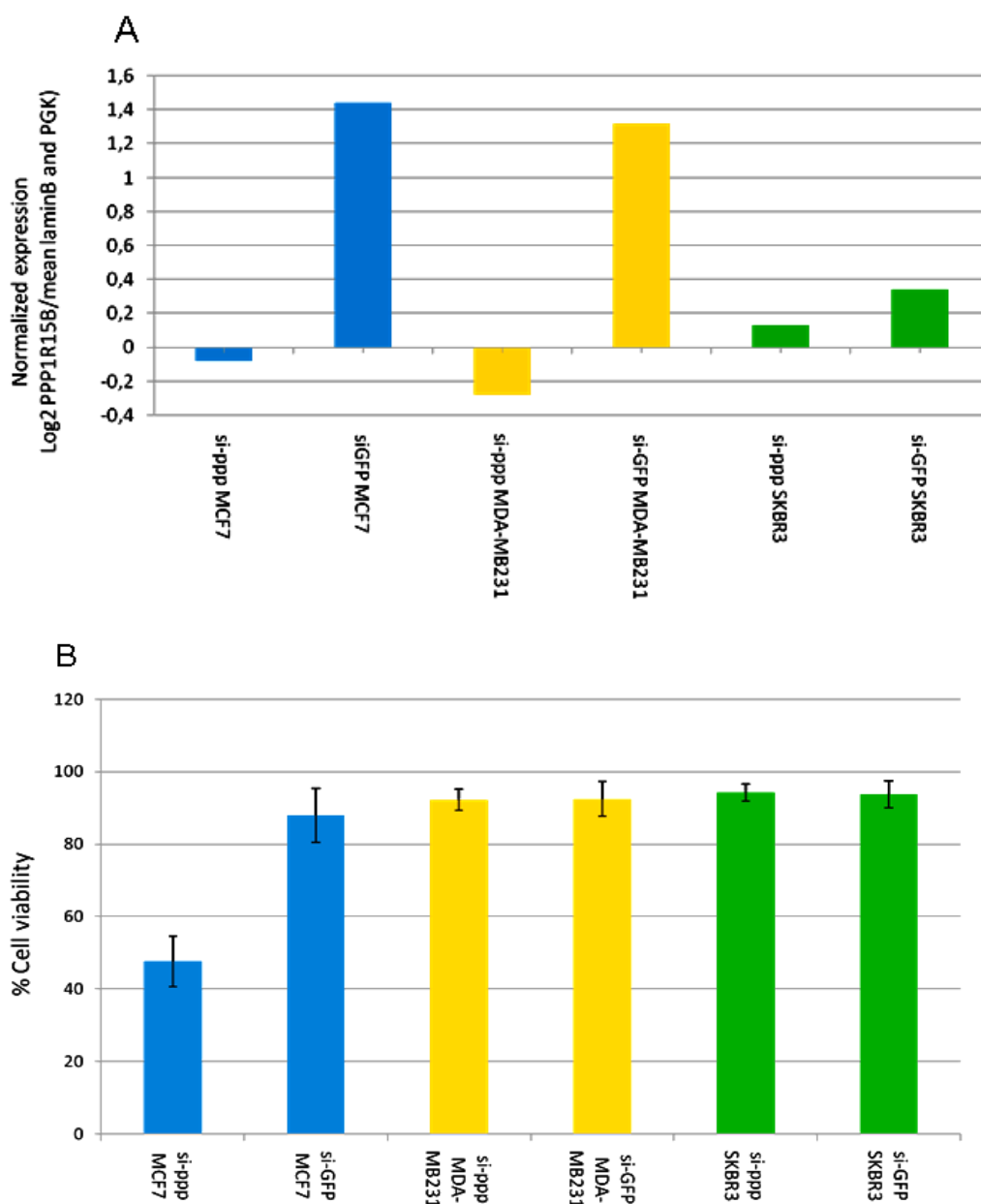


Figure 29- **Silencing efficacy and effect of si-*PPP1R15B* (si-ppp) monitored by qRT-PCR and cell viability assay.** (A) Transfection of si-ppp led to *PPP1R15B* mRNA level reduction. (B) Cell viability was measured 72h after siRNA-PPP, si-GFP (negative control) transfection of MCF7, MDA-MB231 and SKBR3 breast cancer cell lines.

IV Discussion

The completion of the human genome sequence followed by initial functional analyses of the human transcriptome has resulted in the identification of novel genes, most of them uncharacterized or with poorly understood functions (Birney *et al.*, 2007). Currently, for functional analysis of candidate genes, recombinant DNA or RNA molecules are widely used to over-express or to knock-down specific target genes in model cell cultures. When followed by an appropriate read out of the phenotype, such gene modulation approaches can be applied to identify gene functions related to certain cellular pathways (Sturzl *et al.*, 2008). The aim of this study was to exploit the potential of loss-of-function screening to identify novel genes which are involved in apoptosis and cell survival. To reach this goal, we applied a functional genomics approach using RNAi technology in two different cell line models. A normal cell line, human embryonic kidney cells (HEK293T), and the tumorigenic MCF7 cell line were used for RNAi transfection and functional read out assays. Screening in HEK293T cells was carried out using short hairpin-coding constructs (shRNA) targeting 288 poorly characterized human genes. By measuring apoptosis as a readout of loss-of-function screening, *CHMP5* was identified as a candidate for detailed functional and pathway analysis. Further investigation revealed an involvement of CHMP5 in apoptotic cell death and provided evidence on involvement of TNFR1 surface expression as an upstream and NF- κ B signaling as a downstream affected factors. RNAi screening in breast cancer MCF7 cells using siRNAs targeting 107 selected genes over expressed in pNC identified *PPP1R15B* as a validated gene involved in survival and proliferation of MCF7 cells.

IV.1 shRNA screening in non-tumor cells

IV.1.1 An optimized method for screening of apoptotic phenotype mediated by loss-of-function experiments

Ongoing research programs aim to increase the speed of gene function analysis in mammalian cells by i. miniaturization of assays, ii. automatization of experimental processes and iii. improvement and automatization of data recording and management. In order to reach this goal a large number of cell-based assays has been developed over decades of cell culture studies to determine gene function (Sturzl *et al.*, 2008). In 2001, reversely transfected cell microarrays were introduced as an approach for parallel high throughput analysis of gene

function in mammalian cells (Ziauddin and Sabatini, 2001). This method has been applied in various screening settings, such as screening of phenotypes caused by gene silencing or over-expression upon reverse transfection of arrayed cDNA or siRNA molecules (Erflé *et al.*, 2007; Sturzl *et al.*, 2008). The approach has offered the possibility of assessing morphological changes, such as apoptotic body formation, at a high resolution. Previous studies have shown that the reverse transfection assay is a powerful tool to screen for pro-apoptotic genes (Mannherz *et al.*, 2006). In this study, the reverse transfection array was applied to identify putative anti-apoptotic genes based on apoptotic body formation phenotype, detected by fluorescence microscopy as a read out for the screening. Fluorescence microscopy analysis of the transfected cells 72 hours after reverse transfection showed no detectable significant phenotypic changes. As shown in Figure 8, apoptotic cells were detected just in a few shRNA transfected cell clusters (spots on the slide). However, even in positive clusters, the amounts of observed apoptotic cells were not high enough to distinguish the corresponding genes as apoptosis related candidates. Since a sensitive and reproducible detection method was not achieved by this reverse transfection array, the strategy of screening and read out assay was therefore changed to a standard direct transfection and detection of cell death using a sensitive method. A rapid and simple method for measuring apoptosis can be achieved by propidium iodide staining of cells to stain DNA and flow cytometry analysis using FACS, which is able to determine the percentage of apoptotic nuclei or recognize the apoptotic cells in a heterogeneous cell population (Nicoletti *et al.*, 1991). In the current work, we used FACS to facilitate the measurements of apoptosis mediated by 288 shRNAs in a 96-well assay format. PI staining coupled with FACS analysis was also used for further validation analysis and detection of apoptotic cells by single transfection of siRNAs or cDNA constructs.

IV.1.2 Identification of candidate genes on the bases of shRNA screen

The success of an RNAi screen can be assessed by the false-positive and false-negative rates. The false negative rates usually estimated by measuring the hit rate for known positive control and negative control genes in specific phenotype readout. Reproducibility between replicates in each series of assays can provide information on false positive rates (Boutros and Ahringer, 2008). Insufficient silencing of genes might disturb the observable phenotype, and contribute to the false negative rate of the screen. The false positive rate of a primary screen can be estimated using the results of the secondary assays. Most, or all, of the positive hits identified in the primary screen after validation are likely to be 'real'. Secondary screens reveal which genes are of particular relevance (Boutros and Ahringer, 2008).

In this study, four candidates were initially selected upon screening. Of those, three were excluded; one (*Opsin*) due to incorrect sequence of the analyzed gene and two due to non-reproducible results when repeating the experiments. Therefore, the rate of false positives in this study, was as high as one percent, which is a low rate. Such a success rate can be achieved in a well-designed and well-controlled screen. On the other hand, false negative results might be obtained due to problems regarding transfection efficiency and knock-down efficacy of each individual shRNA. In this screen, it was not possible to exclude losing candidates due to a non-effective knock-down. In the present study, reproducible experiments showed fold change increases in apoptosis made by silencing of CHMP5, which was comparable to those made by positive controls, the well-known anti-apoptotic genes, *Birc4*, *Birc5* and *Birc7*. Therefore, we selected *CHMP5* as a proper candidate for further validation assays.

IV.1.2.1 Validation of CHMP5

Validation assays were performed to confirm the involvement of CHMP5 silencing in cell death. The possible risk for RNAi-induced off-target effects has recently been demonstrated. To exclude the possible off-target effects induced by shRNAs used in the first screen, we tested siRNAs targeting different sequences of *CHMP5* mRNA. As it was shown in Figure 12, CHMP5 silencing using both siRNAs increased the level of apoptosis, however, this effect was stronger for one of the siRNAs. Therefore, we used this siRNA in further analyses. The apoptotic phenotype observed by siRNA silencing of CHMP5 suggests that the apoptotic phenotype mediated by sh-CHMP5 was not due to an off-target effect, but was rather a CHMP5-specific phenotype. Quantitative RT-PCR was also used as a sensitive tool to measure target mRNA levels to ensure the effective knock-down in each experiment. To further validate and characterize the CHMP5 anti-apoptotic function, we performed over-expression assays by transfecting a human CHMP5 expression vector (pCMV6-CHMP5) into cells followed by the chemical induction of apoptosis using etoposide. The expected result was a reduction of apoptosis induced via addition of etoposide by over-presentation of an anti-apoptotic gene. In this experiment, induction of apoptosis was compensated by over expression of *Birc4* (positive control) and human CHMP5. Since CHMP5 is an evolutionary conserved gene, over-expression of the murine sequence also affected the percentage of cell death. This over-expression analysis showed that CHMP5 played a role in modulating chemically induced apoptosis and gave rise to the inverse CHMP5-phenotype compared to the CHMP5 loss-of function studies. This further emphasized an anti-apoptotic function for

CHMP5. Rescue experiments were also carried out successfully by co-transfection of human *CHMP5* shRNA together with human or murine CHMP5 over-expression vectors, thereby rescuing the phenotypic effect of CHMP5 over-expression. This represents a stringent way to verify the selectivity and the specificity of the knock-down phenotype.

IV.1.3 Further functional assays

IV.1.3.1 Caspase activity and apoptotic pathway

Common characteristics of most apoptotic processes are the activation of the caspase cascades. In general, activation of upstream caspase-9 is associated with mitochondria-mediated apoptosis (intrinsic pathway), whereas activation of caspase-8 frequently is mediated by death receptor-regulated apoptosis (extrinsic pathway). Activation of either pathway leads to activation of the downstream caspase-3/7. It has also been shown that the connection between these apoptotic pathways can be made by activated caspase-8, which triggers the intrinsic pathway, resulting in activation of caspase-9 and, thereafter, downstream caspases (Kaufmann and Hengartner, 2001; Donepudi and Grutter, 2002; Liu et al., 2005). Investigating CHMP5-mediated caspase cascade activation, we measured active caspase-8, 9 and 3/7 following CHMP5 silencing.

A challenge in caspase activity assays is to figure out the exact time point for correct measurement. The best time point can be identified by the differences between values of the negative and positive controls. In addition, an essential step to set up a caspase activity assay is utilization of proper positive controls for each particular assay. In the apoptosis pathways, FLIP and Birc4 are known as effective inhibitors of caspase 8 and caspase 9 activity (Philchenkov, 2004). Activity of caspase 8 or 9 can be altered by silencing of the FLIP and Birc4, respectively. In order to identify affected key pathway (extrinsic or intrinsic) in the apoptosis mediated by CHMP5 silencing, activated caspase 8 and 9 levels were monitored following CHMP5 modulation. Of significance, caspase 8 and 9 are apical caspases in the apoptotic pathway and, as such, are activated at an earlier time point than caspase 3/7 (terminator caspase in the pathway). In this study, the caspase activity following CHMP5 silencing was measured at different time points, starting 8 hours after transfection and continuously thereafter every 4 hours. The best results were obtained between 16 to 24 hours after transfection for caspase 8, 9, and at 48h for caspase 3/7. Based on our data, CHMP5 deficiency induces apoptosis by activation of caspase-3/7, mainly via caspase-8 extrinsic cascade activation. The slight activation of caspase-9 observed in this study might be a further

downstream consequence in the caspase cascade, due to cross-activation of the intrinsic pathway.

IV.1.3.2 Expression array analysis: genes and pathways affected by CHMP5 modulation

IV.1.3.2.1 Apoptosis related genes and expression changes induced by CHMP5 silencing

Considering the fact that apoptosis is controlled by many factors, and results from an imbalance between activity of genes that promote and genes that repress apoptosis, we conducted a microarray-based study to obtain comprehensive transcriptome patterns following CHMP5 modulation. Characterization of the regulatory effect of CHMP5 on transcriptome patterns indicated that a number of apoptosis-associated genes are dysregulated upon CHMP5 silencing (see tables 1 and 2). Apoptosis-inducer genes included:

- *ATF3* (activating transcription factor 3) which is known to induce apoptosis in cancer and enhances etoposide induced apoptosis in Hela cells, it promotes down regulation of anti-apoptotic genes such as *Bcl2*, *Bcl-XL* and *IAP* families (*Birc4* and *Birc3*) (Yan *et al.*, 2005; Hua *et al.*, 2006; Huang *et al.*, 2008),
- *PPP1R15A* (protein phosphates 1 regulatory subunit15A) that is involved in growth arrest and regulation of apoptosis (Ayllon *et al.*, 2000; Grishin *et al.*, 2001),
- *GADD45A* (Growth arrest and DNA-damage-inducible alpha), which contributes to apoptosis via activation of JNK and/or p38 MAPK signaling pathways (Takekawa and Saito, 1998).

Known genes with anti-apoptotic functions included:

- *CHMP2A* (Charged Multivesicular body Protein 2A, one of the CHMP family genes) (Wu *et al.*, 2006),
- *APBB3* (FE65-like protein), a gene with an apoptosis inhibitory domain (Cao *et al.*, 2000).
- *MSRB2* known as a gene with apoptotic inhibitory function (Kwak *et al.*, 2009).

According to the expression array analysis, CHMP5 indeed affects the activity of other genes involved in apoptosis, underlying its anti-apoptotic function via regulation of genes involved in apoptosis.

IV.1.3.2.2 Pathways affected by CHMP5 modulation

With the advent of microarrays, it was hoped that the knowledge of genome-wide expression levels will speed up the understanding of biological systems. The effect of induction and

repression of target genes on metabolic and regulatory pathways is important in human disease, particularly in cancer (Nakao et al., 1999). In the present study, the main goal of the genome-wide expression array analysis was to identify the impact of CHMP5 expression on other signaling pathways. Expression data were analysed using commercial ingenuity pathway analysis and a homemade comprehensive gene pathway analysis software (Engel et al, *in preparation*). Comprehensive gene pathway analysis software helps to identify pathways, which are potentially involved in human disease, particularly in cancer. Analysis of array data by comprehensive gene pathway analysis revealed that several pathways involved in different cancer types such as AML, prostate, thyroid, endometrial cancer were regulated upon CHMP5 modulation. Further pathways involved in metabolism and degradation of cell products were also affected.

Recent evidence indicates that disrupting the mouse *CHMP5* gene by homologous recombination results in a phenotype of early embryonic lethality, reflecting defective late endosomal function and dysregulation of multiple signaling pathways like NF- κ B and TGF β (transforming growth factor β). Dysregulation of TGF β signaling is attributed to the lack of degradation of internalized receptors (Horii *et al.*, 2006; Shim *et al.*, 2006). More detailed analysis using Ingenuity allowed us to identify genes implicated in the NF- κ B network. Most of those genes were apoptosis-related genes and were up-regulated upon CHMP5 deficiency. Functional study on NF- κ B activity using a reporter assay confirmed that NF- κ B activity is influenced by CHMP5 modulation. Thereby, apoptosis signaling triggered by CHMP5 deficiency can be mediated by the alteration of NF- κ B activity. In this study, apoptosis was observed as consequence of CHMP5 silencing. In addition, investigation of caspase cascade activation showed the impact of CHMP5 deficiency on activation of caspase 8 induced apoptosis and the involvement of the extrinsic apoptosis pathway. On the other hand, pathway analysis and reporter assays confirmed that NF- κ B activity is altered by CHMP5 silencing and over-expression. Previous studies showed that activation of membrane cell death receptors, like TNFR1, leads to activation of the caspase-8 cascade and the NF- κ B pathway (Kaufmann and Hengartner, 2001; Micheau and Tschopp, 2003; Dutta *et al.*, 2006). Interestingly, investigation of upstream molecular mechanisms leading to apoptosis induction by CHMP5 revealed significant changes in cellular surface expression of TNFR1 following CHMP5 modulation. In addition, expression array and IPA analysis revealed regulation of TNFR1-induced apoptotic genes such as *PEA-15* (Condorelli *et al.*, 1999). These observations suggest that TNFR1 could act as an effector to mediate apoptosis induction by CHMP5 deficiency, resulting in activation of the caspase 8 cascade and the extrinsic apoptotic pathway.

IV.1.4 Charged multivesicular body protein 5 (*CHMP5*); One gene, multiple functions

As a result of this screen, *CHMP5* was identified as a gene with an impact on apoptosis. All further experiments testing for specificity of the *CHMP5* knock-down phenotype, *CHMP5* over expression and rescue assays as well as specific caspase-inhibitor experiments and expression array analysis, confirmed an involvement in the apoptotic pathway.

CHMP5 gene is located on chromosome 9 (9p13.3). The *CHMP5* gene product is described as a member of the CHMP-family of coiled-coiled protein homologous to the yeast Vps60/MOS10 gene, and has been shown to be a component of the endosomal sorting complex required for the transport III (ESCRT-III) complex. ESCRT-III is involved in degradation of surface receptor proteins and in formation of endocytic multivesicular bodies (MVBs). It plays an important role in the modulation of various signaling pathways (Shim *et al.*, 2006; Hurley and Ren, 2009; Saksena and Emr, 2009; Wollert *et al.*, 2009). However, in addition to MVB formation, other functions like apoptosis modulation have been discussed for the members of the ESCRT-III complex (Wu *et al.*, 2006).

Interestingly, characterization of the regulatory effect of *CHMP5* on signaling pathways in the current study showed that PPAR, Notch and mTOR signaling were effectively dysregulated upon *CHMP5* modulation. In addition, many NF- κ B associated factors influencing apoptosis were dysregulated upon silencing of *CHMP5*. Likewise, the functional experiments in our study showed significant changes in cell surface expression of TNFR1 and in NF- κ B activity in *CHMP5* modulated cells. It is known that TNFR1 triggers distinct signaling pathways, leading to both to the activation of NF- κ B transcription factors, as well as the induction of apoptosis (Micheau and Tschopp, 2003; Dutta *et al.*, 2006). In addition to the well known functions of NF- κ B, it was recently shown that, in a certain context, NF- κ B activation may result in the expression of pro-apoptotic genes inducing apoptotic pathways (He and Ting, 2002; Siebenlist *et al.*, 2005; Thyss *et al.*, 2005). Moreover, several interaction partners of *CHMP5* in the ESCRTIII complex, like *CHMP2A*, *B*, *CHMP4A* and *CHMP6* (Tsang *et al.*, 2006) have also been shown to be regulated by *CHMP5* modulation. All these findings suggest that the effect of *CHMP5* on apoptosis is mediated via possible changes in the ESCRTIII complex, thereafter resulting in the regulation of different pathways such as NF- κ B-signaling.

CHMP5 is a unique CHMP family protein that does not belong to any other subfamily of CHMP proteins. It may probably play roles beyond those described for the endocytic pathway.

The 5' end of the *CHMP5* gene is separated by only 414 base pairs (bp) from the opposing strand of the *Bag1* gene (Takayama and Reed, 2001), suggesting that both genes may be co-regulated at the transcriptional level. Bag1 is clearly involved in the modulation of apoptosis, cell proliferation, transcription and cell motility as a multifunctional regulator. This could imply that CHMP5 might participate in functions modulated by Bag1.

IV.2 RNAi screen in the breast cancer cells

IV.2.1 Expression profiling revealed candidate genes for functional study

In a recent study, expression profiling of breast cancer patients with complete response and non-response was performed to identify gene expression signatures predicting pathologic complete response to gemcitabine, epirubicin, and docetaxel treatment in primary breast cancer (Thuerigen *et al.*, 2006). In the current work, the expression data obtained from that study was considered to identify genes over-expressed in pNC when compared to the pCR group. Significant analysis of microarrays identified 115 genes that were significantly up-regulated in pNC group. Based on available siRNAs, 107 of these genes were selected as candidate genes for functional screening for their impact on cell survival. A candidate gene, which could be identified in such a screening, may prove to underlie the resistance to therapy or in general acting as a pro survival gene over-expressed in tumor cells.

IV.2.2 siRNA screen and identification of genes involved in cell survival

The major aim of this study was to identify a target gene, whose siRNA-induced knock-down would efficiently trigger cell death. In order to perform a successful screen using siRNAs, efficient delivery of highly functional and specific siRNA molecules into appropriate cells is required. Upon examination of different transfection reagent and approaches, siPORT™ NeoFX™ was selected for reverse transfection of MCF7 cells in a 96 well format. Using this method, the extent of cell death was comparable among different transfection experiments, and positive and negative controls provided the thresholds that allowed us to determine, whether a siRNA can be considered as a positive, negative or neutral effector in the assay.

Several studies showed that the smaller transfected constructs provide better transfection efficiency. SiRNAs with 20-21 nucleotides in length are more easily to transfect than larger expression plasmids coding for shRNAs. Therefore, we used siRNAs (pool sequences) for the screening approach. By using pools of four siRNAs targeting one single gene, we reduced the

costs of screening, but this event might have also increased the chance for off-target effects of a single siRNA on an observed phenotype (Elbashir *et al.*, 2001b). This can be overcome by retesting single siRNAs separately. In order to estimate the hit rate and to minimize the false negative rate, three anti-apoptotic genes were selected as positive controls. Reproducible results from replicate wells provided information about the value of the readout for this screening. The three independent positive controls (*Birc4*, *Birc5* and *Birc7*) used in this screen covered both weak and strong hits, which allowed the detection of weak and strong candidate genes. Weak signals could be caused either by partial knock-down of a gene, which potentially has a strong effect, or a strong knock-down of a gene potentially having a weak effect (Boutros and Ahringer, 2008). A number of negative controls including all-stars negative control, siRNAs targeting *firefly* luciferase or *GFP* tested in this study were used to evaluate off-target effects. A reproducible decrease in cell viability achieved by knock-down of *Birc5*, provided a strong upper threshold for selecting candidates. In addition, to consider the partial knock-down event, siRNAs showing a lower threshold (*Birc4*, and-7, each one representing a weak positive control) were additionally re-tested in the validation experiments. *Birc5* deficiency effectively reduced the cell viability of MCF7 cells, therefore we used si-*Birc5* as a proper positive control for further analysis. All negative controls were used for initial screening. We selected one of them, si-GFP, to be used as negative control in additional assays. Since the gene knock-down efficiency was not tested in the RNAi screen, siRNAs causing reduction in cell viability were further analyzed in the validation assay. Therefore, eight candidates were selected for retesting in single assays and of those, only one (*PPP1R15B*), which was positive in the screen.

IV.2.3 Validation of the candidate gene *PPP1R15B*

Validation experiments are important for identifying the genes that are particularly relevant to the phenotype of interest (Moffat *et al.*, 2006; Boutros and Ahringer, 2008). In this study, validation of a single candidate gene was performed by separately transfecting up to four single siRNA sequences into MCF7 cells. Validation of a candidate gene was scored positive, if at least two out of four siRNA sequences reduced cell viability to a similar degree as the pooled siRNAs targeting the candidate. Recent publications discussed that two or more siRNA sequences that knock-down the target gene and elicit the same phenotype, are sufficient to proof target specificity (Boutros and Ahringer, 2008). In the current study, two of four single siRNAs targeting *PPP1R15B* led to reduction of cell viability comparable to the pooled siRNAs in the screening. The results from the cell viability reduction were in

concordance with knock-down efficiency measured by qRT-PCR. In addition, knock-down efficiency of the most effective single siRNA targeting *PPP1R15B* was also examined at the protein level by western blot analysis. A strong western blot signal is limited by the short half-life of the PPP1R15B protein (about 45min) (Jousse *et al.*, 2003). However, following this straightforward approach, PPP1R15B was identified as a potential validated candidate with a high capacity to reduce cell viability in MCF7 cells after knock-down by using additional functional assays.

IV.2.4 PPP1R15B deficiency reduced cell proliferation and induced apoptosis in breast cancer cell line

The balance between proliferation and apoptosis is crucial in determining the overall growth or regression of the tumor in response to chemotherapy. In the current work, we identified *PPP1R15B* as a gene involved in the viability of MCF7 cells. Reduction of cell viability could be a consequence of a stop in cell proliferation and/or increase in cell death. Therefore, we examined cell proliferation by FACS-based method. As it was shown in 27, cell proliferation is reduced about 50% by PPP1R15B deficiency. An apoptosis assay was performed to determine the effect of the PPP1R15B knock-down in MCF7 cells. Considering the sub-G1 population as apoptotic cells, PPP1R15B deficiency increased apoptosis more than four fold over the negative control.

Activation of caspase 3/7 following PPP1R15B silencing was not increased as strongly as the Birc5 knock-down. This might be due to inappropriate time point for measuring caspase activity for the PPP1R15B knock-down experiment or may indicate that this gene exerts its anti-apoptosis property through other cellular process (like cell proliferation) rather than direct control of apoptosis. Silencing of PPP1R15B could impair the cell proliferation process leading to cell death as a secondary effect or PPP1R15B deficiency does not lead to activate caspase3/7 properly. Reduction of cell proliferation on one hand and induction of apoptosis on the other hand by PPP1R15B silencing in MCF7 breast cancer cells, provided supporting evidence on contribution of this gene to breast cancer.

Cell cycle analysis of the siRNA-PPP1R15B knock-down and control siRNA-GFP revealed significant differences. In the present study, FACS analysis of the stained DNA using propidium iodide showed an arrest in G1 phase of cell cycle distribution by PPP1R15B deficiency. Based on the results obtained from the cell cycle analysis, reduction of proliferative cells could be a consequence of cell cycle arrest following PPP1R15B deficiency. The current study suggests the involvement of PPP1R15B in cell cycle progression and

survival of breast cancer cell line MCF7.

An interesting issue regarding the PPP1R15B is the consequence of knock-down in other breast cancer cells. The phenotypic effect of PPP1R15B silencing may be better detected in cells with higher endogenous expression. Therefore, cell lines such as MDA-MB231 and T47D with expression levels comparable to MCF7 were selected for PPP1R15B knock-down and cell viability assay. Among these cell lines, successful transfection of gene siRNAs was achieved for MCF7 and MDA-MB231. Of those cell lines, only MCF7 showed around 45% reduction in cell viability upon silencing of PPP1R15B. In addition, one of the low *PPP1R15B* expressing cells, SKBR3, was also tested for silencing effect of PPP1R15B. Interestingly, despite successful silencing, deficiency of PPP1R15B did not affect the cell viability of MDA-MB231 and SKBR3 cells. Since breast cancer is a heterogeneous disorder, observed variations in effect of PPP1R15B deficiency on cell viability in different breast cancer cell lines might be due to the different molecular properties of these cells. One major difference between these cells is the exclusive over-presence of estrogen receptor (ER) and progesterone receptor (PR) in MCF7 cells (Sotiriou et al., 2003; Neve et al., 2006). ER refers to a group of receptors that are activated by estrogen hormones (Dahlman-Wright et al., 2006). The main function of the ER is to regulate gene expression, as a DNA binding transcription factor (Dahlman-Wright et al., 2006). However, the ER has additional functions independent of DNA binding (Levin, 2005). The progesterone receptor also known as NR3C3 (nuclear receptor subfamily 3, group C, member 3), is an intracellular steroid receptor that specifically binds to progesterone hormone (Gadkar-Sable et al., 2005). ER and PR both have an effect on cell proliferation through activating the transcription of genes involved in cell growth and proliferation (Lange, 2008). Over presentation of ER or PR (“ER positive” and “PR positive”) in different types of breast cancer cell lines has previously reported (Neve et al., 2006). Of those cell lines tested in this study, MCF7 and T47D are ER positive/PR positive; MDA-MB231 and SKBR3 are described as ER negative/PR negative cell lines (Neve et al., 2006). Considering these molecular differences and our observation that silencing of PPP1R15B resulted in decreased viability only in MCF7 cells, it is likely that PPP1R15B deficiency exerts its effect on cell viability via specific pathways that are regulated by hormone receptors such as estrogen and progesterone receptors.

IV.2.5 PPP1R15B, an interesting target for chemotherapeutic studies

Protein phosphatase 1 regulatory (inhibitor) subunit 15B (*PPP1R15B*) is located on chromosome 1q32.1. Previous studies showed that PPP1R15B has the ability to associate with the catalytic phosphatase PPP1 subunit and to repress eIF2 phosphorylation when over-expressed (Jousse *et al.*, 2003; Harding *et al.*, 2009). Eukaryotic translation initiation factor 2 α (eIF2 α) phosphorylation inhibits protein translation initiation. Therefore, dephosphorylation of eIF2 leads to activation of the protein synthesis machinery. In knock-out PPP1R15B mice, arrest of embryos lacking PPP1R15B at the preimplantation stage was consistent with a role of the protein in eIF2 (α PI) dephosphorylation (Harding *et al.*, 2009). In the current study, we identified the involvement of PPP1R15B in MCF7 cell proliferation and survival. These observations are in concordance with the ability of this gene to dephosphorylate eIF2, which is critical for cell viability.

Expression array analysis of responding and non-responding breast cancer patients to chemotherapy revealed the *PPP1R15B* gene as an over-expressed gene in non-responding patients. Merging patients data and data produced from functional assays in cancer cell lines, suggests to further investigation of a possible role for *PPP1R15B* in resistance to chemotherapy.

V. Literature

- Adams, J.M. (2003). Ways of dying: multiple pathways to apoptosis. *Genes Dev* 17, 2481-2495.
- Ashkenazi, A., and Dixit, V.M. (1998). Death receptors: signaling and modulation. *Science* 281, 1305-1308.
- Ayllon, V., Martinez, A.C., Garcia, A., Cayla, X., and Rebollo, A. (2000). Protein phosphatase 1alpha is a Ras-activated Bad phosphatase that regulates interleukin-2 deprivation-induced apoptosis. *EMBO J* 19, 2237-2246.
- Aza-Blanc, P., Cooper, C.L., Wagner, K., Batalov, S., Deveraux, Q.L., and Cooke, M.P. (2003). Identification of modulators of TRAIL-induced apoptosis via RNAi-based phenotypic screening. *Mol Cell* 12, 627-637.
- Barrett, K.L., Willingham, J.M., Garvin, A.J., and Willingham, M.C. (2001). Advances in cytochemical methods for detection of apoptosis. *J Histochem Cytochem* 49, 821-832.
- Birney, E., Stamatoyannopoulos, J.A., Dutta, A., Guigo, R., Gingeras, T.R., et al. (2007). Identification and analysis of functional elements in 1% of the human genome by the ENCODE pilot project. *Nature* 447, 799-816.
- Bodmer, J.L., Holler, N., Reynard, S., Vinciguerra, P., Schneider, P., Juo, P., Blenis, J., and Tschopp, J. (2000). TRAIL receptor-2 signals apoptosis through FADD and caspase-8. *Nat Cell Biol* 2, 241-243.
- Borner, C. (2003). The Bcl-2 protein family: sensors and checkpoints for life-or-death decisions. *Mol Immunol* 39, 615-647.
- Boutros, M., and Ahringer, J. (2008). The art and design of genetic screens: RNA interference. *Nat Rev Genet* 9, 554-566.
- Brummelkamp, T.R., Bernards, R., and Agami, R. (2002). A system for stable expression of short interfering RNAs in mammalian cells. *Science* 296, 550-553.
- Cao, H., Pratt, N., Mattison, J., Zhao, Y., and Chang, N.S. (2000). Characterization of an apoptosis inhibitory domain at the C-termini of FE65-like protein. *Biochem Biophys Res Commun* 276, 843-850.
- Check, E. (2007). RNA interference: hitting the on switch. *Nature* 448, 855-858.
- Chowdhury, I., Tharakan, B., and Bhat, G.K. (2006). Current concepts in apoptosis: the physiological suicide program revisited. *Cell Mol Biol Lett* 11, 506-525.
- Condorelli, G., Vigliotta, G., Cafieri, A., Trencia, A., Andalo, P., Oriente, F., Miele, C., Caruso, M., Formisano, P., and Beguinot, F. (1999). PED/PEA-15: an anti-apoptotic molecule that regulates FAS/TNFR1-induced apoptosis. *Oncogene* 18, 4409-4415.
- Cotter, T.G. (2009). Apoptosis and cancer: the genesis of a research field. *Nat Rev Cancer* 9, 501-507.
- Crawford, A.M., Kerr, J.F., and Currie, A.R. (1972). The relationship of acute mesodermal cell death to the teratogenic effects of 7-OHM-12-MBA in the foetal rat. *Br J Cancer* 26, 498-503.
- Dahlman-Wright, K., Cavailles, V., Fuqua, S.A., Jordan, V.C., Katzenellenbogen, J.A., Korach, K.S., Maggi, A., Muramatsu, M., Parker, M.G., and Gustafsson, J.A. (2006). International Union of Pharmacology. LXIV. Estrogen receptors. *Pharmacol Rev* 58, 773-781.
- Deveraux, Q.L., Roy, N., Stennicke, H.R., Van Arsdale, T., Zhou, Q., Srinivasula, S.M., Alnemri, E.S., Salvesen, G.S., and Reed, J.C. (1998). IAPs block apoptotic events induced by caspase-8 and cytochrome c by direct inhibition of distinct caspases. *EMBO J* 17, 2215-2223.
- Domchek, S.M., and Weber, B.L. (2006). Clinical management of BRCA1 and BRCA2

- mutation carriers. *Oncogene* 25, 5825-5831.
- Donepudi, M., and Grutter, M.G. (2002). Structure and zymogen activation of caspases. *Biophys Chem* 101-102, 145-153.
- Dutta, J., Fan, Y., Gupta, N., Fan, G., and Gelinas, C. (2006). Current insights into the regulation of programmed cell death by NF-kappaB. *Oncogene* 25, 6800-6816.
- Earnshaw, W.C. (1995). Nuclear changes in apoptosis. *Curr Opin Cell Biol* 7, 337-343.
- Eberwine, J., Yeh, H., Miyashiro, K., Cao, Y., Nair, S., Finnell, R., Zettel, M., and Coleman, P. (1992). Analysis of gene expression in single live neurons. *Proc Natl Acad Sci U S A* 89, 3010-3014.
- Echeverri, C.J., and Perrimon, N. (2006). High-throughput RNAi screening in cultured cells: a user's guide. *Nat Rev Genet* 7, 373-384.
- Elbashir, S.M., Harborth, J., Lendeckel, W., Yalcin, A., Weber, K., and Tuschl, T. (2001a). Duplexes of 21-nucleotide RNAs mediate RNA interference in cultured mammalian cells. *Nature* 411, 494-498.
- Elbashir, S.M., Harborth, J., Weber, K., and Tuschl, T. (2002). Analysis of gene function in somatic mammalian cells using small interfering RNAs. *Methods* 26, 199-213.
- Elbashir, S.M., Lendeckel, W., and Tuschl, T. (2001b). RNA interference is mediated by 21- and 22-nucleotide RNAs. *Genes Dev* 15, 188-200.
- Erfle, H., Neumann, B., Liebel, U., Rogers, P., Held, M., Walter, T., Ellenberg, J., and Pepperkok, R. (2007). Reverse transfection on cell arrays for high content screening microscopy. *Nat Protoc* 2, 392-399.
- Fire, A., Xu, S., Montgomery, M.K., Kostas, S.A., Driver, S.E., and Mello, C.C. (1998). Potent and specific genetic interference by double-stranded RNA in *Caenorhabditis elegans*. *Nature* 391, 806-811.
- Gadkar-Sable, S., Shah, C., Rosario, G., Sachdeva, G., and Puri, C. (2005). Progesterone receptors: various forms and functions in reproductive tissues. *Front Biosci* 10, 2118-2130.
- Ghavami, S., Hashemi, M., Ande, S.R., Yeganeh, B., Xiao, W., Eshraghi, M., Bus, C.J., Kadkhoda, K., Wiechec, E., Halayko, A.J., and Los, M. (2009a). Apoptosis and cancer: mutations within caspase genes. *J Med Genet* 46, 497-510.
- Ghavami, S., Hashemi, M., Ande, S.R., Yeganeh, B., Xiao, W., Eshraghi, M., Bus, C.J., Kadkhoda, K., Wiechec, E., Halayko, A.J., and Los, M. (2009b). Apoptosis and Cancer: Mutations within Caspase Genes. *J Med Genet*.
- Grishin, A.V., Azhipa, O., Semenov, I., and Corey, S.J. (2001). Interaction between growth arrest-DNA damage protein 34 and Src kinase Lyn negatively regulates genotoxic apoptosis. *Proc Natl Acad Sci U S A* 98, 10172-10177.
- Hacker, G. (2000). The morphology of apoptosis. *Cell Tissue Res* 301, 5-17.
- Hanahan, D., and Weinberg, R.A. (2000). The hallmarks of cancer. *Cell* 100, 57-70.
- Hannon, G.J. (2002). RNA interference. *Nature* 418, 244-251.
- Hardin, J.A., Sherr, D.H., DeMaria, M., and Lopez, P.A. (1992). A simple fluorescence method for surface antigen phenotyping of lymphocytes undergoing DNA fragmentation. *J Immunol Methods* 154, 99-107.
- Harding, H.P., Zhang, Y., Scheuner, D., Chen, J.J., Kaufman, R.J., and Ron, D. (2009). Ppp1r15 gene knockout reveals an essential role for translation initiation factor 2 alpha (eIF2alpha) dephosphorylation in mammalian development. *Proc Natl Acad Sci U S A* 106, 1832-1837.
- He, K.L., and Ting, A.T. (2002). A20 inhibits tumor necrosis factor (TNF) alpha-induced apoptosis by disrupting recruitment of TRADD and RIP to the TNF receptor 1 complex in Jurkat T cells. *Mol Cell Biol* 22, 6034-6045.
- Horii, M., Shibata, H., Kobayashi, R., Katoh, K., Yorikawa, C., Yasuda, J., and Maki, M. (2006). CHMP7, a novel ESCRT-III-related protein, associates with CHMP4b and

- functions in the endosomal sorting pathway. *Biochem J* 400, 23-32.
- Hua, B., Tamamori-Adachi, M., Luo, Y., Tamura, K., Morioka, M., Fukuda, M., Tanaka, Y., and Kitajima, S. (2006). A splice variant of stress response gene ATF3 counteracts NF-kappaB-dependent anti-apoptosis through inhibiting recruitment of CREB-binding protein/p300 coactivator. *J Biol Chem* 281, 1620-1629.
- Huang, X., Li, X., and Guo, B. (2008). KLF6 induces apoptosis in prostate cancer cells through up-regulation of ATF3. *J Biol Chem* 283, 29795-29801.
- Hurley, J.H., and Ren, X. (2009). The circuitry of cargo flux in the ESCRT pathway. *J Cell Biol* 185, 185-187.
- Idriss, H.T., and Naismith, J.H. (2000). TNF alpha and the TNF receptor superfamily: structure-function relationship(s). *Microsc Res Tech* 50, 184-195.
- Jackson, A.L., Bartz, S.R., Schelter, J., Kobayashi, S.V., Burchard, J., Mao, M., Li, B., Cavet, G., and Linsley, P.S. (2003). Expression profiling reveals off-target gene regulation by RNAi. *Nat Biotechnol* 21, 635-637.
- Jiang, X., and Wang, X. (2000). Cytochrome c promotes caspase-9 activation by inducing nucleotide binding to Apaf-1. *J Biol Chem* 275, 31199-31203.
- Jousse, C., Oyadomari, S., Novoa, I., Lu, P., Zhang, Y., Harding, H.P., and Ron, D. (2003). Inhibition of a constitutive translation initiation factor 2alpha phosphatase, CREP, promotes survival of stressed cells. *J Cell Biol* 163, 767-775.
- Kamath, R.S., and Ahringer, J. (2003). Genome-wide RNAi screening in *Caenorhabditis elegans*. *Methods* 30, 313-321.
- Kaufmann, S.H., and Hengartner, M.O. (2001). Programmed cell death: alive and well in the new millennium. *Trends Cell Biol* 11, 526-534.
- Kerr, J.F. (2002). History of the events leading to the formulation of the apoptosis concept. *Toxicology* 181-182, 471-474.
- Kerr, J.F., Winterford, C.M., and Harmon, B.V. (1994). Apoptosis. Its significance in cancer and cancer therapy. *Cancer* 73, 2013-2026.
- Kerr, J.F., Wyllie, A.H., and Currie, A.R. (1972). Apoptosis: a basic biological phenomenon with wide-ranging implications in tissue kinetics. *Br J Cancer* 26, 239-257.
- Kiger, A.A., Baum, B., Jones, S., Jones, M.R., Coulson, A., Echeverri, C., and Perrimon, N. (2003). A functional genomic analysis of cell morphology using RNA interference. *J Biol* 2, 27.
- Kittler, J., and Moss, S. (2006). *The Dynamic Synapse: Molecular Methods in Ionotropic Receptor Biology*. Taylor & Francis Group.
- Kittler, R., Pelletier, L., Heninger, A.K., Slabicki, M., Theis, M., Miroslaw, L., Poser, I., Lawo, S., Grabner, H., Kozak, K., Wagner, J., Surendranath, V., Richter, C., Bowen, W., Jackson, A.L., Habermann, B., Hyman, A.A., and Buchholz, F. (2007). Genome-scale RNAi profiling of cell division in human tissue culture cells. *Nat Cell Biol* 9, 1401-1412.
- Koopman, G., Reutelingsperger, C.P., Kuijten, G.A., Keehnen, R.M., Pals, S.T., and van Oers, M.H. (1994). Annexin V for flow cytometric detection of phosphatidylserine expression on B cells undergoing apoptosis. *Blood* 84, 1415-1420.
- Kwak, G.H., Kim, J.R., and Kim, H.Y. (2009). Expression, subcellular localization, and antioxidant role of mammalian methionine sulfoxide reductases in *Saccharomyces cerevisiae*. *BMB Rep* 42, 113-118.
- LaCasse, E.C., Baird, S., Korneluk, R.G., and MacKenzie, A.E. (1998). The inhibitors of apoptosis (IAPs) and their emerging role in cancer. *Oncogene* 17, 3247-3259.
- Lange, C.A. (2008). Integration of progesterone receptor action with rapid signaling events in breast cancer models. *J Steroid Biochem Mol Biol* 108, 203-212.
- Lavrik, I.N., Golks, A., and Krammer, P.H. (2005). Caspases: pharmacological manipulation of cell death. *J Clin Invest* 115, 2665-2672.

- Lettre, G., Kritikou, E.A., Jaeggi, M., Calixto, A., Fraser, A.G., Kamath, R.S., Ahringer, J., and Hengartner, M.O. (2004). Genome-wide RNAi identifies p53-dependent and -independent regulators of germ cell apoptosis in *C. elegans*. *Cell Death Differ* 11, 1198-1203.
- Levin, E.R. (2005). Integration of the extranuclear and nuclear actions of estrogen. *Mol Endocrinol* 19, 1951-1959.
- Li-Weber, M., Giasi, M., and Krammer, P.H. (1998). Involvement of Jun and Rel proteins in up-regulation of interleukin-4 gene activity by the T cell accessory molecule CD28. *J Biol Chem* 273, 32460-32466.
- Li, J., and Yuan, J. (2008). Caspases in apoptosis and beyond. *Oncogene* 27, 6194-6206.
- Li, P., Nijhawan, D., Budihardjo, I., Srinivasula, S.M., Ahmad, M., Alnemri, E.S., and Wang, X. (1997). Cytochrome c and dATP-dependent formation of Apaf-1/caspase-9 complex initiates an apoptotic protease cascade. *Cell* 91, 479-489.
- Liu, Z., Lu, H., Jiang, Z., Pastuszyn, A., and Hu, C.A. (2005). Apolipoprotein I6, a novel proapoptotic Bcl-2 homology 3-only protein, induces mitochondria-mediated apoptosis in cancer cells. *Mol Cancer Res* 3, 21-31.
- Lund, E., Guttinger, S., Calado, A., Dahlberg, J.E., and Kutay, U. (2004). Nuclear export of microRNA precursors. *Science* 303, 95-98.
- Luschen, S., Ussat, S., Scherer, G., Kabelitz, D., and Adam-Klages, S. (2000). Sensitization to death receptor cytotoxicity by inhibition of fas-associated death domain protein (FADD)/caspase signaling. Requirement of cell cycle progression. *J Biol Chem* 275, 24670-24678.
- MacKeigan, J.P., Murphy, L.O., and Blenis, J. (2005). Sensitized RNAi screen of human kinases and phosphatases identifies new regulators of apoptosis and chemoresistance. *Nat Cell Biol* 7, 591-600.
- Mannherz, O., Mertens, D., Hahn, M., and Lichter, P. (2006). Functional screening for proapoptotic genes by reverse transfection cell array technology. *Genomics* 87, 665-672.
- Mattila, J., Kallijarvi, J., and Puig, O. (2008). RNAi screening for kinases and phosphatases identifies FoxO regulators. *Proc Natl Acad Sci U S A* 105, 14873-14878.
- Mello, C.C., and Conte, D., Jr. (2004). Revealing the world of RNA interference. *Nature* 431, 338-342.
- Micheau, O., and Tschopp, J. (2003). Induction of TNF receptor I-mediated apoptosis via two sequential signaling complexes. *Cell* 114, 181-190.
- Moffat, J., Grueneberg, D.A., Yang, X., Kim, S.Y., Kloepfer, A.M., Hinkle, G., Piqani, B., Eisenhaure, T.M., Luo, B., Grenier, J.K., Carpenter, A.E., Foo, S.Y., Stewart, S.A., Stockwell, B.R., Hacohen, N., Hahn, W.C., Lander, E.S., Sabatini, D.M., and Root, D.E. (2006). A lentiviral RNAi library for human and mouse genes applied to an arrayed viral high-content screen. *Cell* 124, 1283-1298.
- Mousses, S., Caplen, N.J., Cornelison, R., Weaver, D., Basik, M., Hautaniemi, S., Elkahloun, A.G., Lotufo, R.A., Choudary, A., Dougherty, E.R., Suh, E., and Kallioniemi, O. (2003). RNAi microarray analysis in cultured mammalian cells. *Genome Res* 13, 2341-2347.
- Nakao, M., Bono, H., Kawashima, S., Kamiya, T., Sato, K., Goto, S., and Kanehisa, M. (1999). Genome-scale Gene Expression Analysis and Pathway Reconstruction in KEGG. *Genome Inform Ser Workshop Genome Inform* 10, 94-103.
- Neumann, B., Held, M., Liebel, U., Erfle, H., Rogers, P., Pepperkok, R., and Ellenberg, J. (2006). High-throughput RNAi screening by time-lapse imaging of live human cells. *Nat Methods* 3, 385-390.
- Neve, R.M., Chin, K., Fridlyand, J., Yeh, J., Baehner, F.L., Fevr, T., Clark, L., Bayani, N., Coppe, J.P., Tong, F., Speed, T., Spellman, P.T., DeVries, S., Lapuk, A., Wang, N.J.,

- Kuo, W.L., Stilwell, J.L., Pinkel, D., Albertson, D.G., Waldman, F.M., McCormick, F., Dickson, R.B., Johnson, M.D., Lippman, M., Ethier, S., Gazdar, A., and Gray, J.W. (2006). A collection of breast cancer cell lines for the study of functionally distinct cancer subtypes. *Cancer Cell* *10*, 515-527.
- Nicoletti, I., Migliorati, G., Pagliacci, M.C., Grignani, F., and Riccardi, C. (1991). A rapid and simple method for measuring thymocyte apoptosis by propidium iodide staining and flow cytometry. *J Immunol Methods* *139*, 271-279.
- Nollen, E.A., Garcia, S.M., van Haften, G., Kim, S., Chavez, A., Morimoto, R.I., and Plasterk, R.H. (2004). Genome-wide RNA interference screen identifies previously undescribed regulators of polyglutamine aggregation. *Proc Natl Acad Sci U S A* *101*, 6403-6408.
- Paddison, P.J., Caudy, A.A., Bernstein, E., Hannon, G.J., and Conklin, D.S. (2002). Short hairpin RNAs (shRNAs) induce sequence-specific silencing in mammalian cells. *Genes Dev* *16*, 948-958.
- Parkin, D.M., Bray, F., Ferlay, J., and Pisani, P. (2001). Estimating the world cancer burden: Globocan 2000. *Int J Cancer* *94*, 153-156.
- Parton, M., Dowsett, M., and Smith, I. (2001). Studies of apoptosis in breast cancer. *BMJ* *322*, 1528-1532.
- Peter, M.E., and Krammer, P.H. (2003). The CD95(APO-1/Fas) DISC and beyond. *Cell Death Differ* *10*, 26-35.
- Philchenkov, A. (2004). Caspases: potential targets for regulating cell death. *J Cell Mol Med* *8*, 432-444.
- Pscherer, A., Schliwka, J., Wildenberger, K., Mincheva, A., Schwaenen, C., Dohner, H., Stilgenbauer, S., and Lichter, P. (2006). Antagonizing inactivated tumor suppressor genes and activated oncogenes by a versatile transgenesis system: application in mantle cell lymphoma. *FASEB J* *20*, 1188-1190.
- Rahman, N., Seal, S., Thompson, D., Kelly, P., Renwick, A., Elliott, A., Reid, S., Spanova, K., Barfoot, R., Chagtai, T., Jayatilake, H., McGuffog, L., Hanks, S., Evans, D.G., Eccles, D., Easton, D.F., and Stratton, M.R. (2007). PALB2, which encodes a BRCA2-interacting protein, is a breast cancer susceptibility gene. *Nat Genet* *39*, 165-167.
- Reed, J.C. (1999). Dysregulation of apoptosis in cancer. *J Clin Oncol* *17*, 2941-2953.
- Renwick, A., Thompson, D., Seal, S., Kelly, P., Chagtai, T., Ahmed, M., North, B., Jayatilake, H., Barfoot, R., Spanova, K., McGuffog, L., Evans, D.G., Eccles, D., Easton, D.F., Stratton, M.R., and Rahman, N. (2006). ATM mutations that cause ataxia-telangiectasia are breast cancer susceptibility alleles. *Nat Genet* *38*, 873-875.
- Riedl, S.J., and Shi, Y. (2004). Molecular mechanisms of caspase regulation during apoptosis. *Nat Rev Mol Cell Biol* *5*, 897-907.
- Rines, D.R., Gomez-Ferreria, M.A., Zhou, Y., DeJesus, P., Grob, S., Batalov, S., Labow, M., Huesken, D., Mickanin, C., Hall, J., Reinhardt, M., Natt, F., Lange, J., Sharp, D.J., Chanda, S.K., and Caldwell, J.S. (2008). Whole genome functional analysis identifies novel components required for mitotic spindle integrity in human cells. *Genome Biol* *9*, R44.
- Rodriguez, J., and Lazebnik, Y. (1999). Caspase-9 and APAF-1 form an active holoenzyme. *Genes Dev* *13*, 3179-3184.
- Rosenblum, B.B., Lee, L.G., Spurgeon, S.L., Khan, S.H., Menchen, S.M., Heiner, C.R., and Chen, S.M. (1997). New dye-labeled terminators for improved DNA sequencing patterns. *Nucleic Acids Res* *25*, 4500-4504.
- Saksena, S., and Emr, S.D. (2009). ESCRTs and human disease. *Biochem Soc Trans* *37*, 167-172.
- Salvesen, G.S., and Dixit, V.M. (1997). Caspases: intracellular signaling by proteolysis. *Cell* *91*, 443-446.

- Salvesen, G.S., and Duckett, C.S. (2002). IAP proteins: blocking the road to death's door. *Nat Rev Mol Cell Biol* 3, 401-410.
- Sanger, F., Nicklen, S., and Coulson, A.R. (1977). DNA sequencing with chain-terminating inhibitors. *Proc Natl Acad Sci U S A* 74, 5463-5467.
- Schulze-Osthoff, K., Ferrari, D., Los, M., Wesselborg, S., and Peter, M.E. (1998). Apoptosis signaling by death receptors. *Eur J Biochem* 254, 439-459.
- Sgonc, R., Gruschwitz, M.S., Dietrich, H., Recheis, H., Gershwin, M.E., and Wick, G. (1996). Endothelial cell apoptosis is a primary pathogenetic event underlying skin lesions in avian and human scleroderma. *J Clin Invest* 98, 785-792.
- Shi, Y. (2002). Mechanisms of caspase activation and inhibition during apoptosis. *Mol Cell* 9, 459-470.
- Shim, J.H., Xiao, C., Hayden, M.S., Lee, K.Y., Trombetta, E.S., Pypaert, M., Nara, A., Yoshimori, T., Wilm, B., Erdjument-Bromage, H., Tempst, P., Hogan, B.L., Mellman, I., and Ghosh, S. (2006). CHMP5 is essential for late endosome function and down-regulation of receptor signaling during mouse embryogenesis. *J Cell Biol* 172, 1045-1056.
- Shiozaki, E.N., Chai, J., Rigotti, D.J., Riedl, S.J., Li, P., Srinivasula, S.M., Alnemri, E.S., Fairman, R., and Shi, Y. (2003). Mechanism of XIAP-mediated inhibition of caspase-9. *Mol Cell* 11, 519-527.
- Siebenlist, U., Brown, K., and Claudio, E. (2005). Control of lymphocyte development by nuclear factor-kappaB. *Nat Rev Immunol* 5, 435-445.
- Singh, A., Ni, J., and Aggarwal, B.B. (1998). Death domain receptors and their role in cell demise. *J Interferon Cytokine Res* 18, 439-450.
- Snove, O., Jr., and Holen, T. (2004). Many commonly used siRNAs risk off-target activity. *Biochem Biophys Res Commun* 319, 256-263.
- Sotiriou, C., Neo, S.Y., McShane, L.M., Korn, E.L., Long, P.M., Jazaeri, A., Martiat, P., Fox, S.B., Harris, A.L., and Liu, E.T. (2003). Breast cancer classification and prognosis based on gene expression profiles from a population-based study. *Proc Natl Acad Sci U S A* 100, 10393-10398.
- Sturzl, M., Konrad, A., Sander, G., Wies, E., Neipel, F., Naschberger, E., Reipschlagel, S., Gonin-Laurent, N., Horch, R.E., Kneser, U., Hohenberger, W., Erfle, H., and Thureau, M. (2008). High throughput screening of gene functions in mammalian cells using reversely transfected cell arrays: review and protocol. *Comb Chem High Throughput Screen* 11, 159-172.
- Takayama, S., and Reed, J.C. (2001). Molecular chaperone targeting and regulation by BAG family proteins. *Nat Cell Biol* 3, E237-241.
- Takekawa, M., and Saito, H. (1998). A family of stress-inducible GADD45-like proteins mediate activation of the stress-responsive MTK1/MEKK4 MAPKKK. *Cell* 95, 521-530.
- Tamm, I., Schriever, F., and Dorken, B. (2001). Apoptosis: implications of basic research for clinical oncology. *Lancet Oncol* 2, 33-42.
- Thornberry, N.A., and Lazebnik, Y. (1998). Caspases: enemies within. *Science* 281, 1312-1316.
- Thuerigen, O., Schneeweiss, A., Toedt, G., Warnat, P., Hahn, M., Kramer, H., Brors, B., Rudlowski, C., Benner, A., Schuetz, F., Tews, B., Eils, R., Sinn, H.P., Sohn, C., and Lichter, P. (2006). Gene expression signature predicting pathologic complete response with gemcitabine, epirubicin, and docetaxel in primary breast cancer. *J Clin Oncol* 24, 1839-1845.
- Thyss, R., Virolle, V., Imbert, V., Peyron, J.F., Aberdam, D., and Virolle, T. (2005). NF-kappaB/Egr-1/Gadd45 are sequentially activated upon UVB irradiation to mediate epidermal cell death. *EMBO J* 24, 128-137.

- Tsang, H.T., Connell, J.W., Brown, S.E., Thompson, A., Reid, E., and Sanderson, C.M. (2006). A systematic analysis of human CHMP protein interactions: additional MIT domain-containing proteins bind to multiple components of the human ESCRT III complex. *Genomics* 88, 333-346.
- Tschuch, C., Schulz, A., Pscherer, A., Werft, W., Benner, A., Hotz-Wagenblatt, A., Barrionuevo, L.S., Lichter, P., and Mertens, D. (2008). Off-target effects of siRNA specific for GFP. *BMC Mol Biol* 9, 60.
- Urruticoechea, A., Smith, I.E., and Dowsett, M. (2005). Proliferation marker Ki-67 in early breast cancer. *J Clin Oncol* 23, 7212-7220.
- Vaux, D.L., and Korsmeyer, S.J. (1999). Cell death in development. *Cell* 96, 245-254.
- Vaux, D.L., and Strasser, A. (1996). The molecular biology of apoptosis. *Proc Natl Acad Sci U S A* 93, 2239-2244.
- Wajant, H., Pfizenmaier, K., and Scheurich, P. (2003). Tumor necrosis factor signaling. *Cell Death Differ* 10, 45-65.
- Wang, X. (2001). The expanding role of mitochondria in apoptosis. *Genes Dev* 15, 2922-2933.
- Webb, B.L., Diaz, B., Martin, G.S., and Lai, F. (2003). A reporter system for reverse transfection cell arrays. *J Biomol Screen* 8, 620-623.
- Wheeler, D.B., Carpenter, A.E., and Sabatini, D.M. (2005). Cell microarrays and RNA interference chip away at gene function. *Nat Genet* 37 *Suppl*, S25-30.
- Wollert, T., Wunder, C., Lippincott-Schwartz, J., and Hurley, J.H. (2009). Membrane scission by the ESCRT-III complex. *Nature* 458, 172-177.
- Wu, W., Hodges, E., and Hoog, C. (2006). Thorough validation of siRNA-induced cell death phenotypes defines new anti-apoptotic protein. *Nucleic Acids Res* 34, e13.
- Wyllie, A.H. (1980). Glucocorticoid-induced thymocyte apoptosis is associated with endogenous endonuclease activation. *Nature* 284, 555-556.
- Yan, C., Jamaluddin, M.S., Aggarwal, B., Myers, J., and Boyd, D.D. (2005). Gene expression profiling identifies activating transcription factor 3 as a novel contributor to the proapoptotic effect of curcumin. *Mol Cancer Ther* 4, 233-241.
- Yan, N., and Shi, Y. (2005). Mechanisms of apoptosis through structural biology. *Annu Rev Cell Dev Biol* 21, 35-56.
- Zheng, L., Liu, J., Batalov, S., Zhou, D., Orth, A., Ding, S., and Schultz, P.G. (2004). An approach to genomewide screens of expressed small interfering RNAs in mammalian cells. *Proc Natl Acad Sci U S A* 101, 135-140.
- Ziauddin, J., and Sabatini, D.M. (2001). Microarrays of cells expressing defined cDNAs. *Nature* 411, 107-110.

VI. Supplementary data

Table 5- Expression Arrest™ shRNA library.

| Column A | Column B | Column C | Column D |
|-------------|-------------------|---------------|---------------------------|
| Oligo ID | Current Accession | Release Plate | Fold change in cell death |
| v2HS_99386 | NM_031284 | 2082 | 1,27 |
| v2HS_108899 | XM_303656 | 2082 | 1,04 |
| v2HS_106350 | XM_298971 | 2082 | 1,19 |
| v2HS_109826 | XM_304205 | 2082 | 1,12 |
| v2HS_102054 | XM_114087 | 2082 | 1,17 |
| v2HS_93615 | NM_000546 | 2082 | 0,91 |
| v2HS_93536 | NM_000533 | 2082 | 1,97 |
| v2HS_96705 | NM_015485 | 2082 | 1,08 |
| v2HS_98358 | NM_022755 | 2082 | 1,59 |
| v2HS_99751 | NM_052897 | 2082 | 1,02 |
| v2HS_92212 | M36341 | 2082 | 1,02 |
| v2HS_107692 | XM_299635 | 2082 | 0,85 |
| v2HS_99682 | NM_052875 | 2082 | 1,12 |
| v2HS_81744 | NM_015229 | 2082 | 0,72 |
| v2HS_100819 | XM_040866 | 2082 | 1,27 |
| v2HS_108244 | XM_303544 | 2082 | 1,10 |
| v2HS_108043 | XM_302939 | 2082 | 1,08 |
| v2HS_95675 | NM_014848 | 2082 | 0,68 |
| v2HS_105509 | XM_298808 | 2082 | 0,74 |
| v2HS_92458 | NM_000339 | 2082 | 0,89 |
| v2HS_109992 | XM_304234 | 2082 | 0,70 |
| v2HS_103048 | XM_208555 | 2082 | 0,84 |
| v2HS_102694 | XM_167168 | 2082 | 0,89 |
| v2HS_99423 | NM_031290 | 2082 | 0,63 |
| v2HS_102635 | XM_167134 | 2082 | 0,70 |
| v2HS_95765 | NM_014867 | 2082 | 0,75 |
| v2HS_107848 | XM_299667 | 2082 | 0,93 |
| v2HS_93983 | NM_001050 | 2082 | 1 |

Supplementary

| | | | |
|-------------|-----------|------|------|
| v2HS_110454 | XM_304313 | 2082 | 0,77 |
| v2HS_93419 | NM_000513 | 2082 | 2,63 |
| v2HS_107955 | XM_302911 | 2082 | 0,54 |
| v2HS_97513 | NM_016091 | 2082 | 0,57 |
| v2HS_100633 | X64991 | 2082 | 0,76 |
| v2HS_96026 | NM_014913 | 2082 | 0,61 |
| v2HS_93189 | NM_000465 | 2082 | 0,66 |
| v2HS_101845 | XM_093799 | 2082 | 0,72 |
| v2HS_98400 | NM_022762 | 2082 | 0,87 |
| v2HS_105370 | XM_292364 | 2082 | 0,49 |
| v2HS_100815 | XM_040860 | 2082 | 0,77 |
| v2HS_106158 | XM_298934 | 2082 | 0,70 |
| v2HS_109934 | XM_304223 | 2082 | 1,18 |
| v2HS_95129 | NM_006992 | 2082 | 1,07 |
| v2HS_91909 | AF278761 | 2082 | 1,07 |
| v2HS_102558 | XM_167044 | 2082 | 0,91 |
| v2HS_108982 | XM_303669 | 2082 | 0,84 |
| v2HS_108635 | XM_303610 | 2082 | 0,79 |
| v2HS_95112 | NM_006989 | 2082 | 0,88 |
| v2HS_93697 | NM_000565 | 2082 | 0,94 |
| v2HS_95204 | NM_014755 | 2082 | 1,92 |
| v2HS_92868 | NM_000409 | 2082 | 0,79 |
| v2HS_108611 | XM_303606 | 2082 | 0,78 |
| v2HS_109733 | XM_303799 | 2082 | 0,88 |
| v2HS_106179 | XM_298937 | 2082 | 0,88 |
| v2HS_99525 | NM_052842 | 2082 | 0,67 |
| v2HS_96984 | NM_015571 | 2082 | 1,03 |
| v2HS_110197 | XM_304270 | 2082 | 1,07 |
| v2HS_100355 | NM_178531 | 2082 | 0,79 |
| v2HS_50067 | NM_005120 | 2082 | 0,70 |
| v2HS_110808 | XM_304375 | 2082 | 0,71 |
| v2HS_94144 | NM_001085 | 2082 | 0,89 |
| v2HS_97570 | NM_016101 | 2082 | 0,84 |
| v2HS_101802 | XM_087245 | 2082 | 0,66 |
| v2HS_107407 | XM_299577 | 2082 | 0,55 |
| v2HS_102025 | XM_114057 | 2082 | 1,39 |

Supplementary

| | | | |
|-------------|-----------|------|------|
| v2HS_91785 | AF065858 | 2082 | 0,70 |
| v2HS_95024 | NM_006963 | 2082 | 0,53 |
| v2HS_107440 | XM_299583 | 2082 | 0,68 |
| v2HS_94640 | NM_001178 | 2082 | 0,97 |
| v2HS_95167 | NM_006999 | 2082 | 0,75 |
| v2HS_108711 | XM_303624 | 2082 | 0,75 |
| v2HS_105242 | XM_292336 | 2082 | 0,65 |
| v2HS_99735 | NM_052888 | 2082 | 0,71 |
| v2HS_117956 | NM_032143 | 2082 | 0,83 |
| v2HS_97583 | NM_016103 | 2082 | 0,75 |
| v2HS_100161 | NM_177979 | 2082 | 0,75 |
| v2HS_110113 | XM_304256 | 2082 | 0,70 |
| v2HS_110270 | XM_304282 | 2082 | 0,87 |
| v2HS_126426 | XM_303961 | 2082 | 1,06 |
| v2HS_97249 | NM_016039 | 2082 | 1,92 |
| v2HS_95179 | NM_014751 | 2082 | 1,05 |
| v2HS_101450 | XM_085974 | 2082 | 1,10 |
| v2HS_105530 | XM_298811 | 2082 | 1,14 |
| v2HS_110899 | XM_304392 | 2082 | 0,89 |
| v2HS_92324 | NM_000315 | 2082 | 1,78 |
| v2HS_100667 | XM_027054 | 2082 | 0,76 |
| v2HS_109597 | XM_303776 | 2082 | 0,64 |
| v2HS_99318 | NM_031273 | 2082 | 0,83 |
| v2HS_110719 | XM_304358 | 2082 | 0,76 |
| v2HS_101990 | XM_114028 | 2082 | 0,68 |
| v2HS_104670 | XM_291735 | 2082 | 0,60 |
| v2HS_108399 | XM_303571 | 2082 | 0,75 |
| v2HS_97310 | NM_016050 | 2082 | 0,8 |
| v2HS_101013 | XM_062958 | 2082 | 0,72 |
| v2HS_110467 | XM_304315 | 2082 | 0,57 |
| v2HS_97528 | NM_016094 | 2082 | 0,84 |
| v2HS_108139 | XM_302970 | 2082 | 1,92 |
| v2HS_128761 | XM_305060 | 2052 | 0,73 |
| v2HS_111583 | NM_000590 | 2052 | 0,66 |
| v2HS_129996 | XM_305270 | 2052 | 0,72 |
| v2HS_122689 | XM_291991 | 2052 | 1,08 |

Supplementary

| | | | |
|-------------|--------------|------|------|
| v2HS_126883 | XM_304437 | 2052 | 0,62 |
| v2HS_118105 | BC044246 | 2052 | 0,66 |
| v2HS_125581 | XM_303817 | 2052 | 0,81 |
| v2HS_123108 | XM_292566 | 2052 | 0,92 |
| v2HS_116405 | NM_024096 | 2052 | 1,75 |
| v2HS_118242 | NM_052948 | 2052 | 1,17 |
| v2HS_130113 | XM_305290 | 2052 | 1,74 |
| v2HS_122936 | XM_292500 | 2052 | 1,61 |
| v2HS_122468 | XM_291898 | 2052 | 1,93 |
| v2HS_129041 | XM_305109 | 2052 | 1,25 |
| v2HS_114320 | NM_009171 | 2052 | 1,57 |
| v2HS_112211 | Z34811 | 2052 | 1,5 |
| v2HS_121965 | XM_210044 | 2052 | 1,43 |
| v2HS_118049 | NM_032167 | 2052 | 1,35 |
| v2HS_110975 | NM_015052 | 2052 | 1,78 |
| v2HS_118743 | NM_178838 | 2052 | 1 |
| v2HS_126466 | XM_303967 | 2052 | 0,96 |
| v2HS_122423 | XM_291886 | 2052 | 1,03 |
| v2HS_120958 | XM_167317 | 2052 | 1,37 |
| v2HS_123173 | XM_292594 | 2052 | 1,07 |
| v2HS_129828 | XM_305242 | 2052 | 1,08 |
| v2HS_130080 | XM_305284 | 2052 | 2 |
| v2HS_115280 | AK082587 | 2052 | 1,16 |
| v2HS_128067 | XM_304640 | 2052 | 0,94 |
| v2HS_129692 | XM_305220 | 2052 | 0,92 |
| v2HS_124791 | XM_299758 | 2052 | 1,29 |
| v2HS_117818 | NM_032119 | 2052 | 0,77 |
| v2HS_129789 | XM_305236 | 2052 | 1,31 |
| v2HS_112775 | NM_001237 | 2052 | 1,23 |
| v2HS_121954 | XM_210027 | 2052 | 1,01 |
| v2HS_127399 | XM_304524 | 2052 | 1,36 |
| v2HS_122326 | XM_370662 | 2052 | 1,07 |
| v2HS_122903 | XM_292488 | 2052 | 0,98 |
| v2HS_112317 | NM_001006628 | 2052 | 1,92 |
| v2HS_125901 | XM_303870 | 2052 | 1,44 |
| v2HS_112682 | NM_001219 | 2052 | 1,27 |

Supplementary

| | | | |
|-------------|--------------|------|------|
| v2HS_119731 | XM_086791 | 2052 | 0,70 |
| v2HS_121188 | XM_174639 | 2052 | 0,69 |
| v2HS_120464 | XM_115026 | 2052 | 0,89 |
| v2HS_120416 | NM_002154 | 2052 | 0,83 |
| v2HS_113461 | NM_001365 | 2052 | 0,76 |
| v2HS_117194 | NM_031418 | 2052 | 0,92 |
| v2HS_125239 | XM_299852 | 2052 | 1 |
| v2HS_128718 | XM_305053 | 2052 | 1,12 |
| v2HS_128323 | XM_304683 | 2052 | 1,28 |
| v2HS_111231 | AF527534 | 2052 | 1,31 |
| v2HS_119467 | XM_065172 | 2052 | 1,78 |
| v2HS_113420 | BC035974 | 2052 | 1,18 |
| v2HS_125723 | XM_303841 | 2052 | 1,34 |
| v2HS_115032 | NM_203379 | 2052 | 1,21 |
| v2HS_126958 | XM_304450 | 2052 | 1,26 |
| v2HS_114178 | NM_002073 | 2052 | 1,31 |
| v2HS_118113 | NM_052918 | 2052 | 1,51 |
| v2HS_125448 | XM_299892 | 2052 | 1,62 |
| v2HS_124685 | XM_299737 | 2052 | 1,70 |
| v2HS_112699 | NM_001223 | 2052 | 1,21 |
| v2HS_125791 | XM_303852 | 2052 | 1,25 |
| v2HS_114451 | NM_015641 | 2052 | 1,02 |
| v2HS_128707 | XM_305051 | 2052 | 1,44 |
| v2HS_125400 | XM_299882 | 2052 | 1 |
| v2HS_118023 | NM_032160 | 2052 | 1,11 |
| v2HS_119805 | BX648094 | 2052 | 1,15 |
| v2HS_112649 | U88965 | 2052 | 1,23 |
| v2HS_129103 | XM_305119 | 2052 | 1,18 |
| v2HS_111256 | AJ276510 | 2052 | 1,23 |
| v2HS_122375 | NM_001002925 | 2052 | 1 |
| v2HS_127678 | XM_304571 | 2052 | 1,72 |
| v2HS_115755 | NM_016410 | 2052 | 2,63 |
| v2HS_125023 | XM_299802 | 2052 | 1,21 |
| v2HS_120996 | XM_167360 | 2052 | 0,94 |
| v2HS_114602 | NM_015681 | 2052 | 1,07 |
| v2HS_119659 | XM_086666 | 2052 | 1,78 |

Supplementary

| | | | |
|-------------|--------------|------|------|
| v2HS_121275 | XM_370839 | 2052 | 1,10 |
| v2HS_128423 | XM_305003 | 2052 | 1,02 |
| v2HS_125280 | XM_299861 | 2052 | 1,47 |
| v2HS_118363 | NM_052972 | 2052 | 1,31 |
| v2HS_121120 | XM_168122 | 2052 | 1,03 |
| v2HS_118180 | NM_052938 | 2052 | 0,83 |
| v2HS_119967 | XM_088114 | 2052 | 1,01 |
| v2HS_118548 | NM_172251 | 2052 | 1,13 |
| v2HS_126142 | XM_303911 | 2052 | 0,87 |
| v2HS_112549 | NM_000793 | 2052 | 0,78 |
| v2HS_115696 | NM_016395 | 2052 | 0,75 |
| v2HS_112786 | NM_001239 | 2052 | 0,75 |
| v2HS_116030 | NM_016482 | 2052 | 0,8 |
| v2HS_126390 | XM_303955 | 2052 | 0,72 |
| v2HS_129466 | XM_305180 | 2052 | 1,04 |
| v2HS_113750 | NM_001430 | 2052 | 2,07 |
| v2HS_116053 | NM_016486 | 2052 | 0,89 |
| v2HS_116865 | NM_030791 | 2052 | 0,86 |
| v2HS_115813 | NM_016436 | 2052 | 0,90 |
| v2HS_120275 | NM_199282 | 2052 | 0,98 |
| v2HS_124509 | XM_299704 | 2050 | 1,45 |
| v2HS_128475 | XM_305012 | 2050 | 0,92 |
| v2HS_118580 | AK098243 | 2050 | 1,16 |
| v2HS_127050 | XM_304465 | 2050 | 1,27 |
| v2HS_116165 | AK022973 | 2050 | 0,87 |
| v2HS_111723 | NM_000617 | 2050 | 1,05 |
| v2HS_114504 | NM_015653 | 2050 | 0,91 |
| v2HS_111088 | BC013143 | 2050 | 1,44 |
| v2HS_115378 | NM_016311 | 2050 | 1,14 |
| v2HS_115382 | NM_016312 | 2050 | 1 |
| v2HS_128033 | XM_304634 | 2050 | 1 |
| v2HS_122367 | XM_291857 | 2050 | 1,31 |
| v2HS_122129 | NM_001004760 | 2050 | 1,67 |
| v2HS_114552 | NM_015668 | 2050 | 1,12 |
| v2HS_118457 | NM_148676 | 2050 | 1,66 |
| v2HS_122909 | XM_292489 | 2050 | 1,53 |

Supplementary

| | | | |
|-------------|-----------|------|------|
| v2HS_115009 | AF169802 | 2050 | 1,08 |
| v2HS_111447 | K01241 | 2050 | 1,31 |
| v2HS_126828 | XM_304428 | 2050 | 1,15 |
| v2HS_116976 | NM_030811 | 2050 | 1,36 |
| v2HS_115237 | NM_016279 | 2050 | 1,34 |
| v2HS_119556 | NM_024789 | 2050 | 1,37 |
| v2HS_119045 | AB040926 | 2050 | 1,51 |
| v2HS_127432 | XM_304530 | 2050 | 1,37 |
| v2HS_114427 | NM_015634 | 2050 | 1,60 |
| v2HS_116953 | NM_023668 | 2050 | 1,20 |
| v2HS_123529 | XM_293001 | 2050 | 1,31 |
| v2HS_127318 | XM_304510 | 2050 | 1,41 |
| v2HS_119242 | NM_052892 | 2050 | 1,18 |
| v2HS_125203 | XM_299837 | 2050 | 1,29 |
| v2HS_126354 | XM_303949 | 2050 | 1,27 |
| v2HS_125335 | XM_299871 | 2050 | 1,24 |
| v2HS_126875 | XM_304436 | 2050 | 1,24 |
| v2HS_127377 | XM_304519 | 2050 | 1,05 |
| v2HS_120350 | AB037792 | 2050 | 1,10 |
| v2HS_123622 | AK049977 | 2050 | 1,13 |
| v2HS_112799 | NM_058241 | 2050 | 1,43 |
| v2HS_129658 | XM_305214 | 2050 | 1,06 |
| v2HS_120046 | XM_094565 | 2050 | 1,03 |
| v2HS_124163 | XM_293204 | 2050 | 1,10 |
| v2HS_126951 | XM_304448 | 2050 | 0,99 |
| v2HS_111995 | NM_000682 | 2050 | 0,91 |
| v2HS_118009 | NM_027654 | 2050 | 1,03 |
| v2HS_124122 | XM_293182 | 2050 | 1,29 |
| v2HS_122024 | XM_210107 | 2050 | 2,31 |
| v2HS_114339 | NM_015602 | 2050 | 1,85 |
| v2HS_117152 | NM_002138 | 2050 | 1,64 |
| v2HS_122701 | XM_291994 | 2050 | 1,12 |
| v2HS_115983 | NM_016472 | 2050 | 1,11 |
| v2HS_115853 | NM_016445 | 2050 | 0,78 |
| v2HS_116025 | NM_016481 | 2050 | 0,90 |
| v2HS_127044 | XM_304464 | 2050 | 0,98 |

Supplementary

| | | | |
|-------------|--------------|------|------|
| v2HS_120227 | NM_008393 | 2050 | 0,77 |
| v2HS_122178 | XM_210195 | 2050 | 1,01 |
| v2HS_122475 | XM_291899 | 2050 | 0,97 |
| v2HS_116270 | NM_022895 | 2050 | 0,86 |
| v2HS_115029 | NM_016233 | 2050 | 0,85 |
| v2HS_129600 | XM_305203 | 2050 | 0,97 |
| v2HS_124612 | XM_299723 | 2050 | 0,92 |
| v2HS_118381 | NM_052997 | 2050 | 0,78 |
| v2HS_116669 | NM_030752 | 2050 | 0,92 |
| v2HS_129743 | XM_305228 | 2050 | 1,31 |
| v2HS_121369 | XM_208853 | 2050 | 1,05 |
| v2HS_128874 | XM_305079 | 2050 | 1,18 |
| v2HS_114438 | BC013144 | 2050 | 0,92 |
| v2HS_120607 | NM_001005198 | 2050 | 0,78 |
| v2HS_112158 | NM_000710 | 2050 | 0,78 |
| v2HS_116118 | NM_005678 | 2050 | 0,77 |
| v2HS_124174 | XM_293205 | 2050 | 0,76 |
| v2HS_126743 | XM_304414 | 2050 | 0,76 |
| v2HS_111793 | J03171 | 2050 | 1,02 |
| v2HS_130166 | XM_305299 | 2050 | 0,76 |
| v2HS_120737 | NM_001004745 | 2050 | 1,03 |
| v2HS_121335 | XM_208821 | 2050 | 1,91 |
| v2HS_112035 | NM_000689 | 2050 | 1,11 |
| v2HS_118847 | NR_000039 | 2050 | 0,89 |
| v2HS_112726 | NM_033339 | 2050 | 0,88 |
| v2HS_113000 | NM_001275 | 2050 | 1,23 |
| v2HS_115106 | NM_016249 | 2050 | 0,74 |
| v2HS_128362 | XM_304691 | 2050 | 1,25 |
| v2HS_116349 | AK052018 | 2050 | 1,17 |
| v2HS_130073 | XM_305283 | 2050 | 0,96 |
| v2HS_115416 | NM_016322 | 2050 | 1,30 |
| v2HS_112218 | AB086123 | 2050 | 1,02 |
| v2HS_118086 | NM_017871 | 2050 | 0,94 |
| v2HS_113011 | NM_001277 | 2050 | 1,89 |
| v2HS_126311 | XM_303941 | 2050 | 1,38 |
| v2HS_127080 | XM_304470 | 2050 | 1,21 |

Supplementary

| | | | |
|-------------|-----------|------|------|
| v2HS_118618 | NM_178812 | 2050 | 1,28 |
| v2HS_122948 | XM_292504 | 2050 | 1,11 |
| v2HS_112634 | NM_001211 | 2050 | 0,98 |
| v2HS_126432 | XM_303962 | 2050 | 1,04 |
| v2HS_112186 | NM_000715 | 2050 | 0,89 |
| v2HS_123963 | XM_293131 | 2050 | 1,05 |
| v2HS_111636 | NM_000599 | 2050 | 0,81 |
| v2HS_121684 | AF255565 | 2050 | 1,12 |

*Column A: specific Oligo IDs in the library. Column B: Respective gene accession numbers. Column C: Original plate number in Expression Arrest™ shRNA library. Column D: Fold changes in cell death measured by PI staining and FACS analysis (normalized to negative control sh-luciferase).

Table 6- 107 siRNA from Qiagen human siRNA library.

| Column A | Column B | Column C |
|------------|-------------------------------------|-------------------------------|
| QiagenID | Current Accession | Fold change in cell viability |
| HsDGV3_44 | NM_005763 | 1,13 |
| HsDGV3_28 | NM_004827 | 1,21 |
| HsDGV3_81 | NM_000020 | 1,09 |
| HsDGV3_44 | NM_000689 | 1,02 |
| HsNMV1_90 | NM_001154 | 1,17 |
| HsDGV3_28 | NM_014629 | 0,97 |
| HsNMV1_210 | NM_005738 | 1,16 |
| HsDGV3_12 | NM_004318 NM_032466 NM_032468 | 1,16 |
| HsNMV1_91 | NM_001698 | 1,16 |
| HsDGV3_81 | NM_001204 | 0,94 |
| HsDGV3_45 | NM_000060 | 1,15 |
| HsNMV1_130 | NM_014550 | 1,06 |
| HsDGV3_48 | NM_001239 | 1,05 |
| HsNMV1_158 | NM_030911 | 1,05 |
| HsDGV3_9 | NM_003671 NM_033331 | 1,12 |
| HsNMV1_111 | NM_003956 | 1,05 |

Supplementary

| | | |
|------------|-------------------------------------|------|
| HsNMV1_92 | NM_001280 | 1,13 |
| HsNMV1_111 | NM_012129 | 1,21 |
| HsNMV1_106 | NM_003277 | 1,04 |
| HsNMV1_116 | NM_016138 | 1,02 |
| HsNMV1_117 | NM_006371 | 0,91 |
| HsDGV3_79 | NM_005730 | 0,97 |
| HsNMV1_217 | NM_021800 | 1,06 |
| HsDGV3_8 | NM_015291 | 1,10 |
| HsNMV1_93 | NM_001374 | 1,13 |
| HsNMV1_124 | NM_015296 | 1,00 |
| HsDGV3_48 | NM_001964 | 0,98 |
| HsDGV3_82 | NM_005233 NM_182644 | 0,89 |
| HsDGV3_48 | NM_005239 | 0,90 |
| HsDGV3_12 | NM_012161 NM_033535 | 1,03 |
| HsDGV3_26 | NM_013231 | 1,01 |
| HsNMV1_122 | NM_014947 | 1,05 |
| HsDGV3_52 | NM_002015 | 1,15 |
| HsNMV1_121 | NM_007285 | 1,02 |
| HsNMV1_149 | NM_022087 | 0,94 |
| HsDGV3_24 | NM_018841 | 0,99 |
| HsDGV3_2 | NM_001004051 NM_138437 | 0,93 |
| HsDGV3_66 | NM_001018102 NM_015532 | 1,08 |
| HsNMV1_122 | NM_014282 | 1,06 |
| HsNMV1_120 | NM_007072 | 0,93 |
| HsDGV3_15 | NM_032549 | 0,98 |
| HsDGV3_78 | NM_005539 | 0,90 |
| HsDGV3_79 | NM_014937 NM_198330 NM_198331 | 0,90 |
| HsDGV3_59 | NM_003749 | 0,91 |
| HsDGV3_80 | NM_032833 | 0,48 |
| HsDGV3_43 | NM_015074 NM_183416 | 0,94 |

Supplementary

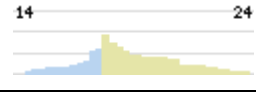
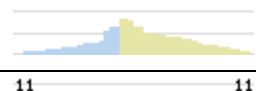
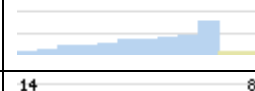
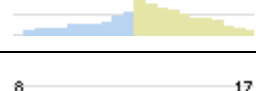
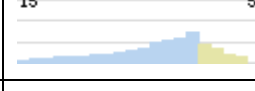
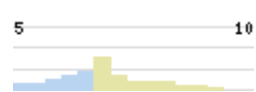
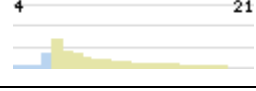
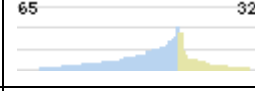
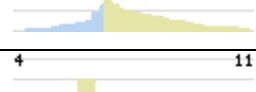
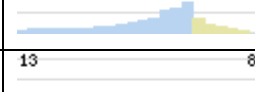
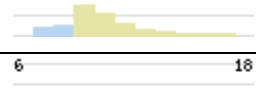
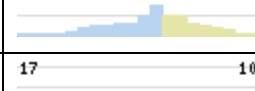
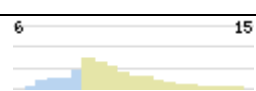
| | | |
|------------|-------------------------------------|------|
| HsNMV1_91 | NM_001206 | 0,78 |
| HsNMV1_108 | NM_033631 | 0,73 |
| HsDGV3_38 | NM_000081 NM_001005736 | 0,73 |
| HsDGV3_89 | NM_012301 | 1,16 |
| HsDGV3_29 | NM_000898 | 1,23 |
| HsDGV3_85 | NM_003618 | 1,07 |
| HsDGV3_60 | NM_002387 | 0,96 |
| HsDGV3_53 | NM_004992 | 1,00 |
| HsDGV3_26 | NM_002404 | 1,15 |
| HsNMV1_99 | NM_005938 | 1,06 |
| HsDGV3_66 | NM_024848 | 1,02 |
| HsDGV3_76 | NM_145015 | 0,99 |
| HsDGV3_49 | NM_002487 | 1,14 |
| HsDGV3_59 | NM_015277 | 1,06 |
| HsDGV3_88 | NM_033116 | 0,90 |
| HsNMV1_206 | NM_014057 | 1,07 |
| HsNMV1_101 | NM_006196 | 1,16 |
| HsDGV3_83 | NM_002595 | 1,18 |
| HsDGV3_55 | NM_006202 | 1,15 |
| HsDGV3_65 | NM_021255 | 1,03 |
| HsDGV3_50 | NM_016831 | 1,00 |
| HsDGV3_10 | NM_014819 | 0,87 |
| HsNMV1_98 | NM_000216 | 1,02 |
| HsDGV3_79 | NM_002841 | 0,96 |
| HsDGV3_79 | NM_002847 NM_130842 NM_130843 | 0,96 |
| HsDGV3_36 | NM_006908 NM_018890 NM_198829 | 1,05 |
| HsNMV1_103 | NM_000983 | 1,00 |
| HsNMV1_147 | NM_020974 | 1,19 |
| HsNMV1_119 | NM_006642 | 0,95 |
| HsNMV1_111 | NM_003919 | 1,26 |
| HsNMV1_120 | NM_007001 | 0,97 |
| HsDGV3_88 | NM_032840 | 0,78 |

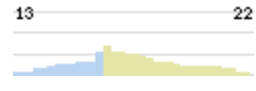
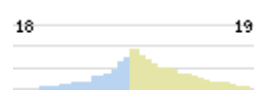
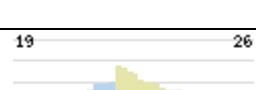
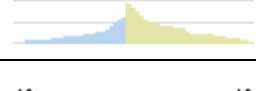
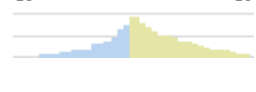
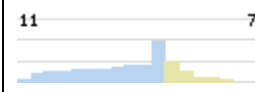
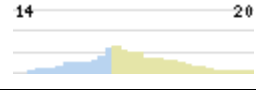
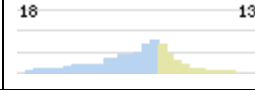
Supplementary

| | | |
|------------|---------------------------|------|
| HsNMV1_220 | NM_052851 | 0,90 |
| HsNMV1_129 | NM_006588 | 0,94 |
| HsNMV1_168 | NM_080737 | 0,95 |
| HsNMV1_124 | NM_007375 | 1,05 |
| HsNMV1_136 | NM_018201 | 1,02 |
| HsDGV3_85 | NM_000459 | 1,05 |
| HsNMV1_135 | NM_018975 | 0,92 |
| HsDGV3_85 | NM_001024847 NM_003242 | 1,03 |
| HsDGV3_21 | NM_032027 | 1,05 |
| HsNMV1_137 | NM_017775 | 0,76 |
| HsNMV1_116 | NM_006048 | 0,73 |
| HsDGV3_16 | NM_022832 | 0,88 |
| HsDGV3_36 | NM_014232 | 0,90 |
| HsNMV1_112 | NM_004781 | 1,10 |
| HsDGV3_31 | NM_052867 | 0,93 |
| HsNMV1_216 | NM_015378 | 1,05 |
| HsNMV1_121 | NM_007187 | 1,06 |
| HsDGV3_85 | NM_003390 | 1,00 |
| HsNMV1_147 | NM_020899 | 1,16 |
| HsDGV3_28 | NM_015336 | 0,78 |
| HsNMV1_158 | NM_030634 | 1,28 |
| HsNMV1_162 | NM_032497 | 0,97 |
| HsNMV1_162 | NM_032342 | 0,65 |
| HsNMV1_137 | NM_017787 | 1,13 |
| HsNMV1_187 | NM_153367 | 0,98 |
| HsNMV1_156 | NM_025057 | 1,13 |
| HsNMV1_119 | NM_018691 | 0,92 |
| HsNMV1_153 | NM_024573 | 1,38 |
| HsNMV1_122 | NM_014929 | 1,10 |

*Column A: Specific Oligo IDs in the library. Column B: Respective gene accession numbers. Column C: Fold changes in cell viability measured by CTG assay (normalized to negative control si-GFP).

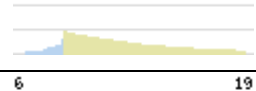
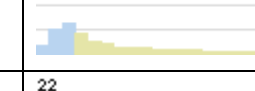
Table 7 (A)- Top 20 pathways which are affected by CHMP5 over-expression 48h after transfection.

| Down-Regulated pathways by CHMP5 over-expression after 48h | | | Up- Regulated pathways by CHMP5 over-expression after 48h | | |
|--|---|-------|---|---|-------|
| A | B | C | D | E | F |
| Pathway Name | Histogram | Score | Pathway Name | Histogram | Score |
| Endometrial cancer |  | 359 | Ribosome |  | 326 |
| Acute myeloid leukemia |  | 352 | Caprolactam degradation |  | 294 |
| Thyroid cancer |  | 347 | Biosynthesis of steroids |  | 291 |
| Huntington's disease |  | 313 | Benzoate degradation via CoA ligation |  | 286 |
| Polyunsaturated fatty acid biosynthesis |  | 307 | Aminosugars metabolism |  | 273 |
| Sphingolipid metabolism |  | 293 | Oxidative phosphorylation |  | 225 |
| Methionine metabolism |  | 272 | Keratan sulfate biosynthesis |  | 215 |
| Insulin signaling pathway |  | 264 | Limonene and pinene degradation |  | 211 |
| Carbon fixation |  | 208 | Proteasome |  | 172 |
| Glycosaminoglycan degradation |  | 208 | Glycosylphosphatidylinositol(GPI)-anchor biosynthesis |  | 162 |
| Selenoamino acid metabolism |  | 208 | Propanoate metabolism |  | 152 |
| Amyotrophic lateral sclerosis (ALS) |  | 206 | DNA polymerase |  | 146 |
| Glycan structures - degradation |  | 192 | Riboflavin metabolism |  | 141 |

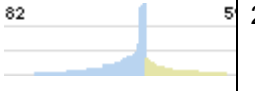
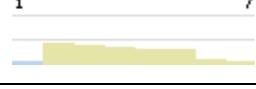
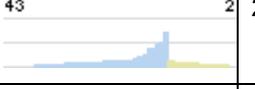
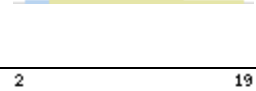
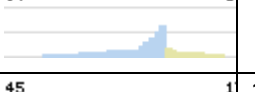
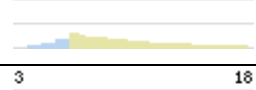
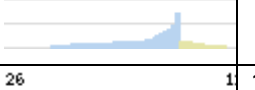
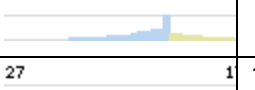
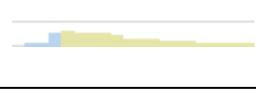
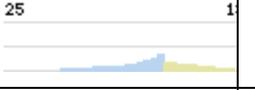
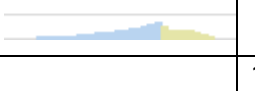
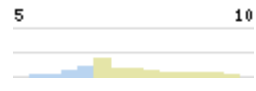
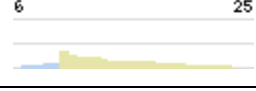
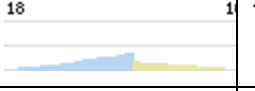
| | | | | | |
|--|---|-----|---|---|-----|
| Notch signaling pathway |  | 175 | Butanoate metabolism |  | 141 |
| Pathogenic Escherichia coli infection - EHEC |  | 168 | SNARE interactions in vesicular transport |  | 135 |
| Adipocytokine signaling pathway |  | 165 | TGF-beta signaling pathway |  | 134 |
| Prostate cancer |  | 165 | gamma-Hexachlorocyclohexane degradation |  | 134 |
| Pathogenic Escherichia coli infection - EPEC |  | 161 | Porphyrin and chlorophyll metabolism |  | 116 |
| Aminoacyl-tRNA biosynthesis |  | 148 | Fatty acid metabolism |  | 102 |
| Pentose phosphate pathway |  | 129 | p53 signaling pathway |  | 101 |

*Column A and D: name of the pathways, column B and E histogram of the genes which are down or up regulated in proper pathways, column C and F: Scores which are obtained by CGPA-software for each pathway.

Table 7 (B)- **Top 20 pathways which are affected by CHMP5 silencing 48h after transfection.**

| Down- Regulated pathways by CHMP5 knock-down after 48h | | | Up- Regulated pathways by CHMP5 knock-down after 48h | | |
|--|---|-------|--|---|-------|
| A | B | C | F | G | H |
| Pathway Name | Histogram | Score | Pathway Name | Histogram | Score |
| Valine, leucine and isoleucine degradation |  | 359 | Cell cycle |  | 326 |
| Propanoate metabolism |  | 352 | p53 signaling pathway |  | 294 |
| Oxidative phosphorylation |  | 347 | Urea cycle and metabolism of amino groups |  | 291 |
| Citrate cycle (TCA cycle) |  | 313 | Bladder cancer |  | 286 |

Supplementary

| | | | | | |
|---|---|-----|--|---|-----|
| Fatty acid metabolism |  | 307 | MAPK signaling pathway |  | 273 |
| Ubiquinone biosynthesis |  | 293 | Chronic myeloid leukemia |  | 225 |
| Glycosylphosphatidylinositol(GPI)-anchor biosynthesis |  | 272 | Thyroid cancer |  | 215 |
| Proteasome |  | 264 | Notch signaling pathway |  | 211 |
| Caprolactam degradation |  | 208 | Acute myeloid leukemia |  | 172 |
| Aminoacyl-tRNA biosynthesis |  | 208 | Prostate cancer |  | 162 |
| Pentose phosphate pathway |  | 208 | Endometrial cancer |  | 152 |
| Limonene and pinene degradation |  | 206 | Non-small cell lung cancer |  | 146 |
| Benzoate degradation via CoA ligation |  | 192 | mTOR signaling pathway |  | 141 |
| beta-Alanine metabolism |  | 175 | Pathogenic Escherichia coli infection - EPEC |  | 141 |
| Pyruvate metabolism |  | 168 | Small cell lung cancer |  | 135 |
| Biosynthesis of steroids |  | 165 | Pathogenic Escherichia coli infection - EHEC |  | 134 |
| Polyunsaturated fatty acid biosynthesis |  | 165 | Colorectal cancer |  | 134 |
| Butanoate metabolism |  | 161 | Cholera - Infection |  | 116 |
| Glutamate metabolism |  | 148 | Parkinson's disease |  | 102 |
| Arginine and proline metabolism |  | 129 | Renal cell carcinoma |  | 101 |

*Column A and D: name of the pathways, column B and E histogram of the genes which are down or up regulated in proper pathways, column C and F: Scores which are obtained by CGPA-software for each pathway.

Table 8- Down-regulated and up-regulated genes upon CHMP5 over-expression at different time points.

| A | | | | | | B | | | | | |
|--------------------------|--------------------|------|--------------------------|--------------------|------|--------------------------|--------------------|------|--------------------------|--------------------|------|
| Down-regulated genes | | | | | | Up-regulated genes | | | | | |
| CHMP5 Overexpression-48h | | | CHMP5 Overexpression-72h | | | CHMP5 Overexpression-48h | | | CHMP5 Overexpression-72h | | |
| gene name | fold change (log2) | rank | gene name | fold change (log2) | rank | gene name | fold change (log2) | rank | gene name | fold change (log2) | rank |
| PKM2 | -1.64 | 1 | LBR | -1.42 | 2 | CHMP5 | 3.74 | 1 | CHMP5 | 3.71 | 1 |
| LBR | -1.38 | 4 | UCP2 | -0.76 | 3 | HIST1H1C | 2.33 | 2 | HIST1H1C | 3.12 | 2 |
| ATP2A2 | -1.31 | 5 | C6orf68 | -1.16 | 5 | HIST2H2AA3 | 2.06 | 3 | HIST2H2AA3 | 3.03 | 3 |
| FKBP1A | -1.23 | 7 | FKBP1A | -1.157 | 6 | HIST2H2AC | 1.63 | 4 | HIST2H2AC | 2.96 | 4 |
| SPTBN1 | -1.17 | 9 | PKM2 | -1.133 | 7 | CLEC2D | 1.56 | 5 | HIST2H2AA3 | 1.75 | 7 |
| C6orf68 | -1.17 | 10 | EZH2 | -1.09 | 8 | WDR79 | 1.56 | 6 | HIST1H2BD | 1.63 | 8 |
| RRM2 | -1.15 | 11 | SBDS | -1.07 | 9 | DCBLD1 | 1.25 | 7 | DCBLD1 | 1.37 | 11 |
| TPM3 | -1.12 | 13 | ATP2A2 | -1.07 | 10 | iNUTF2 | 1.22 | 9 | SIPA1L1 | 1.17 | 13 |
| DHX9 | -1.12 | 15 | GTF2I | -1.06 | 11 | IL18 | 1.22 | 10 | IL18 | 1.17 | 14 |
| HNRPK | -1.11 | 17 | TRUB1 | -0.97 | 13 | CU055 | 1.11 | 14 | CU055 | 1.12 | 17 |
| EZH2 | -1.09 | 20 | S6A15 | -0.97 | 14 | C15orf51 | 1.07 | 16 | EIF5A | 1.1 | 18 |
| GP137 | -1.08 | 21 | RRM2 | -0.96 | 17 | ZNF135 | 1.05 | 18 | WDR79 | 1.07 | 21 |
| GTF2I | -1.08 | 22 | STAU1 | -0.95 | 18 | MCAR1 | 1.05 | 19 | SIRT7 | 1.03 | 23 |
| USP22 | -1.08 | 24 | SREBF2 | -0.92 | 22 | PRNPIP | 1.03 | 21 | SPSB3 | 1.01 | 25 |
| TRUB1 | -1.08 | 25 | PFN2 | -0.76 | 23 | NDUFB10 | 1.01 | 23 | ZNF135 | 0.99 | 28 |
| SBDS | -1.07 | 26 | SLC25A24 | -0.9 | 24 | SIPA1L1 | 0.93 | 29 | PRNPIP | 0.96 | 33 |
| SLC25A22 | -1.06 | 27 | ACTB | -0.86 | 27 | HIST1H4D | 0.92 | 32 | SCRIB | 0.94 | 35 |
| MGRN1 | -1.06 | 29 | Q5TA31 | -0.92 | 28 | TAX1BP3 | 0.91 | 35 | C15orf51 | 0.92 | 42 |
| SREBF2 | -1.06 | 30 | HSF1 | -0.97 | 30 | IFI6 | 0.91 | 36 | MPDU1 | 0.9 | 45 |
| LLGL1 | -1.04 | 32 | FAM100A | -0.88 | 31 | GCC2 | 0.91 | 38 | RNF126 | 0.89 | 46 |
| SLC25A24 | -1.01 | 34 | HNRPK | -0.87 | 37 | M6PRBP1 | 0.9 | 40 | MCAR1 | 0.88 | 48 |
| UCP2 | -0.99 | 36 | SLC25A22 | -0.86 | 39 | C9orf10 | 0.89 | 42 | JARID2 | 0.88 | 50 |
| HSF1 | -0.99 | 37 | GPR89A | -0.86 | 41 | SNF8 | 0.88 | 45 | SNF8 | 0.87 | 52 |
| CCDC95 | -0.97 | 39 | ATP2A2 | -0.87 | 43 | RNF126 | 0.85 | 49 | iNUTF2 | 0.86 | 54 |
| ACTB | -0.96 | 43 | CCDC95 | -1.07 | 46 | JARID2 | 0.85 | 50 | M6PRBP1 | 0.85 | 57 |
| ATP2A2 | -0.96 | 44 | SNAP23 | -0.9 | 51 | EIF5A | 0.85 | 51 | CLEC2D | 0.84 | 61 |
| WBSCR1 | -0.96 | 50 | CV005 | -1.07 | 52 | Q6ZUY0 | 0.81 | 60 | PRKDC | 0.83 | 64 |
| Q5TA31 | -0.95 | 51 | PKMYT1 | -0.8 | 54 | MPDU1 | 0.79 | 66 | C9orf10 | 0.83 | 65 |
| STAU1 | -0.93 | 57 | GP137 | -0.8 | 56 | SIRT7 | 0.78 | 71 | Q6ZUY0 | 0.82 | 69 |
| PFN2 | -0.92 | 63 | HOXB9 | -0.79 | 60 | SPSB3 | 0.78 | 74 | GCC2 | 0.82 | 70 |
| FAM100A | -0.91 | 68 | TPM3 | -0.78 | 63 | HIST1H2BD | 0.78 | 76 | IFI6 | 0.82 | 71 |
| SNAP23 | -0.9 | 69 | SPTBN1 | -0.77 | 67 | AKT1S1 | 0.77 | 81 | NDUFB10 | 0.81 | 72 |
| HOXB9 | -0.89 | 71 | USP22 | -0.76 | 68 | HIST2H2AA3 | 0.76 | 91 | HIST1H4D | 0.81 | 75 |
| ATXN7L3 | -0.89 | 72 | LLGL1 | -0.76 | 73 | PRKDC | 0.75 | 97 | AKT1S1 | 0.78 | 83 |
| MCM3 | -0.88 | 78 | DDB1 | -0.75 | 74 | SCRIB | 0.74 | 99 | TAX1BP3 | 0.76 | 86 |
| HSPD1 | -0.88 | 80 | HSPD1 | -0.84 | 78 | | | | | | |
| GPR89A | -0.87 | 82 | MGRN1 | -0.73 | 81 | | | | | | |
| DDB1 | -0.87 | 88 | DHX9 | -0.72 | 91 | | | | | | |
| S6A15 | -0.86 | 89 | MCM3 | -0.88 | 93 | | | | | | |
| CV005 | -0.85 | 94 | ATXN7L3 | -1.25 | 94 | | | | | | |
| PKMYT1 | -0.85 | 99 | WBSCR1 | -0.73 | 96 | | | | | | |

*Common genes of top 100 in comparison of time points 48h and 72h (A, B)

AGGCAGC**TTCC**CGC**TC**CCTGCAATT Murine cDNA-CHMP5 sequence

AGGCAGC**ATCT**GC**AC**CTGCAATT Human sh-CHMP5 sequence

Figure 30- Murine cDNA-CHMP5 (nucleotide 609-631) and Human sh-CHMP5 (nucleotide 631-653) sequences. The mismatches are shown in bold.

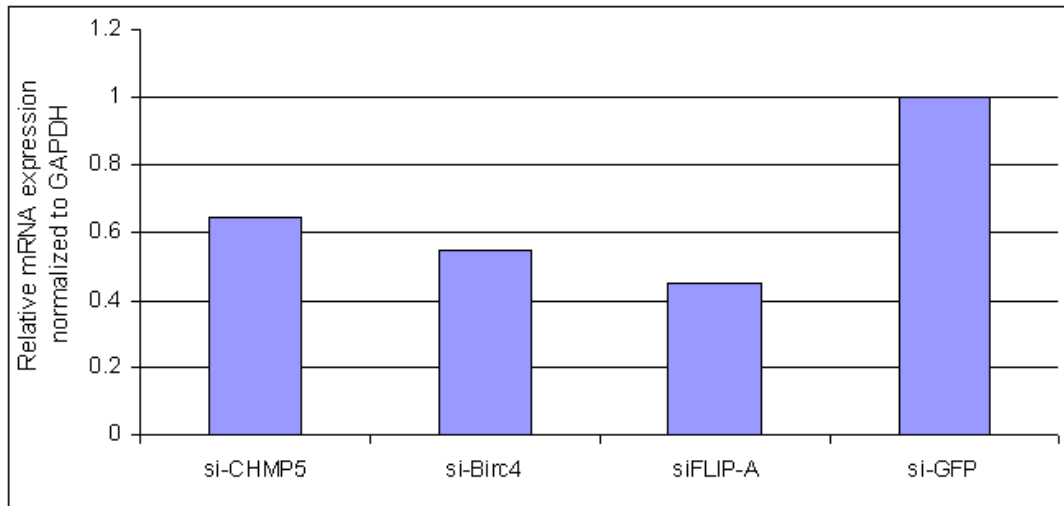


Figure 31- **Expression of CHMP5, Birc4 and FLIP in transfected HEK293T cells.** The level of CHMP5, Birc4 and FLIP mRNA was measured by qRT-PCR 48h after transfection and values were normalized to GAPDH mRNA levels, which was used as loading control. Si-GFP transfected cells used as negative control.

Publications

Articles based on this thesis

Maria Shahmoradgoli, Otto Mannherz, Felix Engel, Stefanie Heck, Martina Seiffert, Armin Pscherer, Peter Lichter.

'Anti-apoptotic function of Charged Multivesicular Body Protein 5 (CHMP5) revealed by RNAi-screening' *In revision*

Maria Shahmoradgoli, Otto Mannherz, Natalia Becker, Michael Boutros, Peter Lichter.

'Identification of PPP1R15B gene as a survival factor in breast cancer cells' *In preparation.*

Acknowledgments

- My parents and the best in my life Yasser;
- Prof. Otmar Wiestler for introducing me to Prof. Peter Lichter;
- My supervisor Prof. Peter Lichter for the opportunity to start my PhD in his lab, suggesting the topic, his scientific support, and his guidance on writing this thesis;
- Prof. Eckart Meese for providing me with the great opportunity to start my PhD at Saarland university, department of human genetics and his advices as a member of my PhD committee;
- Armin Pscherer for his excellent support, our weekly discussions, ideas and advices;
- My colleague, Dr.Otto Mannherz, for his great support at the beginning of my work at DKFZ and teaching me the lab methods;
- Dr. Michael Rogers, for critical revisions and valuable comments;
- Dr. Martina Seiffert and Dr. Stefanie Heck for helpful discussions;
- Prof. Michael Boutros, for insightful discussions and his advices as member of my PhD advisory committee;
- Dr. Karsten Richter for his kind help during my scientific life in the office number 1.105;
- Dr. Alexandra Farfsing, a lady full of positive energy, for comprehensive discussions from lab to home;
- Members of the bioinformatics group, especially Felix Engel and Natalia Becker for the Chip analysis;
- All my former and current colleagues in the Oncogenomics lab, at the Division of Molecular Genetics, and of course all my friends at DKFZ, and,
- Paymaan Jafar-Nejad.

Curriculum Vitae

Name

Maria

Family name

Shahmoradgoli Najafabadi

Date and place of birth

Aug 19, 1978, Esfahan, Iran

Education

March 2005 - 2009, German Cancer Research Center (DKFZ), Heidelberg, Germany
PhD candidate in Molecular Biology.

Sep 2001 – Nov 2003, Science and Research Campus, Azad University,
Tehran, Iran.

Master of Science in Molecular-Cellular Biology (*Top grade student in entrance examination*).

Sep 1996- March 2000, Falavarjan Campus, Azad University, Esfahan, Iran.
Bachelor of Science in Microbiology.

Sep 1992- Jun 1996, Mahboobeh Danesh high school, Esfahan, Iran.
High school degree in Experimental Sciences (Diploma/12th Grade).

Publications based on previous works

M.Shahmoradgoli, O. Mueller, N. Kutzner, B. Noorinayer, MR. Zali (2006). Gene symbol: APC. Disease: Familial adenomatous polyposis coli. Accession #Hd0518
Human Genetics: 118(6):776.

M.Shahmoradgoli Najafabadi, M.Ohadi, F.Valaie, Y.Riazalhosseini, F.Mohammadbeigi, H.Najmabadi (2005). Association between the DRD2 A1 allele and opium-addiction in Iranian population. *American Journal of Medical Genetics Part B; 134(1):39-41.*

Heidelberg 30.11.2009